

F
O
S
S
I
L
E
N
E
R
G
Y

DOE/BC/14881-12
(DE95000158)

**IMPROVING RESERVOIR
CONFORMANCE USING GELLED POLYMER SYSTEMS**

Annual Report for the Period
September 25, 1993 to September 24, 1994

By
D. W. Green and G. P. Willhite

July 1995

Performed Under Contract No. DE-AC22-92BC14881

The University of Kansas
Lawrence, Kansas



**Bartlesville Project Office
U. S. DEPARTMENT OF ENERGY
Bartlesville, Oklahoma**

DISCLAIMER

This report was prepared as an account of work sponsored by an agency of the United States Government. Neither the United States Government nor any agency thereof, nor any of their employees, makes any warranty, expressed or implied, or assumes any legal liability or responsibility for the accuracy, completeness, or usefulness of any information, apparatus, product, or process disclosed, or represents that its use would not infringe privately owned rights. Reference herein to any specific commercial product, process, or service by trade name, trademark, manufacturer, or otherwise does not necessarily constitute or imply its endorsement, recommendation, or favoring by the United States Government or any agency thereof. The views and opinions of authors expressed herein do not necessarily state or reflect those of the United States Government.

This report has been reproduced directly from the best available copy.

Available to DOE and DOE contractors from the Office of Scientific and Technical Information, P.O. Box 62, Oak Ridge, TN 37831; prices available from (615) 576-8401.

Available to the public from the National Technical Information Service, U.S. Department of Commerce, 5285 Port Royal Rd., Springfield VA 22161

DOE/BC/14881-12
Distribution Category UC-122

Improving Reservoir Conformance Using
Gelled Polymer Systems

Annual Report for the Period
September 25, 1993 to September 24, 1994

By
D. W. Green
and
G. P. Willhite

July 1995

Work Performed Under Contract No. DE-AC22-92BC14881

Prepared for
U.S. Department of Energy
Assistant Secretary for Fossil Energy

Jerry Casteel, Project Manager
Bartlesville Project Office
P.O. Box 1398
Bartlesville, OK 74005

Prepared by
The University of Kansas
4006 Learned
Lawrence, KS 66045-2223

Table of Contents

	<u>Page No.</u>
List of Figures	iv
List of Tables	vii
Abstract	ix
Executive Summary	x
Chapter 1 Introduction	1-1
Chapter 2 Development of the KUSP1 Polysaccharide and Derivatives	2-1
Chapter 3 Gelation of KUSP1 by Ester Hydrolysis	3-1
Chapter 4 Permeability Modification by In Situ Gelation of a KUSP1-Ester System in Porous Media	4-1
Chapter 5 Rock-Fluid Interations and Injectivity of KUSP1 in Porous Media	5-1
Chapter 6 In Situ Gelation of KUSP1 by Supercritical Carbon Dioxide	6-1
Chapter 7 Effect of Steady Shear on the Gelation of a Polyacrylamide- Chromium(III) System	7-1
Chapter 8 Investigation of the Polyacrylamide-Aluminum Cirate Gel System	8-1
Chapter 9 Simulation of Alkali-Sandstone Interactions in Core-Flood Experiments	9-1

List of Figures

<u>Figure No.</u>	<u>Title</u>	<u>Page No.</u>
3.1	Effect of Ester Concentration on Viscosity and pH Behavior. 2.0% KUSP1, 1.0 N NaOH, and 0% NaCl. MEP/NaOH => mole ratio of ester to NaOH.	3-5
3.2	Effect of KUSP1 Concentration on Viscosity and pH Behavior. 1.0 N NaOH, 0.75 moles MEP/mole NaOH and 0% NaCl.	3-6
3.3	Effect of NaOH Concentration on Viscosity and pH Behavior. 2.0% KUSP1, 0.75 moles MEP/mole NaOH and 0% NaCl.	3-7
3.4	Effect of NaCl Concentration on Viscosity and pH Behavior. 2.0% KUSP1, 1.0 N NaOH, and 0.75 moles MEP/mole NaOH.	3-8
3.5	Simulated and Measured NaOH Concentration as a Function of Time. 0% KUSP1, 0% NaCl and 0.75 moles of MEP/mole NaOH.	3-10
3.6	Simulated and Measured pH as Function of Time. 0% KUSP1, 0% NaCl and 0.75 moles of MEP/mole NaOH.	3-11
4.1	Controlled pH Reduction by Hydrolysis of MEP Ester. Initial NaOH Concentration was 0.10 N.	4-3
4.2	Gelation Induced by pH Reduction. Initial Concentrations - 0.10 N NaOH, 0.06 M MEP Ester.	4-4
4.3	Pressure Drops During Injection of Gel Solution in Sandpack #1.	4-5
4.4	Tracer Concentrations in Effluent During Pre- and Post-treatment Tests.	4-6
5.1	Apparent Viscosities for Individual Sections of a Berea Core Indicating Front-End Loading.	5-2
5.2	Apparent Viscosity in Individual Sections of a Berea Plug Indicating Front-End Loading.	5-3
5.3	Consumption of Hydroxide with Time by the Rock Matrix for Solutions Containing 1.0 M Sodium Hydroxide.	5-8
5.4	Consumption of Hydroxide with Time by the Rock Matrix for Solutions Containing 0.1 M Sodium Hydroxide.	5-9
6.1	Typical Effluent pH During Injection of Carbon Dioxide In a Berea Core Saturated with KUSP1 and 1N Sodium Hydroxide.	6-6

6.2	Typical Production Rate of Liquid During Injection of Carbon Dioxide In a Berea Core Saturated with KUSP1 and 1N Sodium Hydroxide.	6-8
7.1	Viscosity Behavior During Gelation Under Shear. Data from Weissenberg Rheometer and for Long Time Periods.	7-4
7.2	Viscosity Behavior During Gelation Under Shear. Data from Weissenberg Rheometer and for Early Time Periods.	7-5
7.3	Viscosity Behavior During Gelation Under Shear for Long Time Periods. Data from Bohlin Rheometer (parallel plates, gap = 0.5 mm).	7-6
7.4	Viscosity Behavior During Gelation Under Shear. Data from Bohlin Rheometer (parallel plates) and for Early Time Periods.	7-7
7.5	Development of Storage Modulus During Gelation Under Shear. Data from Weissenberg Rheometer and for Long Time Periods.	7-8
7.6	Development of Storage Modulus During Gelation Under Shear. Data from Weissenberg Rheometer and for Early Time Periods.	7-9
7.7	Determination of Gel Times from Rheological Data. Sample Subjected to Shear Rate of 0.74 s ⁻¹	7-10
7.8	Rheological Data for Sample Subjected to a Shear Rate of 14.88 s ⁻¹ . Rapid Rise in Viscosity and G'-G" Cross-over Not Observed.	7-12
7.9	Comparison of Viscosity Behavior for Replicate Experiments. Sample Subjected to Shear Rate of 0.74 s ⁻¹ on Wiessenberg Rheometer.	7-14
7.10	Comparison of Viscosity Behavior at Two Gap Settings Using Parallel-Plate Geometry. Sample Subjected to Shear Rate of 14.88 s ⁻¹ on Bohlin Rheometer.	7-15
7.11	Stress as a Function of Time for Selected Shear Rates. Data from Weissenberg Rheometer.	7-17
7.12	Development of Storage Modulus with Time for Replicate Samples Subjected to Oscillatory Shear Only. Data from Weissenberg Rheometer.	7-18
8.1	Transition Pressures Determined from TGU and Flow Rate Curves. Solution Composition: 900 ppm HiVis 350, 45 ppm Al ⁺⁺⁺ and 0.5% KCl.	8-3
8.2	Development of Transition Pressure with Time. Solution Composition: 300 ppm HiVis 3500, 15 ppm Al ⁺⁺⁺ and 0.5% KCl.	8-4
8.3	Viscosity as a Function of Shear Rate and Age. Solution Composition: 900 ppm HiVis 3500 and 0.5% KCl.	8-6

8.4	Comparison of Experimental Viscosity Data with Correlation. Solution Composition: HiVis polymer and 0.5% KCl.	8-7
8.5	Comparison of Chromatograms for Two Polyacrylamides.	8-8
9.1	Simulated histories of the reduced concentrations of sodium and hydroxide compared to experimental data of Jenson and Radke (correction factor = 5, $K_i = 1E4$ (moles/liter) $^{-2}$, $n_T = 0.125$ meq/(100g solid)).	9-5
9.2	Simulated histories of the reduced concentrations of sodium and hydroxide compared to experimental data of Novassad and Novassad (correction factor = 5, $K_i = 1E4$ (moles/liter) $^{-2}$, $n_T = 0.4$ meq/(100g solid)).	9-7
9.3	Simulated histories of the reduced concentrations of sodium and hydroxide compared to experimental data reported by Bunge and Radke (correction factor = 0.14, $K_i = 1E2$ (moles/liter) $^{-2}$, $n_T = 1.25$ meq/(100g solid)).	9-9

List of Tables

<u>Table No.</u>	<u>Title</u>	<u>Page No.</u>
2.1	Growth of <i>Cellulomonas flavigena</i> in 40,000 liters vessels.	2-3
3.1	Composition of Samples and Gel Times.	3-4
4.1	Permeability Reductions Using KUSP1-Ester Gelant.	4-7
5.1	Rock-Fluid Interactions.	5-6
6.1	Permeability Reduction by CO ₂ Injection at 0.5 ml/min.	6-3
6.2	Stability of Permeability Reduction.	6-3
6.3	Reversibility of Permeability Reduction.	6-3
6.4	Permeability Reduction by CO ₂ Injection in the Absence of Polymer.	6-4
6.5	Permeability Reduction by CO ₂ Injection in the Presence of Polymer.	6-4
6.6	Permeability Reduction by CO ₂ Injection at 0.005 ml/min.	6-5
7.1	Gel Times as determined by G'-G" Cross-over and Rapid Rise in Viscosity.	7-13
9.1	Summary of the reference physical parameters used in the simulations.	9-4
9.2	Summary of the physical parameters for the alkaline flood by Radke and Jenson.	9-4
9.3	Summary of the physical parameters for the alkaline flood by Novassad and Novassad.	9-6

Abstract

The objectives of the research program are to (1) identify and develop polymer systems which have potential to improve reservoir conformance of fluid displacement processes, (2) determine the performance of these systems in bulk and in porous media, and (3) develop methods to predict their performance in field applications. The research focuses on three types of aqueous gel systems - a polysaccharide (KUSP1) that gels as a function of pH, a polyacrylamide-chromium(III) system and a polyacrylamide-aluminum citrate system. This report describes work conducted during the second year of a three-year program. Progress was made in the utilization of KUSP1 as a gelling agent. It was shown that gels can be formed in situ in porous media using CO₂ or ester hydrolysis to lower pH. An ester was identified that could be used in field-scale operations. It was determined that KUSP1 will form strong gels when ortho boric acid is added to the system. It was also determined, in cooperation with Abbott Laboratories, that KUSP1 can be produced on a commercial scale. Rheological studies showed that shear rate significantly affects gelation time and gel strength. The effect of rock-fluid interactions at alkaline conditions was examined experimentally and through mathematical modeling. A model was developed that treats non-equilibrium conditions and this is an improvement over previously published models.

Executive Summary

OBJECTIVES

The general objectives of this research program are to 1) identify and develop gelled polymer systems which have potential to improve reservoir conformance of fluid displacement processes, 2) to determine the performance of these systems in bulk and in porous media, and 3) to develop methods to predict the capability of these systems to recover oil from petroleum reservoirs.

The research focuses on three types of gel systems — an aqueous polysaccharide (KUSP1) system that gels as a function of pH, a chromium-based system where polyacrylamide and xanthan are crosslinked by Cr(III) and a polyacrylamide-aluminum citrate system.

The laboratory research is directed at the fundamental understanding of the physics and chemistry of the gelation process in bulk form and in porous media. This knowledge will be used to develop conceptual and mathematical models of the gelation process. Mathematical models will then be extended to predict the performance of gelled polymer treatments in oil reservoirs.

The project is divided into five major tasks. These are:

- Development and Selection of Gelled Polymer Systems
- Physical and Chemical Characterization of Gel Systems
- Flow and Gelation in Rock Materials
- Mathematical Modeling of Gel Systems
- Sponsor International Forums on Gelled Polymer Treatments

A summary of progress in each task is described in the following sections.

SUMMARY OF PROGRESS

Development and Selection of Gelled Polymer Systems

Research activities focused on development of the KUSP1 polysaccharide gel system, and an examination of the polyacrylamide-aluminum citrate system. The polyacrylamide-aluminum citrate system was selected for study because a suitable organic crosslinked system was not identified.

KUSP1 System. KUSP1 is an unbranched (1→3)- β -D-glucan which is produced by bacterial activity in a simple medium containing an excess of glucose as the carbon and energy source and is deposited as a capsule surrounding the bacterium. The polymer is separated from the capsule by dissolution in 1N NaOH. KUSP1 forms a gel when the pH is reduced to the vicinity of 10.8. The polymer is insoluble in water and organic solvents. The polymer is not toxic.

Microbial polysaccharides have variations in their degree of polymerization, or polydispersivity. Several parameters may influence the polydispersivity, including growth conditions, stage of the culture and activity of the hydrolytic enzymes. For this reason, standardized procedures were sought which yielded

maximum amounts of the polymer. This was accomplished, first with small (500 ml) batch cultures and later with 1-liter table-top fermentors. Results indicated that a 72 hr incubation period was optimum.

Large-scale production of KUSP1 was investigated in cooperation with Abbott Laboratories, North Chicago, Illinois. Fermentation was carried out in a 40,000-liter fermentor vessel which was operated at conditions very similar to those developed from the laboratory optimization study. A yield of 9.1 g (dry weight) of KUSP1 was produced per liter of culture. This was slightly better than the laboratory results.

As stated, KUSP1 forms a gel when the pH is reduced to about 10.8. It was also determined that KUSP1 can be gelled using ortho boric acid, and that gels produced in this manner have improved characteristics over those obtained by the method of simple pH reduction. The ortho boric acid system is being investigated further.

Polyacrylamide-Aluminum System. Gelation behavior was examined using a screen viscometer device and rheological measurements. An experimental apparatus is being developed to measure the growth of gel aggregates in this system.

Physical and Chemical Characterization of Gel Systems

Rheological or kinetic studies were carried out on three gel systems. A study of the effect of shear rate on gelation was conducted using a polyacrylamide-Cr(III) gel. Kinetic studies of the rate of hydrolysis of an ester system were done as a possible way to control pH and thus gel time for the KUSP1 gel system. For the third system, polyacrylamide-aluminum citrate, gelation behavior was examined using a screen-viscometer device. Results of these studies follow.

Rheological Studies (Polyacrylamide-Cr(III) System). Since a gel solution is subjected to shear when it is pumped through a well and into a reservoir rock, the effect of shear on the gelation process was examined. Experiments were performed using cone-and-plate geometry on a Weissenberg R-19 rheometer, and using parallel-plate geometry on a Bohlin CS rheometer. Steady shear experiments and parallel superposition experiments (simultaneous application of oscillatory shear and steady shear) were conducted. Shear rates examined ranged from 0.47 to 47 s^{-1} . The effect of shear on gelation was interpreted primarily from the time-dependent data of shear viscosity, storage modulus and loss modulus. The gel system used was a polyacrylamide crosslinked by Cr(III). Gelation time was measured by two methods which correlated quite well. The first was the time at which the solution viscosity started to increase rapidly, while the second was the time at which the storage modulus and loss modulus curves crossed.

Several general observations resulted from the experiments. There is an induction period during which very small increases in shear viscosity and storage modulus occur. Apparently during this period aggregates formed by the gelation process are small and do not significantly affect the magnitude of the shear viscosity or storage modulus. Following this induction period there is an abrupt increase in the values of the parameters, indicating the onset of gelation. At low shear rates, less than 2.35 s^{-1} , this gel time is decreased as shear rate is increased. Gels formed at higher shear rates were weaker than those formed at low shear rates, and at rates greater than 40 s^{-1} no gels were formed at all.

One problem with the experimental approach was an apparent occurrence of slip at the rheometer platen walls during the latter stages of the gelation process.

Kinetic Studies (KUSP1 System). KUSP1 is a microbial polysaccharide which dissolves in alkaline media and forms a gel when the pH drops to about 10.8. Control of the rate of pH decrease is one way to control the gelation time of this system. A method to decrease the pH in a controlled and predictable fashion is through the use of an ester. Ester hydrolysis is used to produce an acid that reduces the pH. After evaluating many esters, mono-ethyl phthalate (MEP) was found to be suitable for this application. Criteria used to evaluate the esters were cost, ease of preparation, solubility in water, rate of hydrolysis and toxicity.

Experiments were conducted to examine the effects of MEP ester, sodium hydroxide and sodium chloride concentrations on the rate of pH reduction and viscosity increase in KUSP1 solutions. Additional runs in which KUSP1 concentration was varied were also conducted. Data were developed which allow gelation times to be set a priori by proper variation of the system concentrations. These data can be used for design of field implementation of the KUSP1 gel process. A kinetic model is being developed to describe the rate of pH reduction. The current model describes pH reduction in the absence of polymer, but does not satisfactorily describe the process when KUSP1 is present at concentrations required for gelation to occur.

Screen Viscometer Studies (Polyacrylamide-Aluminum System). The polyacrylamide-aluminum citrate system in the form of a colloidal dispersion gel was developed by TIORCO Inc., Englewood, CO. The formulation consists of low concentrations of a partially hydrolyzed polyacrylamide and a chelated aluminum citrate solution. Typical concentrations used in this system are 300 ppm polymer and 15 ppm Al^{3+} . These systems are reported to be slow forming which allows large volumes to be injected during field applications with the intent of altering flow patterns distant from the wellbore. It is speculated that polymer colloids, or gel aggregates, are formed which are then apparently filtered from solution by the rock, thereby reducing the permeability.

Different formulations of this system were analyzed using a screen viscometer type device (TGU apparatus) developed by TIORCO, Inc. Measurements on the device can be used as indicators of gelation time and gel strength. Data were obtained which were consistent with results reported in the literature. It was determined that very small concentrations of chlorine in the solution, on the order of 0.25 ppm, caused the polymer to degrade significantly and inhibited gel formation. Studies are continuing with this system.

Flow and Gelation in Rock Materials

Gelation experiments in porous media were conducted with KUSP1 and with the polyacrylamide-aluminum citrate system. For the KUSP1 system, pH reduction to form a gel was accomplished using either carbon dioxide or hydrolysis of mono-ethyl phthalate ester (MEP). The porous medium used was either an unconsolidated sand or a Berea core. Experiments were also conducted to assess the importance of rock-fluid interactions on pH change.

In Situ Gelation of KUSP1 by CO_2 . KUSP1 gels potentially can be used to increase volumetric sweep efficiency in the CO_2 miscible displacement process. CO_2 will dissolve into high-pH KUSP1 solutions, form an acid and thereby lower the pH. When CO_2 is present in sufficient quantities, the pH will be lowered to the gelation pH, approximately 10.8.

Low pressure experiments and preliminary experiments using CO_2 at supercritical conditions were conducted in Berea cores. A high-pressure core displacement apparatus was constructed for the latter

experiments. The initial results indicate that KUSP1 can be gelled in situ with CO₂ either in gaseous form at low pressure or at CO₂ supercritical conditions. Permeability reduction factors on the order of 3-15 were obtained in these initial experiments at supercritical conditions. Additional runs at supercritical conditions will be made.

In Situ Gelation of KUSP1 Using Ester Hydrolysis. In situ gelation experiments with KUSP1 in unconsolidated sandpacks and Berea cores were carried out in which gelation resulted from lowering of pH through hydrolysis of MEP ester. In these experiments, the permeability of the porous medium was first measured. Then the gel system, including the ester, was injected into the porous medium and allowed to stand for a pre-determined gelation time. After gelation occurred, brine was flowed through the medium and a post-treatment permeability was determined. Permeability was reduced by a factor on the order of 260 in Berea cores and 4700 in unconsolidated sands. Continued flow of brine through the systems has shown that the gels are quite stable, with very little change in permeability occurring over many pore volumes injected.

In Situ Gelation of the Polyacrylamide-Aluminum Citrate System. Experiments were conducted in unconsolidated sandpacks. The polymer solution and aluminum citrate solution were mixed in an in-line mixer located just ahead of the sandpack. Flow rates and the length of the pack were set such that there was sufficient residence time in the packs for gelation to occur. The early experiments were plagued with the formation of gels either on the entry or effluent sand retaining screens. Gels did not form in the sandpack. The problem of the retaining screens and gelation conditions will be addressed in future experiments.

pH Change Resulting from Rock-Fluid Interactions. Since KUSP1 forms a gel when solution pH is lowered sufficiently, the effect of rock-fluid interactions on solution pH was examined. KUSP1 solutions were injected into several porous medium types, including unconsolidated sands, Berea core, and carbonate field cores. In all cases, the initial solution pH was high, at values where KUSP1 is soluble. The systems were allowed to set for long periods of time during which solution pH was periodically measured. In no case was there a significant change in pH which would affect the gelation of KUSP1.

Mathematical Modeling of Gel Systems

A mathematical model was developed to describe the effect of rock-fluid interactions on the pH of alkaline solutions flowing through a sandstone. The model incorporates the kinetics of silica dissolution and sodium/hydrogen ion exchange, and is felt to be an improvement over those previously reported in the literature which are based on an assumption of local equilibrium. The model developed here does not assume local equilibrium exists for silica dissolution.

Model calculations were compared to three independent core-flood experimental sets reported in the literature. In all cases, the calculations exhibited the features seen in the data and agreement between the calculations and data was good. While some parameter adjustment was necessary, consistent and reasonable parameters were used in all cases.

Sponsor International Forums on Gelled Polymer Treatments

We participated in the 1993 Society of Petroleum Engineers Forum on Improvements in Conformance Technology. Professor G. Paul Willhite was on the planning committee of that forum. We are planning to sponsor a forum during fiscal year 1995.

SIGNIFICANT ACCOMPLISHMENTS

Progress was made in the utilization of KUSP1 as a gelling agent. It was shown that gels can be formed in situ in porous media using CO₂ or ester hydrolysis to lower pH. An ester was identified that could be used in field-scale operations. It was determined that KUSP1 will form strong gels when ortho boric acid is added to the system. It was also determined, in cooperation with Abbott Laboratories, that KUSP1 can be produced on a commercial scale. Rheological studies showed that shear rate significantly affects gelation time and gel strength. The effect of rock-fluid interactions at alkaline conditions was examined experimentally and through mathematical modeling. A model was developed that treats non-equilibrium conditions and this is an improvement over previously published models.

SIGNIFICANCE TO EOR RESEARCH PLAN

This research supports the DOE Energy Plan to reduce well abandonment and increase oil recovery from existing fields. Improving oil recovery from conformance control is one of the few technologies that are economic at current oil prices. We anticipate the following developments from our research program: 1) development of KUSP1 as an environmentally acceptable gelation system, 2) development of a data base of gelling systems, 3) correlation of permeability reduction from gelation with composition and rock permeability, 4) prediction of gelation and permeability reduction of selected systems in porous rocks and 6) promotion of dialogue on conformance control in the technical community.

RESEARCH PLANS

We will complete research in areas already in progress. More emphasis will be placed on gathering data on in situ gelation in porous media, on correlation of data and on mathematical modeling.

Chapter 1

Introduction

Principal Investigators: D.W. Green, G.P. Willhite, C.S. McCool,
S. Vossoughi, M.J. Michnick and C.S. Buller

The application of gelled polymer treatments to petroleum reservoirs can improve oil recoveries and reduce fluid-handling costs. This research program consists of a laboratory investigation of chemical systems that are applicable for gelled polymer treatments and the development of mathematical models that describe gelled polymer treatments of oil reservoirs.

The gel systems being studied are (1) KUSP1, a biopolymer which gels as a function of pH or by a borate crosslinker, (2) polyacrylamide-chromium(III), and (3) polyacrylamide-aluminum citrate, a system that forms gel aggregates rather than a bulk gel.

Investigations of the KUSP1 system are presented in Chapters 2 through 6. Progress on the development of KUSP1 and its derivatives is presented in Chapter 2. A kinetic study on the use of an ester to reduce pH and initiate gelation of KUSP1 is presented in Chapter 3. Measurement and long-term stability of permeability reductions by a KUSP1-ester system are presented in Chapter 4. Chapter 5 describes a study on the injectivity of KUSP1 and the potential of fluid-rock interactions to reduce the pH of fluids. An investigation of using supercritical carbon dioxide to trigger gelation of KUSP1 is presented in Chapter 6.

A rheological study of the effect of shear on the gelation of the polyacrylamide-chromium(III) system is presented in Chapter 7. Preliminary results of the investigation of the polyacrylamide-aluminum citrate system are presented in Chapter 8. A mathematical model describing interactions between alkali solutions and sandstone rock was developed. Simulation of core flood experiments by this model and using data from the literature are presented in Chapter 9.

Chapter 2

Development of the KUSP1 Polysaccharide and Derivatives

Principal Investigator: C.S. Buller

INTRODUCTION

KUSP1 is a microbial polysaccharide which was isolated and is being developed at the University of Kansas. It is a (1→3)- β -D-glucan which is produced by *Cellulomonas flavigena*, a non-pathogenic soil bacterium. It is not soluble in water but can be dissolved in alkali. When alkaline solutions of it are neutralized, KUSP1 is precipitated as a hydrogel.¹ This unique trait offers possibilities for use of KUSP1 for subterranean permeability modification by in situ gelation. As an attempt to further develop the potential of KUSP1 for use in enhanced oil recovery procedures we undertook to determine if its versatility could be increased by chemically derivatizing it. Additionally, we sought to identify the affect, if any, of variations in growth conditions on the properties of the polyglucan. Finally, we undertook large scale production of KUSP1 to determine whether its production could become economically feasible.

RESULTS AND DISCUSSION

Chemical modification of KUSP1. Several chemical derivatives of KUSP1 were prepared to determine if they had properties suitable for use in enhanced oil recovery procedures. O-carboxymethyl-KUSP1 was prepared according to a method by Green.² The water soluble reaction product, which was attainable in good yields, could not be induced to form gels.

Attempts were made to produce methyl-, propyl, and ethyl- ethers of KUSP1, by nucleophilic substitution reactions, using alkyl halide as the donor and alkaline KUSP1 as the acceptor. These derivatives also were water soluble and did not form gels.

Determination of effects of growth condition on KUSP1 properties. It is well known that microbial polysaccharides often are polydisperse, i.e., they have variations in their degree of polymerization (DP). A variety of conditions, including growth conditions, stage of the culture, and activity of hydrolytic enzymes, may influence the polydispersity. Since the amount of water in hydrogels formed from KUSP1 may be affected by the DP of the polymer, it was important to standardize procedures which yielded maximum amounts of the polymer. This was accomplished, first with small (500 ml) batch cultures, and subsequently with 1 liter table top fermentors. Under the conditions optimized for batch cultures, the maximal yield of KUSP1 obtained after 72 hours of incubation was 9 gms (dry weight) per liter of culture. Although longer incubation times sometimes resulted in slightly larger yields, a 72 hr incubation period was chosen for the standard procedure. Longer incubation periods increased the risk of culture contamination and the chance for development of hydrolytic enzymes was increased. When *C. flavigena* is incubated for prolonged periods in the presence of KUSP1 it begins to produce extracellular (1→3)- β -D-glucanases. Such enzymes, especially those which are endoglucanases, can lower the DP of cell-free KUSP1. These enzymes are also synthesized under conditions in which *C. flavigena* is synthesizing the capsular KUSP1. Fortunately, however, such enzymes remain cell bound and do not significantly alter the polysaccharide during the 72 hour incubation period. If cultures are incubated substantially longer than 72 hours some of the cells autolyze and glucanases are released from the cell.

Large-scale production of KUSP1. Abbott Laboratories, North Chicago, Illinois, was contracted for the scale-up of growth procedures of *Cellulomonas flavigena*, under conditions leading to the production of KUSP1. Some of the results of such a large scale fermentor culture are shown in Table 2.1. The process was carried out in a 40,000 liter multipurpose fermentor vessel, operated under conditions which were very similar to those procedures which had been developed and standardized for flask cultures and 1 liter table top fermentors (Task 1.1.3.). The fermentation process was carried out for 72 hours. Table 2.1 indicates that 9.11 gms (dry weight) of KUSP1 was produced per liter of the culture. That yield is slightly better than could be obtained in small batch cultures operated under optimal conditions. This is very encouraging, since simple scale-up of volume usually results in substantial decreases in product yields.

CONCLUSIONS

There is an extensive literature on the preparation and properties of ethers of cellulose.³ Because of the similarity of KUSP1 ((1→3)- β -D-glucan) to cellulose ((1→4)- β -D-glucan), most of the procedures developed for cellulose could readily be modified for production of methyl-, propyl, and ethyl- ethers of KUSP1. All were water soluble and none produced hydrogels.

The growth conditions developed for small laboratory scale fermentors and for shake batch cultures, proved to be suitable for use in large scale (40,000 liter) cultures. Even so, it is not possible to make useful estimates of the cost of production of KUSP1 on a commercial scale. However, if KUSP1 is found to have important industrial applications, and if there is a large scale demand for it, then there will be extensive scale-up efforts, and fermentors dedicated to the growth of *C. flavigena* will be designed. *Cellulomonas flavigena* can be grown in inexpensive media, and growth yields can be similar to those obtained for the cost efficient production of xanthan gum by *Xanthomonas campestris*.

REFERENCES

1. Buller, C.S. and K.C. Voepel, "Production and Purification of an Extracellular Polyglucan Produced by *Cellulomonas flavigena*," *J. Ind. Microbiol.*, 5 (1990) 139-146.
2. Green, J.W. "O-Carboxymethylcellulose," From *Methods in Carbohydrate Chemistry, Vol III*, R.L. Whistler, J.W. Green, and J.N. BeMiller (eds.) Academic Press (1963) 322-327.
3. Nicholson, M.D. and F.M. Merritt, "Cellulose Ethers," Ch. 15, From *Cellulose Chemistry and its Applications*, T.P. Newell and S.H. Zeronian (eds), Ellis Horwood LTD (1985) 363-383.

Table 2.1: Growth of *Cellulomonas flavigena* in 40,000-liter vessels.

Age of culture (hrs)	Residual Glucose (gm/liter)	Packed cell volume (% of culture)	Glucan (gm/liter of culture)
0	27.7	-	-
12	26.3	0.7	0.12
24	21.3	3.5	0.65
36	16.5	5.5	2.48
48	11.8	5.4	4.60
60	6.8	5.3	6.72
72	4.4	5.5	9.11

The minimal salts culture medium, designated as CM9, was of the following composition (g/l): KH₂PO₄, 3.18; K₂HPO₄, 5.20; MgSO₄, 0.12; yeast extract (Difco), 0.50. NH₄Cl was used as a nitrogen source. The pH of the medium was adjusted to 6.8. Corn syrup, which was sterilized separately, was added to a final concentration of 2.8% (w/v).

Chapter 3

Gelation of KUSP1 by Ester Hydrolysis

Principal Investigators: Don Green, Paul Willhite, Stan McCool
Graduate Research Assistant: Ashok Fichadia

INTRODUCTION

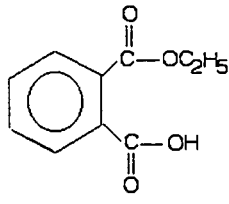
KUSP1 is a microbial polysaccharide which dissolves in alkaline media. The solution gels when the alkaline medium is neutralized to an extent where the pH is around 10.8 or lower. This change of KUSP1's physical state from a solution to a gel is the basis for potential use in permeability modification treatments applied to oil reservoirs.

The reduction in pH can be achieved by a variety of methods including bubbling carbon dioxide through the solution or adding acid, both of which produce gels. A method to decrease the pH in a controlled and predictable fashion is through the use of an ester. The ester hydrolyses to produce an acid that reduces the pH. After evaluating many esters, mono-ethyl phthalate (MEP) was found to be suitable for this application. Criteria used to evaluate the esters were cost, ease of preparation, solubility in water, rate of hydrolysis and toxicity.

The objective of work described in this chapter was to determine the applicability of using MEP to gel bulk KUSP1 solutions. This was accomplished by investigating the effect of component concentrations on the rate of gelation. A mathematical model of the kinetics describing the pH reduction was developed and tested against the experimental data.

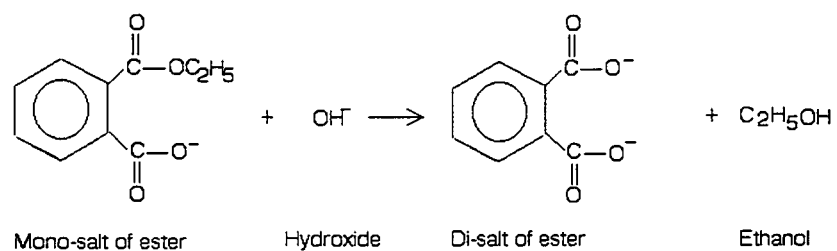
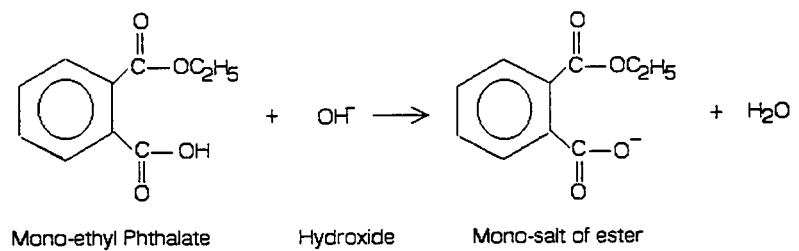
BACKGROUND

The chemical structure of the MEP ester is



Mono-ethyl Phthalate

Two acid groups are made available when MEP is added to an alkaline solution according to the following reactions.



The first reaction is fast and results in an immediate drop in the pH of the solution. Ester hydrolysis shown by the second reaction is rate-limiting and produces a slow reduction in pH. Hydrolysis of MEP provides the means to control the rate of gelation of KUSP1.

EXPERIMENTAL

KUSP1 polymer stock was received as a wet gel at neutral pH and at concentrations of approximately 4 weight percent. The stock gel also contained 0.2% sodium azide to prevent microbial growth.

MEP was prepared by dissolving phthalic anhydride in ethanol at a mole ratio of 1:3, respectively. The mixture was incubated at 45 °C for 24 hours. It was assumed that all the anhydride was converted to MEP ester.

Samples were prepared in two steps. First, polymer solutions were prepared by mixing appropriate amounts of stock gel, NaOH, water and, in some cases, NaCl. The stock gel dissolved in the alkaline solution. The second step was the addition of the appropriate amount of MEP solution to the polymer solution. Gel formed around each drop of the MEP solution as it was added to the polymer solution. The gel formed due to the localized low pH surrounding the drop which, in turn, was a result of the first reaction described above. The samples were stirred for two minutes after MEP addition to dissolve the gel drops and to ensure adequate mixing. A drop in pH of the sample would occur during this mixing step. Samples were maintained at 25 °C by a waterbath.

Viscosity and pH of the samples were determined as a function of time. The pH of the sample was measured using a Fisher Accumet pH meter equipped with a combination electrode. In some runs, the pH was electronically recorded through a data acquisition system. Small aliquots of the sample were withdrawn periodically to determine viscosity. Measurements were performed on a Brookfield microviscometer equipped with a cone-and-plate geometry.

RESULTS AND DISCUSSION

Preliminary experiments showed that the initial mole ratio of MEP ester to NaOH was a key parameter for the gelation of KUSP1. Mole ratios less than or equal to 0.4 would not produce gelation while immediate gelation occurred at mole ratios greater than 1.0. These results were consistent with the reaction sequence described above in that two acid groups are supplied by the ester.

A series of samples was prepared with selected concentrations of polymer, MEP ester, sodium hydroxide and sodium chloride in order to determine the effect of each component on the pH and viscosity behavior. Compositions of these systems are shown in Table 3.1. The concentration of MEP ester was adjusted so that the initial mole ratios between the ester and NaOH were set at 0.75 and 0.5.

The effect of ester concentration on the gelation of KUSP1 is shown in Figure 3.1 for samples containing 2.0% KUSP1 and 1.0 mole NaOH per kg solution. The initial pH of these samples was 13.2 before addition of the MEP ester solution. An immediate drop in pH was observed with the addition of ester at time equal to zero. Thereafter, the pH values decreased with time. As the pH of the sample containing the MEP/NaOH molar ratio of 0.75 decreased to approximately 10.8, the viscosity increased sharply. The gel time for this sample was 8.6 hours. Similar behavior was observed for the sample containing the MEP/NaOH molar ratio of 0.5, but at a slower rate resulting in a gel time of 64 hours. Higher ester concentrations increased the rate at which the pH dropped and decreased the gel time. Gel times for all the samples are given in Table 3.1.

The effect of polymer concentration on the gelation behavior is shown in Figure 3.2. The initial pH drop that accompanied the ester addition was greater at higher polymer concentration. Thereafter, the pH profiles were similar. The initial viscosity of the 3.0% KUSP1 sample was approximately 60 cp, significantly higher than the samples containing 1.0% and 2.0% polymer. The high viscosity indicated some initial gel structure which likely led to a faster increase in viscosity in comparison to the lower polymer concentrations. The viscosity of the 3.0% KUSP1 sample is probably too high for field treatments. Samples with 1.0% and 2.0% polymer gelled at similar times, between 8 and 10 hours.

The effect of NaOH concentration on the gelation of KUSP1 was determined by preparing samples containing 2.0% KUSP1 and maintaining the ester/NaOH molar ratio constant. Figure 3.3 presents pH and viscosity data for samples containing 1.0, 0.316 and 0.10 N NaOH at a ester/NaOH molar ratio of 0.75. The data show that at constant ester/NaOH ratio, samples containing higher concentrations of NaOH and ester gelled sooner even though the initial pH after mixing was higher.

Some samples were prepared with 2.0% NaCl to determine if added salt would affect the gelation behavior. Typical data for similar samples with and without NaCl are shown in Figure 3.4. Added salt had no significant effect on the rate of pH drop or the development of viscosity.

Table 3.1: Composition of Samples and Gel Times.

Run #	KUSP1 concentration (wt. %)	NaOH concentration (moles/liter)	MEP ester concentration (moles ester / mole NaOH)	NaCl concentration (wt. %)	Gel time (hours)
1	0.0	1.0	0.75	0.0	No gel
2	"	"	0.50	"	"
3	"	0.316	0.75	"	"
4	"	"	0.50	"	"
5	"	0.10	0.75	"	"
6	"	"	0.50	"	"
7	1.0	1.0	0.75	0.0	9.0
8	"	"	0.50	"	118.0
9	2.0	1.0	0.75	0.0	8.5
10	"	"	0.75	2.0	8.6
11	"	"	0.50	0.0	64.0
12	"	"	0.50	2.0	62.0
13	"	0.316	0.75	0.0	9.5
14	"	"	0.75	2.0	10.5
15	"	"	0.50	0.0	33.0
16	"	"	0.50	2.0	29.0
17	"	"	0.40	0.0	No gel
18	"	"	0.40	2.0	No gel
19	"	0.10	0.75	0.0	17.0
20	"	"	0.50	"	64.0
21	3.0	1.0	0.75	0.0	6.5
22	"	"	0.50	"	45.0

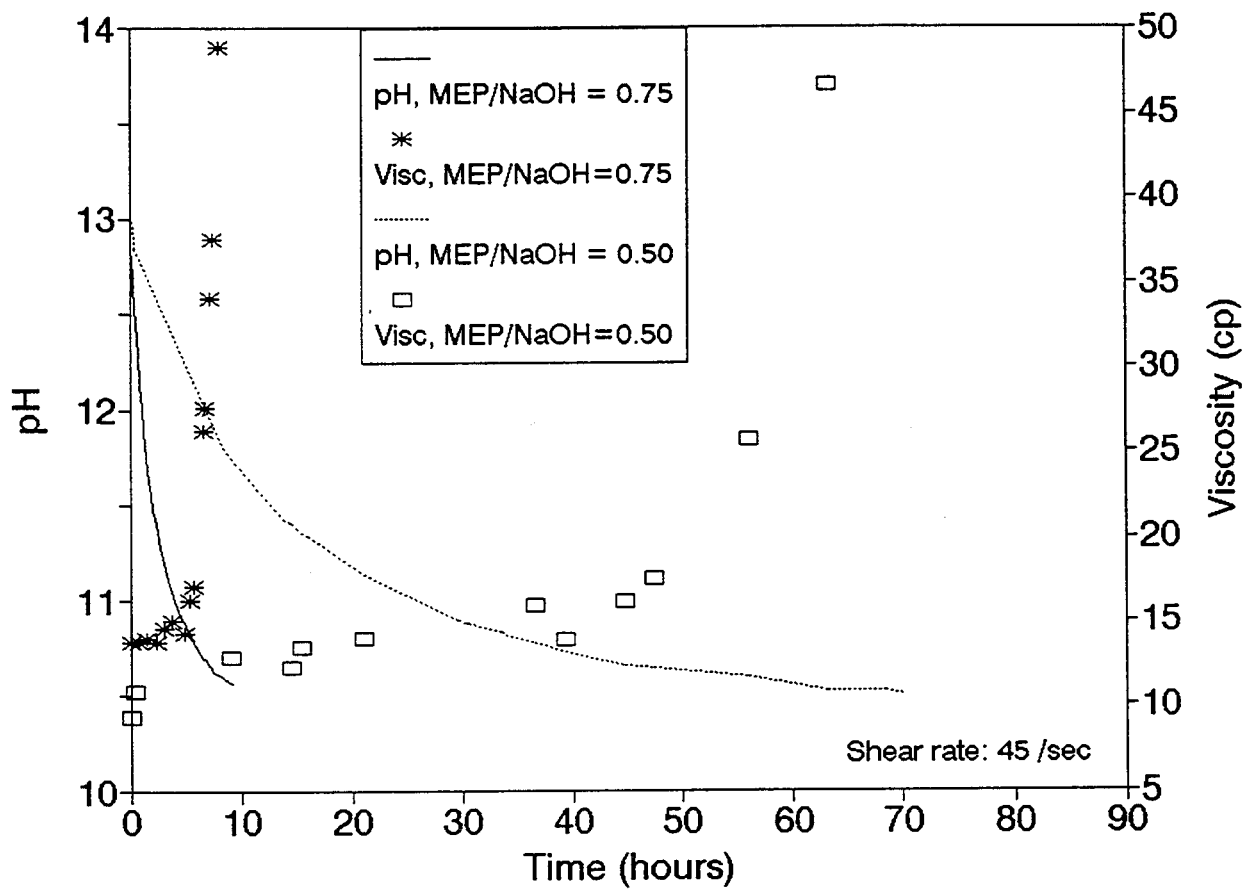


Figure 3.1: Effect of Ester Concentration on Viscosity and pH Behavior.
 2.0% KUSP1, 1.0 N NaOH, and 0% NaCl.
 $\text{MEP/NaOH} = >$ mole ratio of ester to NaOH.

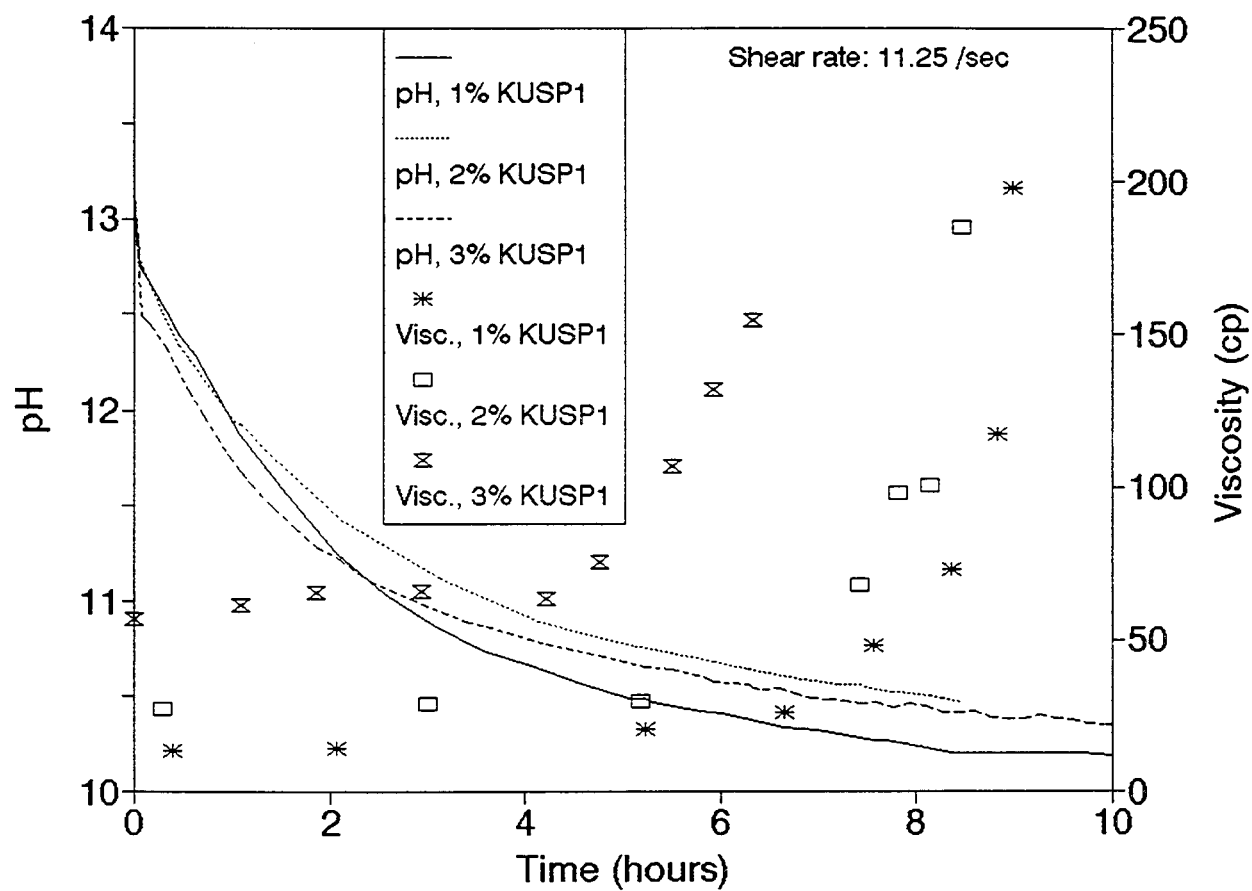


Figure 3.2: Effect of KUSP1 Concentration on Viscosity and pH Behavior.
 1.0 N NaOH, 0.75 moles MEP/mole NaOH and 0% NaCl.

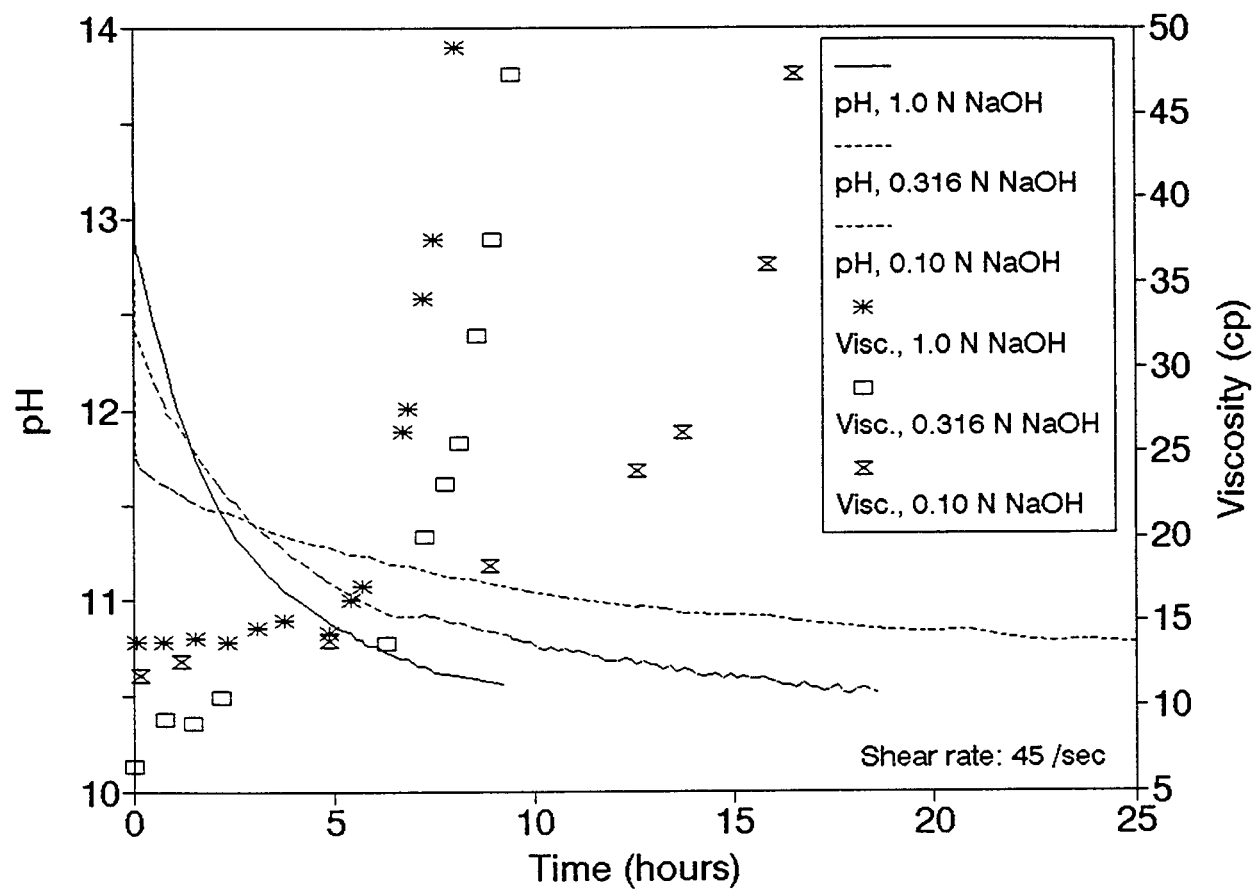


Figure 3.3: Effect of NaOH Concentration on Viscosity and pH Behavior.
2.0% KUSP1, 0.75 moles MEP/mole NaOH and 0% NaCl.

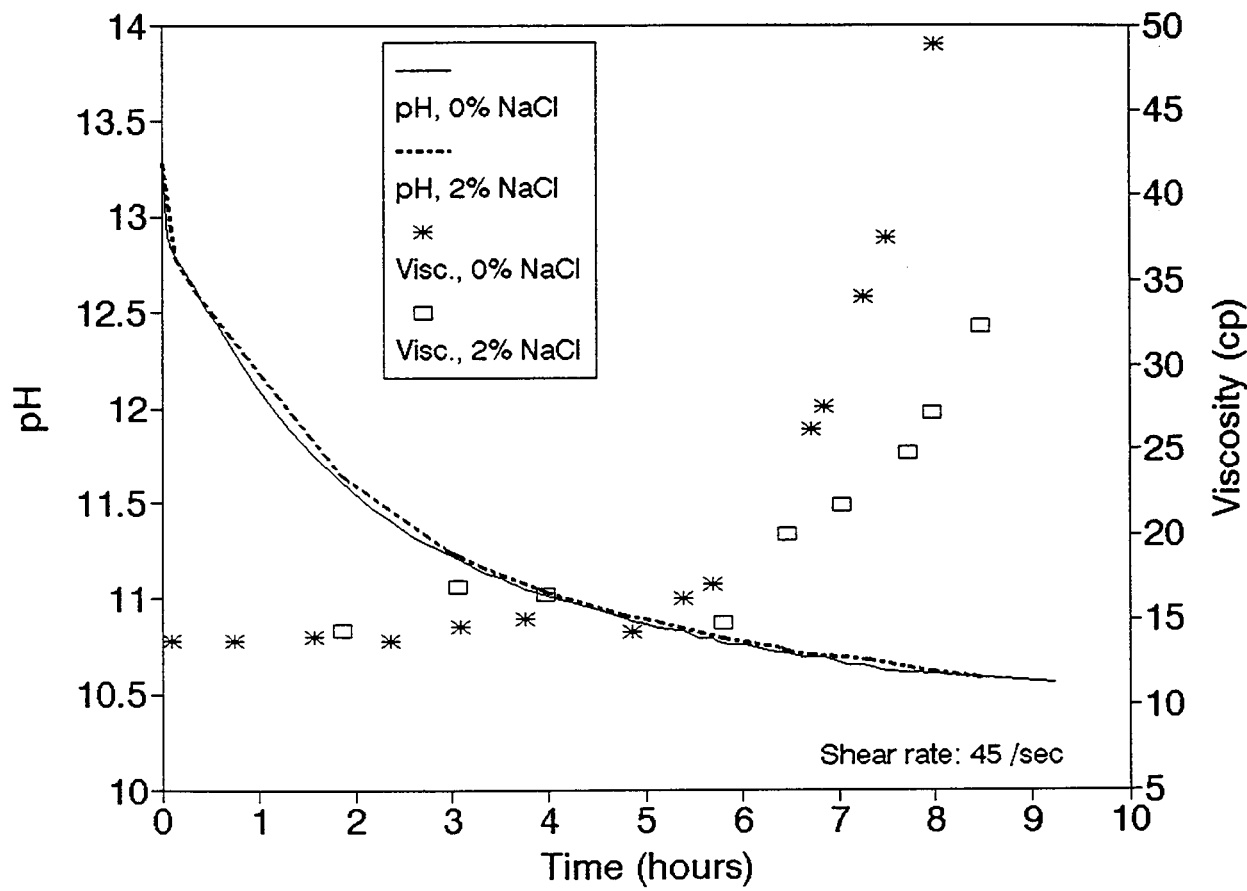


Figure 3.4: Effect of NaCl Concentration on Viscosity and pH Behavior.
2.0% KUSP1, 1.0 N NaOH, and 0.75 moles MEP/mole NaOH.

KINETIC MODELING

The reaction between the MEP ester and NaOH was modeled assuming that the rate of reaction was first order in both NaOH concentration (C_A) and MEP concentration (C_B). The ordinary differential equation describing the kinetics was

$$\frac{dC_A}{dt} = -k * C_A * C_B \quad (3.1)$$

The stoichiometry of the reaction between MEP (after the initial pH drop) and NaOH is

$$C_{A0} - C_A = C_{B0} - C_B \quad (3.2)$$

An analytical solution for Equations 3.1 and 3.2 (when C_{A0} does not equal C_{B0}) is

$$C_A = \frac{C_{A0} * \delta * \exp(-k*\delta*t)}{C_{B0} - C_{A0} * \exp(-k*\delta*t)} \quad (3.3)$$

$$\text{where } \delta = C_{B0} - C_{A0}$$

The concentration of NaOH and pH are predicted knowing C_{A0} and C_{B0} , the initial concentrations at time $t=0$. C_{B0} was determined from the amount of ester added and the volume of the system. C_{A0} was determined from the pH value measured after the addition of ester to the solution and the subsequent drop in pH. The measured pH was converted to C_{A0} via a calibration curve.

The model was applied to data obtained for six samples that were prepared without polymer (see Table 3.1 for compositions). The value of rate constant k was varied until the calculated pH profile matched the experimental data. The criterion for checking the validity of the model was that the rate constant be the same for all data sets. Typical results are shown in Figures 3.5 and 3.6 for initial NaOH concentrations of 1.0 N and 0.316N and a MEP/NaOH molar ratio of 0.75. Figure 3.5 shows calculated and measured NaOH concentration as a function of time. The same data in terms of pH are presented in Figure 3.6. The model represents the experimental data reasonably well with a reaction constant, k , of 5.0 liter/mole/sec.

The kinetic model did not give satisfactory simulations of the pH profile for solutions containing polymer. A single value of the rate constant did not match all the sets of experimental data. Interactions between the KUSP1 polymer with NaOH and MEP ester need to be incorporated in the model. However, these interactions are not understood at present.

CONCLUSIONS

The following conclusions were drawn from this study.

1. The KUSP1 polymer can be gelled in a predictable and controlled manner using the MEP ester.
2. Gel times ranging from instantaneous to a few days can be achieved using the KUSP1-MEP system.
3. The gel time decreased with increasing polymer concentration, MEP concentration and NaOH concentration. Added NaCl had an insignificant effect on pH drop or viscosity buildup.
4. Kinetic modeling predicted the pH profile well for solutions that did not contain polymer. However, the model did not satisfactorily describe the pH profile in solutions containing polymer.

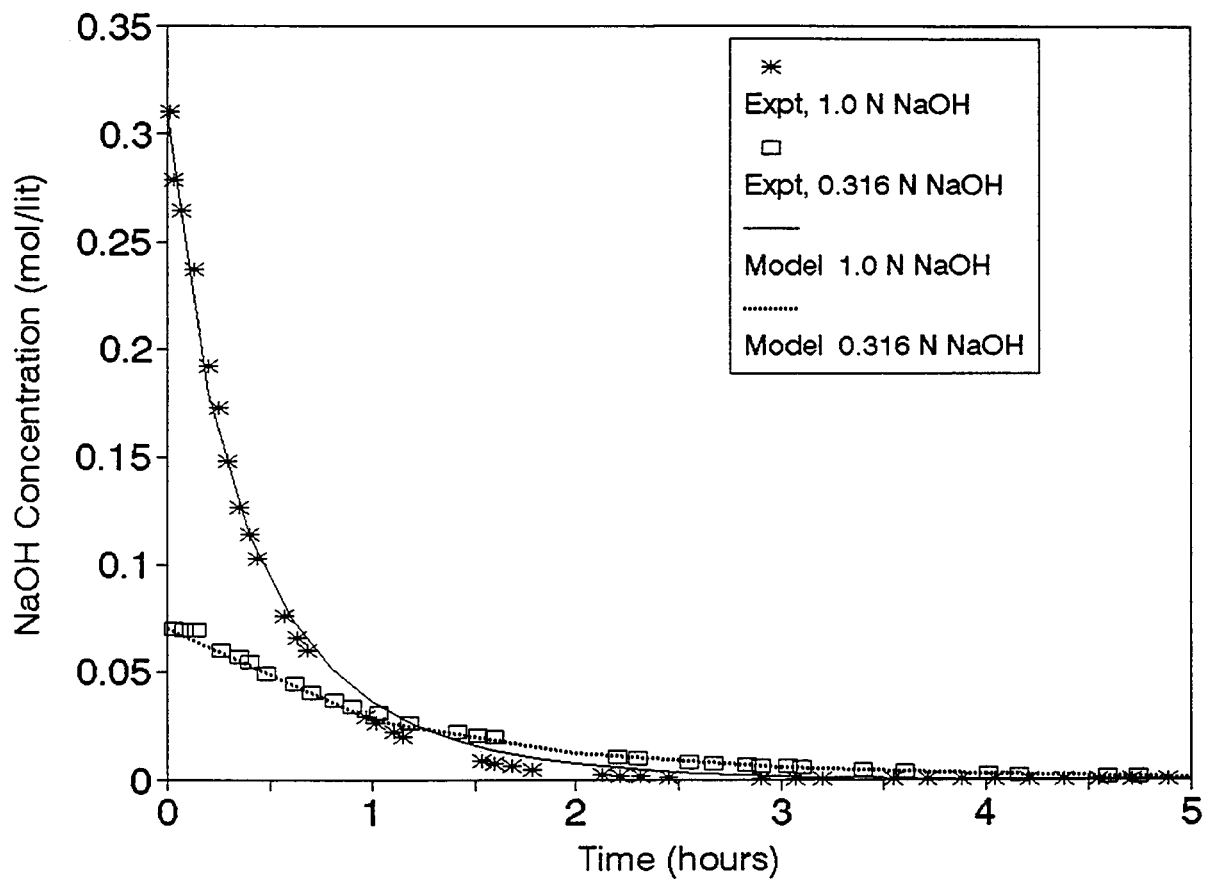


Figure 3.5: Simulated and Measured NaOH Concentration as a Function of Time.
0% KUSP1, 0% NaCl and 0.75 moles of MEP/mole NaOH.

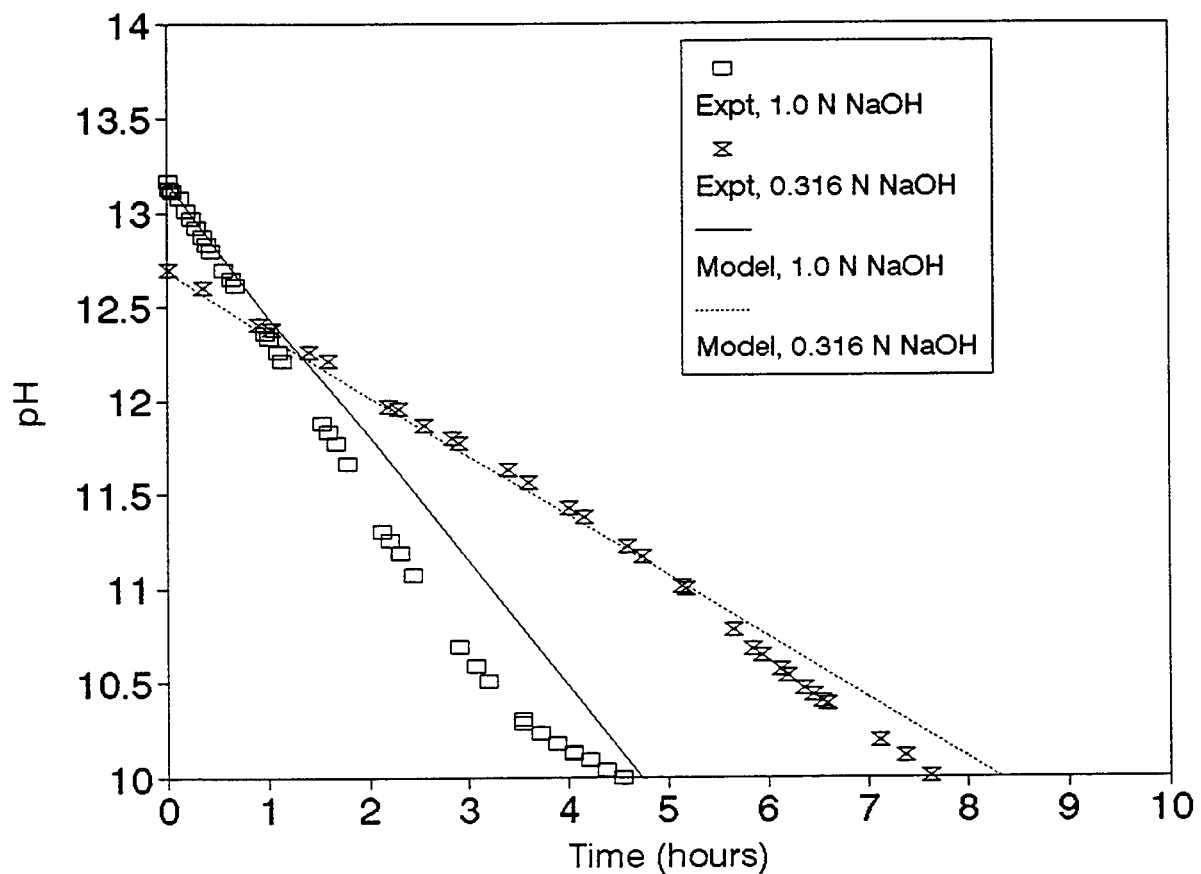


Figure 3.6: Simulated and Measured pH as Function of Time.
0% KUSP1, 0% NaCl and 0.75 moles of MEP/mole NaOH.

Chapter 4

Permeability Modification by In Situ Gelation of a KUSP1-Ester System in Porous Media

Principal Investigators: G.P. Willhite, D.W. Green and C.S. McCool

Graduate Research Assistant: Ajay Kumar Shaw

INTRODUCTION

The polymer system investigated in this phase of the research work is composed of a biopolymer (KUSP1) and an ester (monoethyl phthalate, MEP). KUSP1 is obtained from the bacterium - *cellulomonas flavigena*. An alkali solution of this polymer forms a gel when its pH is lowered to a value of about 10.8. The pH of the solution is reduced over a selected time interval by an ester hydrolysis reaction.

The purpose of this work was to determine the magnitude of permeability reduction produced by the gelation of the KUSP1-ester system. The effectiveness and long-term stability of the treatments in sandpacks, Berea cores and field cores were to be investigated.

EXPERIMENTAL

Preliminary bottle tests were conducted to determine the behavior of the gel system in bulk form and to determine a suitable formulation for testing in porous media. Viscosity and pH were monitored for samples that were prepared at selected concentrations. The gel time of the sample was defined as the time at which the viscosity increased rapidly.

Flow experiments were conducted in sandpacks and Berea cores using the following procedure.

1. The porous medium was prepared.

Sandpacks - One-foot long, 1.5" ID holders with pressure ports spaced 2" along the length were packed with sand. Wedron Silica sand and Oklahoma #1 sand were used for Sandpacks 1 and 2, respectively.

Berea cores - One-foot long, 2"x 2" cross-section Berea cores were fitted with endplates and coated with epoxy. Pressure ports were installed along the length at 2" intervals.

2. The sandpack or Berea core was saturated with brine and the porosity was determined gravimetrically.

Permeabilities of the total medium and of each section were determined. A tracer test was conducted to evaluate the flow characteristics of the medium. The tracer was a step change in salt concentration.

3. The sandpack or Berea core was saturated with 0.1 N NaOH solution. Approximately two pore volumes of gel solution were injected through the porous medium over a period of about an hour. The injection was completed in much less time than the bulk gelation time of approximately 35 hours. Solution injected in the Berea cores contained 1.0% NaCl and no salt was added to the solutions injected in the sandpacks.

4. The sandpack or Berea core was shut-in for three to four days to allow gelation to occur.

5. Brine (water for sandpacks) was injected to determine the post-treatment permeabilities. A tracer test was conducted to assess changes in the flow characteristics of the medium produced by the treatment.
6. Fluid was injected through the sandpack or Berea core using a constant head of fluid and measuring the flow rate. The long-term stability of the treatment was assessed by determining the permeability as a function of time over a period of many weeks.

RESULTS and DISCUSSION

Bottle tests. The purpose of the first series of bottle tests was to determine the pH-time behavior of solutions containing the MEP ester. Solutions were prepared that contained 0.1N NaOH and selected concentrations of the MEP ester. The solutions were maintained at 25 °C. The pH was measured as a function of time and is shown in Figure 4.1 for different MEP ester concentrations. Acid is produced by the hydrolysis of the ester which reduces the pH. Since the KUSP1 polymer gels at a pH of 10.8, the results indicated that gelation would occur for MEP concentrations of 0.05 M and greater for solutions prepared with 0.1 N NaOH.

A second series of bottle tests were conducted with solutions that contained 2.0% KUSP1 polymer. These bottle tests were conducted to determine a suitable formulation for testing in porous media. Samples were prepared in 1.0 and 0.1 N NaOH and contained MEP ester at mole ratios of ester-to-NaOH of 0.6 and 0.75. Viscosity and pH as a function of time were measured. These data for a sample containing 0.1 N NaOH and 0.06 M MEP ester are shown in Figure 4.2. At 30 hours, the pH had declined to a value of approximately 10.8 and the viscosity had increased rapidly indicating gelation. This formulation was selected for study in the flow experiments. Gel times of 10 to 20 hours were observed for solutions that contained 0.75 moles of ester per mole of NaOH.

Flow experiments. Three gel treatments in porous media have been performed to date, two in sandpacks and one in a Berea core. The gel solution contained 2.0% KUSP1 polymer, 0.1 N NaOH and 0.06 M MEP ester. Solutions injected into the Berea core also contained 1.0% NaCl.

Development of flow resistance was not observed during the injection of the gel solutions as shown by the pressure drops measured during the injection of the gel solution in sandpack #1 in Figure 4.3. The pressure drop increased as the more viscous gel solution displaced the resident water through each section. Consistent gelation behavior was observed between the injected solution and effluent samples collected after one pore volume had been injected. After the gelation of these samples, post-treatment permeabilities were measured. The permeabilities of the sandpacks or Berea core were reduced significantly by the gel treatments as shown in Table 4.1. Pressure drops measured across 2-inch long sections of the porous media showed that the permeability reduction was uniform along the length. The difference in the magnitudes of the permeability reduction between the two sandpacks was attributed to changes in the preparation of the polymer stock solution.

Flow characteristics of the porous media before and after the gel treatment were interpreted from tracer tests. Tracer concentrations in the effluent for tests conducted with the Berea core are shown in Figure 4.4. Comparison of the tracer profiles showed that brine injected after the gel treatment contacted 90% of the pore volume even though the permeability was reduced by a factor of 290. This indicated that the

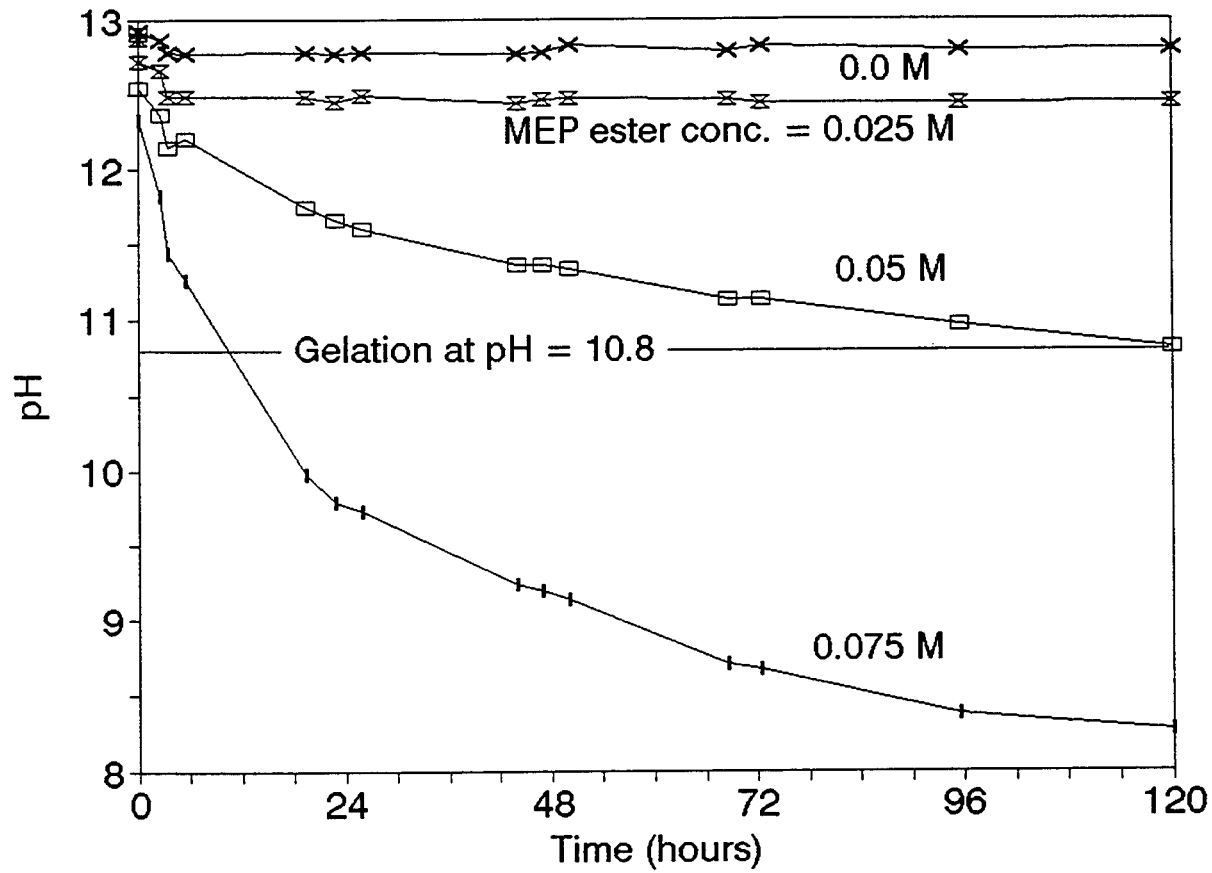


Figure 4.1: Controlled pH Reduction by Hydrolysis of MEP Ester.
Initial NaOH Concentration was 0.10 N.

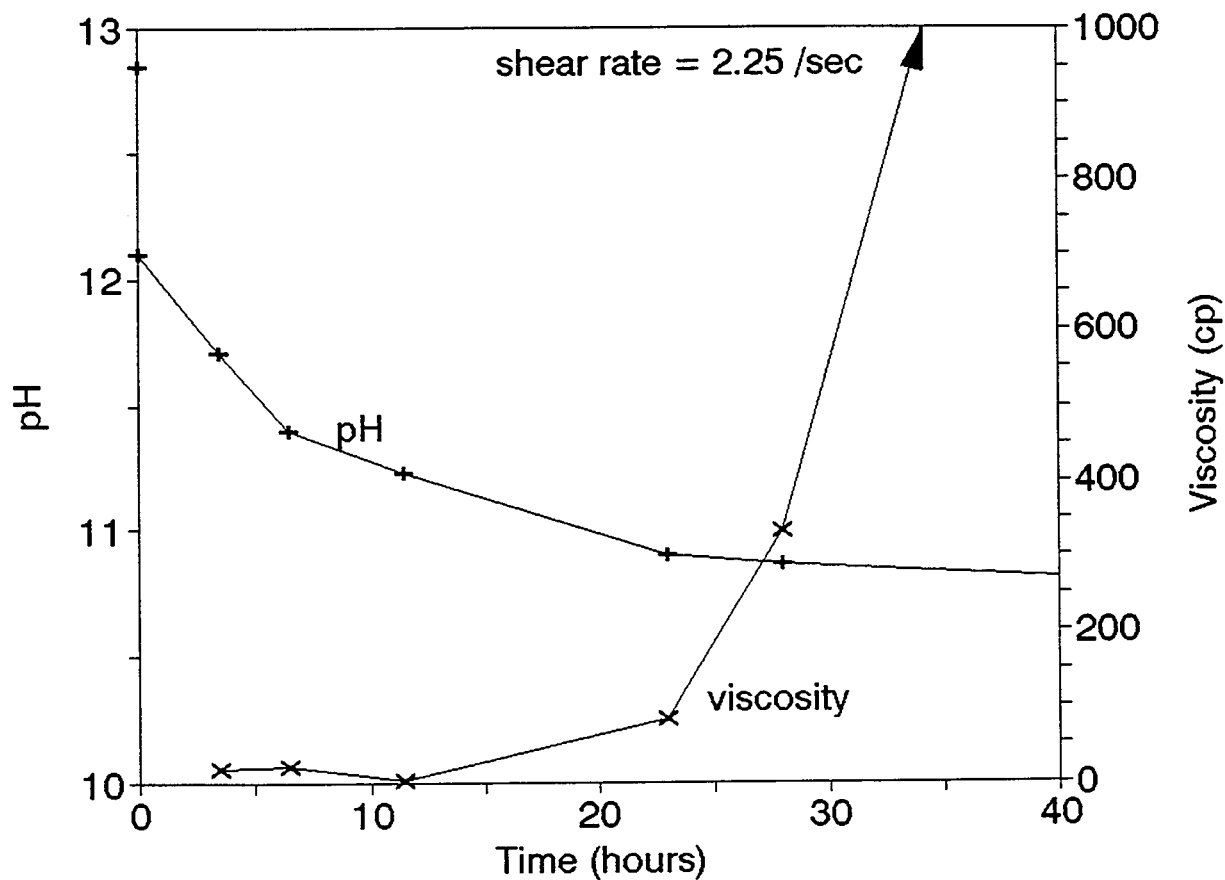


Figure 4.2: Gelation Induced by pH Reduction.
Initial Concentrations - 0.10 N NaOH, 0.06 M MEP Ester.

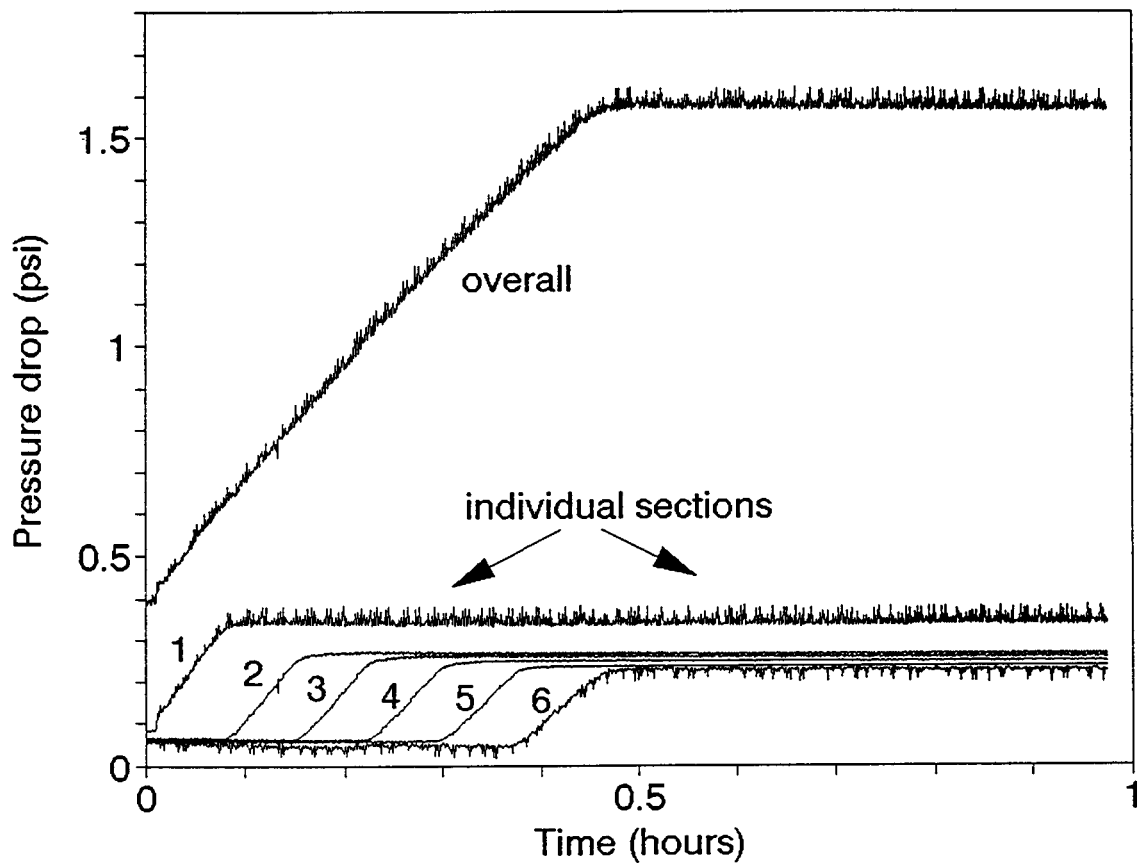


Figure 4.3: Pressure Drops During Injection of Gel Solution in Sandpack #1.

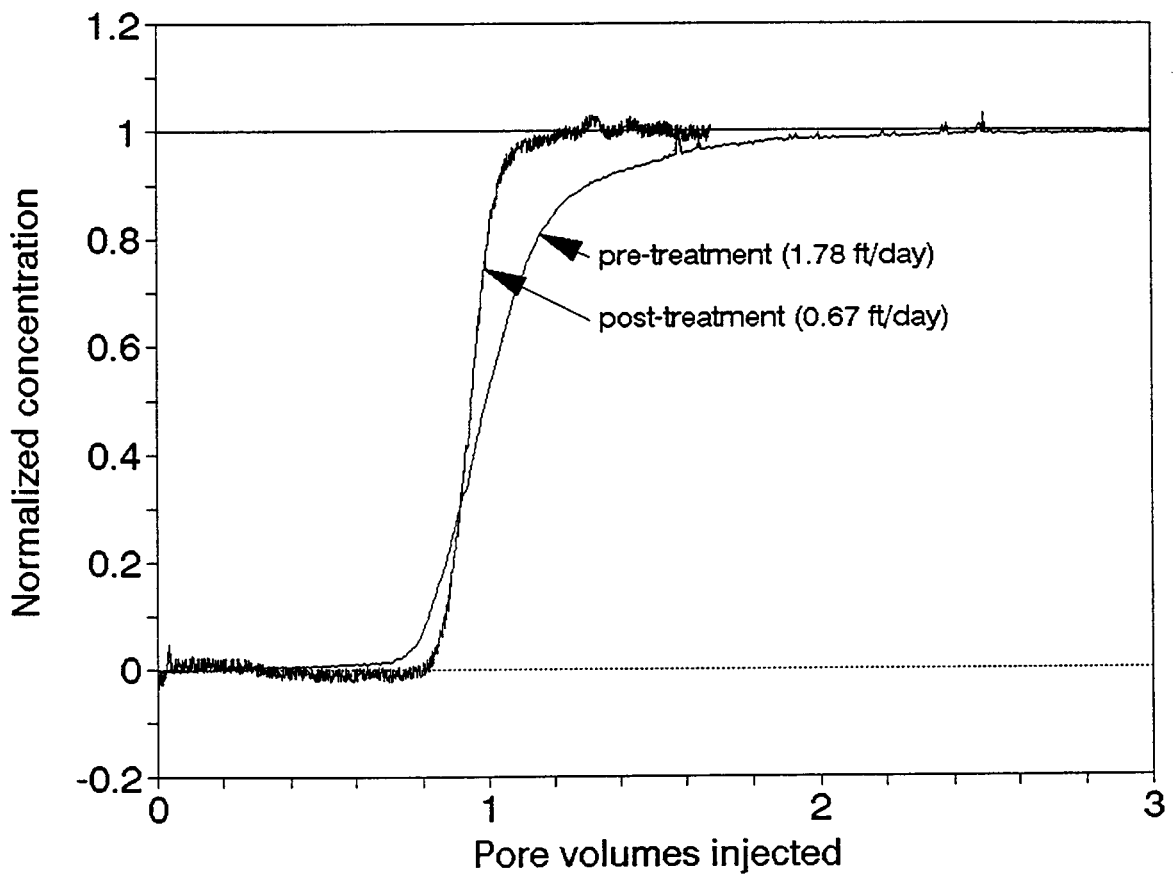


Figure 4.4: Tracer Concentrations in Effluent During Pre- and Post-treatment Tests.

Table 4.1 : Permeability Reductions Using KUSP1-Ester Gelant.

	Pre-Treatment Permeability, k_i (md)	Post-Treatment Permeability, k_f (md)	Permeability Reduction Factor k_f/k_i
Sandpack #1	8700	34	260
Sandpack #2	9400	2.0	4700
Berea #1	160	0.54	290

brine in the gel structure was mobile. The injected tracer solution flowed through the gel displacing the brine originally held in the gel structure.

Stability of the permeability-reduction treatments is being assessed by continuously injecting brine under a constant head and measuring the flow rate. Preliminary results show that the gel is quite stable. For example, over 200 pore volumes of brine were flowed through sandpack #1 over a period of 3 months without a change in permeability.

FUTURE PLANS

Permeability reduction by the gelation of the KUSP1-ester system will be tested in carbonate core material. The effect of a residual oil saturation on the gelation and long-term stability of the KUSP1-ester system will be examined.

Chapter 5

Rock-Fluid Interaction and Injectivity of KUSP1 in Porous Media

Principal Investigators: G.P. Willhite, D.W. Green and M.J. Michnick
Graduate Research Assistant: Saibal Bhattacharya

INTRODUCTION

KUSP1 is a biopolymer, (1→3)- β -d-glucan, which is soluble in sodium or potassium hydroxide above pH 11 and forms a gel at pH values between 11 and 10.8. Alkaline solutions of KUSP1 capable of forming gels have solution viscosities on the order of 3-5 cp and thus can be injected at low injection pressures. This polymer is being studied for in situ modification of reservoir permeability to improve sweep efficiency of secondary and tertiary oil recovery processes. KUSP1 is not toxic and does not rely upon metal ions to promote gelation. To attain in situ permeability modification, a KUSP1 solution has to be injected into the reservoir to significant depths at reasonable surface injection pressures and without appreciable loss of the polymer as it propagates through the porous media. However, a mechanism that will cause the pH of the injected polymer solution to decrease to less than 11 is required for in situ gelation.

Several mechanisms of reducing pH to attain in situ gelation of KUSP1 are being evaluated in this project. The research described in this chapter was carried out to determine if interactions between alkaline solution containing KUSP1 and representative reservoir rock would reduce the pH of the injected fluid to levels required for in situ gelation.

RESULTS AND DISCUSSION

The initial experimental plan was based upon injection of KUSP1 solutions containing 1.0 M and 0.1 M sodium hydroxide into sandpacks and representative core materials to determine the effects of fluid-rock interaction on the polymer and the pH of the resident polymer solution. However, this plan was modified when it was discovered that the injection of KUSP1 solutions into Berea cores resulted in the development of large pressure drops in the front section of the rocks. Figures 5.1 and 5.2 show the pressure drops, in terms of apparent viscosity, in Berea cores upon injection of an unfiltered KUSP1 solution containing 1.0% polymer, 0.1 M sodium hydroxide and 1% sodium chloride. Apparent viscosities were calculated by Darcy's Law using the initial permeability of the section. The increase in the apparent viscosity of the injected fluid in the first section as compared to subsequent sections revealed a potential problem with KUSP1. This suggested that the KUSP1, as received, contained material that was not dissolved. Consequently, the research program was expanded to include identification of the causes of front-end loading.

Injectivity of KUSP1 solutions in porous media. Filtration of the biopolymer solution through a 5-micron filter did not eliminate the front-end loading problem. Filtration tests at constant pressure using 5-micron filters determined that the pressure increase was caused by the accumulation of a small amount of debris from the KUSP1 solution. A series of filtration tests at constant flow rates showed the addition of sodium chloride enhanced the formation of an insoluble component in the KUSP1 solution in agreement with an earlier work by Kolodziej.¹ A method to remove the insoluble material from the KUSP1 solution was required. Different methods of pre-filtration of the polymer solution were tried before injecting the KUSP1 solution into short Berea plugs. The addition of carbon black and filter aid to the KUSP1 solution

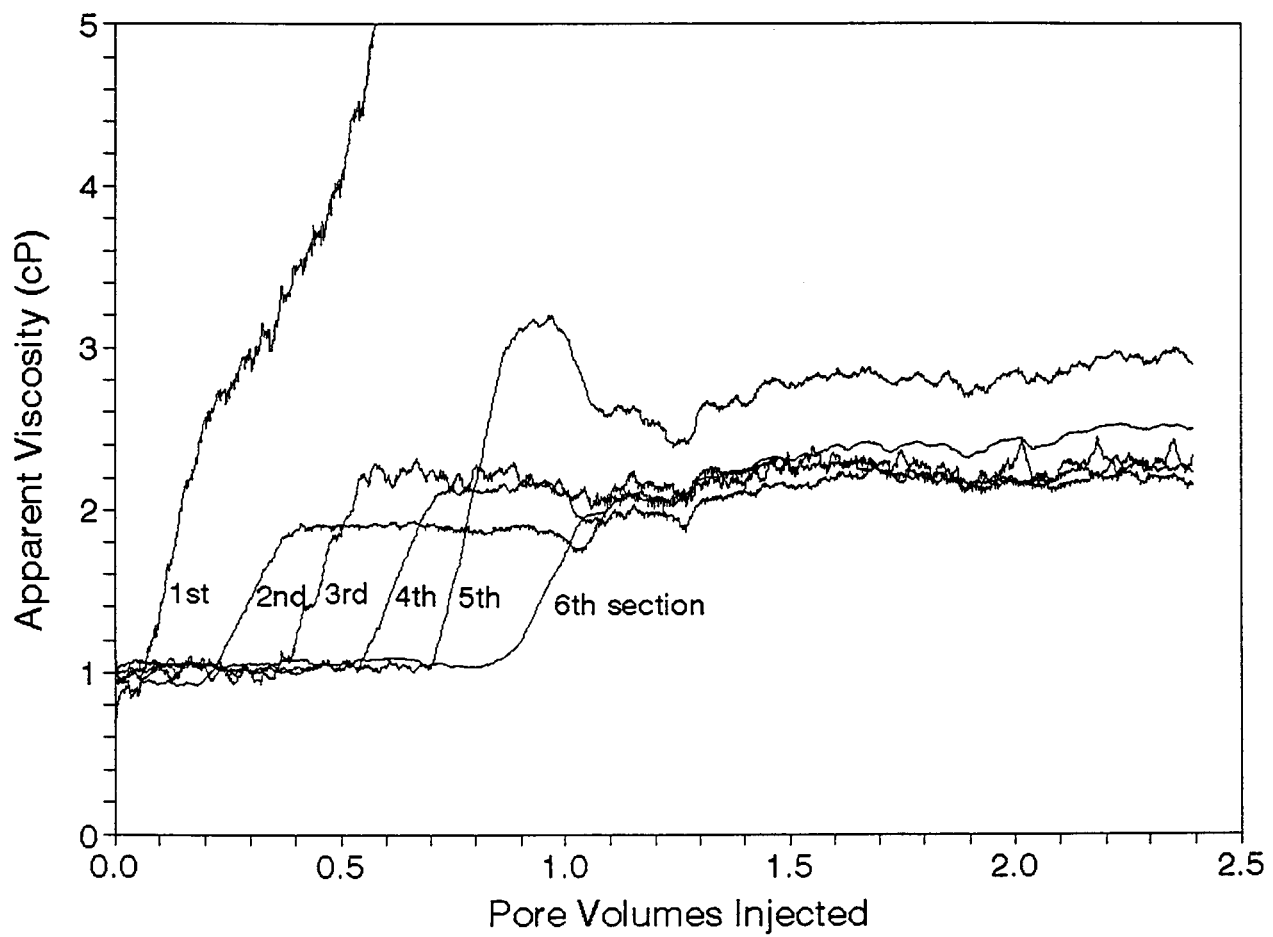


Figure 5.1: Apparent Viscosities for Individual Sections of a Berea Core Indicating Front-End Loading.

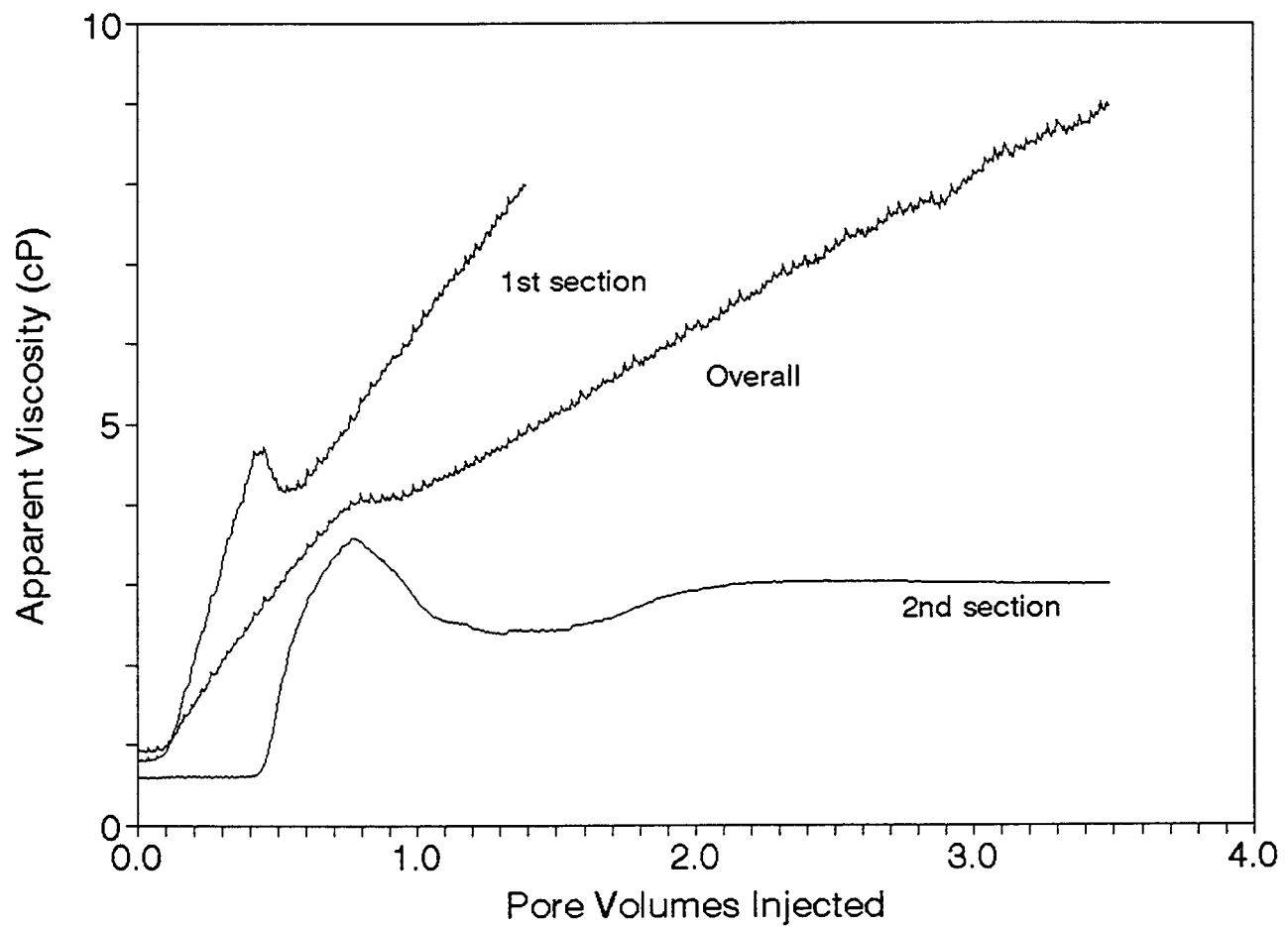


Figure 5.2: Apparent Viscosity in Individual Sections of a Berea Plug
Indicating Front-End Loading.

followed by passage through a 5-micron filter resulted in a polymer solution with reduced front-end loading. Treated KUSP1 solutions were injected into a one-foot long Berea core and the results agreed with the Berea plug tests.

The alkalinity and salinity composition boundaries of KUSP1 solutions were explored using a 5-micron filter test. Results show the sensitivity of filtration is linked with the pH and the sodium chloride content of the polymer solution. KUSP1 must be dissolved in a minimum of 0.1 M sodium hydroxide when the system contains 1% sodium chloride in order to eliminate front-end loading, even after the solution is filtered. Additional details on the development of the filtration tests are presented in Reference 2.

Rock-fluid interactions. A parallel study of the rock-fluid interaction was conducted in Berea sandstone, Baker dolomite, J Alpha grainstone from the Lansing-Kansas City formation, and silica sandpacks. Each core was saturated with a KUSP1 solution of pH 11 or greater. Biopolymer solutions were made up of 1% biopolymer in 1% sodium chloride solution in 1.0 M and 0.1 M sodium hydroxide. The cores were kept at 25 °C for selected periods of shut-in time. Small volumes of the KUSP1 solution were then injected periodically into each core and the effluent collected. The effluent was tested for change in pH, viscosity, and polymer content. Pressure drops measured during these injections were compared with the pressure drops measured during initial injection. No significant change in flow resistance was observed for any of cores studied.

Table 1 contains pH measurements for the effluent samples obtained from the various materials tested. The pH decrease observed was the least for silica sand, followed by Berea sandstone, Baker dolomite, and J Alpha grainstone. The latter rock showed a pH change from 12.8 to 11.8 after 37 days for a KUSP1 solution prepared with 0.1 M sodium hydroxide. The decrease in pH even after 54 days was insufficient to cause the KUSP1 solution to gel. Figures 5.3 and 5.4 illustrate the pH change with time of the displaced KUSP1 solutions containing 0.1 M and 1.0 M sodium hydroxide, respectively, for different types of porous media. A small pH decrease was observed with time, but the pH decrease was insufficient to cause the KUSP1 solutions to gel.

The viscosity of effluent samples collected from the Berea sandstones, Baker dolomite, and J Alpha grainstone are presented in Table 5.1. For comparison, viscosities of the injected solutions that were refrigerated for 18 days were 2.2 cp for the polymer solution prepared in 1.0 M NaOH and 2.6 cp for the polymer solution prepared in 0.1 N NaOH. No significant increase in viscosity of the effluent solutions was observed indicating no gelation occurred in the porous media. Viscosities were determined at a shear rate of 225 s^{-1} and a temperature of 25 °C using a Wells-Brookfield microviscometer. The conclusion was that rock-fluid interactions would not be sufficient to cause the required decrease in pH for the KUSP1 solution to gel in the oil reservoir. Consequently, another method such as reduction of pH by hydrolysis of an ester is required to gel KUSP1 in situ.

Solutions of biopolymer prepared in 1 and 0.1 M sodium hydroxide and 1% sodium chloride show a color change from colorless to yellow and then to yellow-brown with time. The change in color of the effluent samples from the various cores exhibited some degree of color change. The color change corresponded inversely with the pH decrease noted for the various types of core material, except the Baker dolomite effluent. The J Alpha grainstone effluent did not display a color change. The color change is probably indicative of deterioration of the (1→3)- β -D-glucan. However, the biopolymer effluent, for both 1 and 0.1 M sodium hydroxide systems, from Berea, Baker dolomite, and J Alpha grainstone all gelled when the pH was decreased by bubbling carbon dioxide through the solutions. Thus, the deterioration indicated by the change in color did not affect the capability of the polymer to gel when the pH was reduced.

CONCLUSIONS

1. KUSP1 contains small amounts of undissolved material that must be filtered from the solution to avoid filtration on the entrance of the porous media during injection .
2. A method of filtering KUSP1 solutions to remove this material was developed.
3. The amount of undissolved material is sensitive to both solution pH and sodium chloride content. Approximate composition boundaries were found that outlined compositions of injectable solutions.
4. Fluid-rock interactions in sandpacks, Berea sandstone, Baker Dolomite and J Alpha grainstone from the Lansing-Kansas City formation were not sufficient to reduce the pH of injected KUSP1 solutions to promote in situ gelation.
5. Some method to reduce pH, other than rock-fluid interaction, must be used to gel KUSP1.

REFERENCES

1. Kolodziej, E.J., "Mechanisms of Microgel Formation in Xanthan Biopolymer Solutions," SPE paper No. 16730, presented at the 62nd Annual Technical Conference and Exhibition of the Society of Petroleum Engineers, Dallas, TX (Sept. 27-30, 1987).
2. Bhattacharya, S., "Rock-Fluid Interaction and Injectivity of KUSP1 Biopolymer Solutions in Porous Media," M.S. Thesis in preparation, University of Kansas (1995).

Table 5.1: Rock-Fluid Interactions.

Porous Medium		Injected Solution	Test 1	Test 2	Test 3
Type #	Length x dia. Pore Volume Permeability	1.0% KUSP1 1.0% NaCl	Time core was shut-in before injection; Volume of solution injected; pH and viscosity of effluent; Comments.		
Silica sand 1	1 ft x 1.5" 115 ml 2,700 md	1.0 M NaOH pH 12.64 2.0% NaCl	6 days 13 ml pH 12.63	21 days 10 ml pH 12.62	
Silica sand 2	1 ft x 1.5" 118 ml 3,000 md	0.1 M NaOH pH 12.64 2.0% NaCl	21 days 11.5 ml pH 12.63		
Berea sandstone 1	1 ft x 2" 130 ml 297 md	1 M NaOH pH 13.6	15 days 21.2 ml pH13.6	30 days 16 ml pH 13.52	60 days 1.2 ml pH 13.27 gel CO ₂
Berea sandstone 2	1 ft x 2" 132 ml 660 md	1 M NaOH pH 13.77	16 days 13.5 ml pH 13.53	28 days 10 ml pH 13.51	41 days 15 ml pH 13.47
Berea sandstone 3 & 4 (in series)	1" x 2" each #3 5.3 ml 255 md #4 5.0 ml 365 md	0.1 M NaOH pH 12.73	7 days 3 ml pH 12.24	23 days 1.2 ml pH12.03	33 days 1.5 ml pH 12.19
Berea sandstone 5	1" x 2" 4.3 ml 243 md	0.1 M NaOH pH 12.65	9 days 0.8 ml pH 12.36		
Berea sandstone 21	1 ft x 2" 132 ml 677 md	1 M NaOH pH 13.65	34 days 10 ml pH 13.56 visc. 1.9cp dark yellow gelled w/CO ₂	54 days 10 ml pH 13.4 visc. 1.6 cp	
Berea sandstone 22	1 ft x 2" 131 ml 787 md	0.1 M NaOH pH 12.78	35 days 10 ml pH 11.90 visc 2.9 cp yellow	55 days 10 ml pH 11.54 visc 2.6 cp dark yellow gel CO ₂	

Table 5.1 (cont): Rock-Fluid Interactions.

Porous Medium		Injected Solution	Test 1	Test 2
Type #	Length x dia. Pore Volume Permeability	1.0% KUSP1 1.0% NaCl	Time core was shut-in before injection; Volume of solution injected; pH and viscosity of effluent; Comments.	
Baker dolomite 1	3.2" x 1" 10 ml 234 md	1 M NaOH pH 13.66	40 days 5 ml pH 12.8 visc 2.8 cp yellow, gelled w/CO ₂	
Baker dolomite 2	2.9" x 1" 8.7 ml 179 md	1 M NaOH pH 13.66	19 days 4 ml pH 13.59 visc 1.7 cp yellow, gelled w/CO ₂	
Baker dolomite 3	3.2" x 1" 9.9 ml 108 md	0.1 M NaOH pH 12.85	17 days 4 ml pH 12.44 visc 2.1 cp yellow, gelled w/CO ₂	
Baker dolomite 4	3.2" x 1" 10.2 ml 202 md	0.1 M NaOH pH 12.85	37 days 7 ml pH 12.1 visc 1.9 cp dark yellow, gelled w/CO ₂	
J Alpha Limestone 1	2.5" x 1" 7.7 ml 219 md	1 M NaOH pH 13.66	19 days 3 ml pH 13.15 visc 2.0 cp colorless, gelled w/CO ₂	
J Alpha Limestone 2	2.4" x 1" 8.0 ml 223 md	1 M NaOH pH 13.66	40 days 5 ml pH 13.23 visc 1.7 cp lt. yellow, gelled w/CO ₂	
J Alpha Limestone 3	2.4" x 1" 8.5 ml 252 md	0.1 M NaOH pH 12.83	17 days 3.2 ml pH 12.92 visc 2.3 cp colorless, gelled w/CO ₂	37 days 2 ml pH 11.79 visc 1.9 cp colorless, gelled w/CO ₂

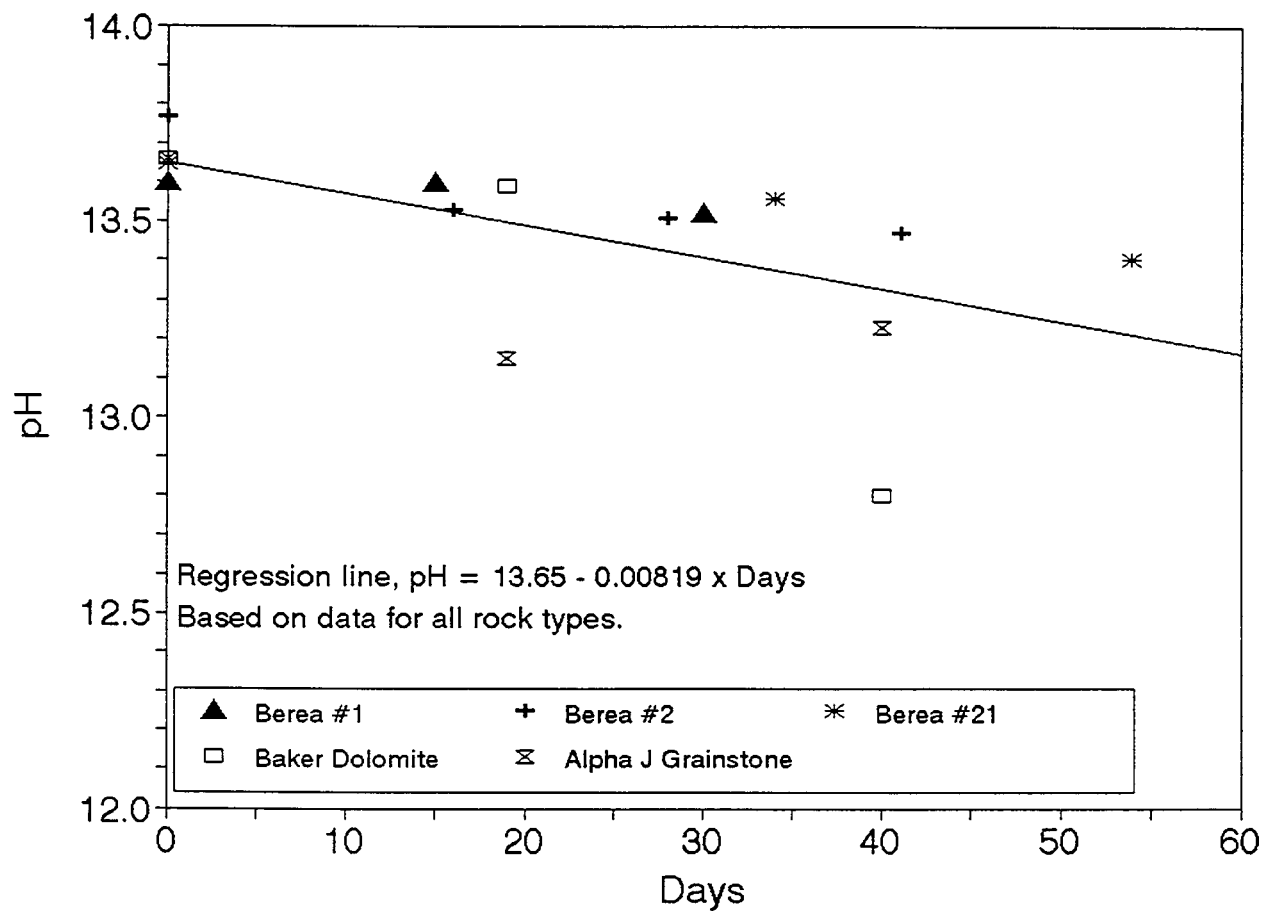


Figure 5.3: Consumption of Hydroxide with Time by the Rock Matrix for Solutions Containing 1.0 M Sodium Hydroxide.

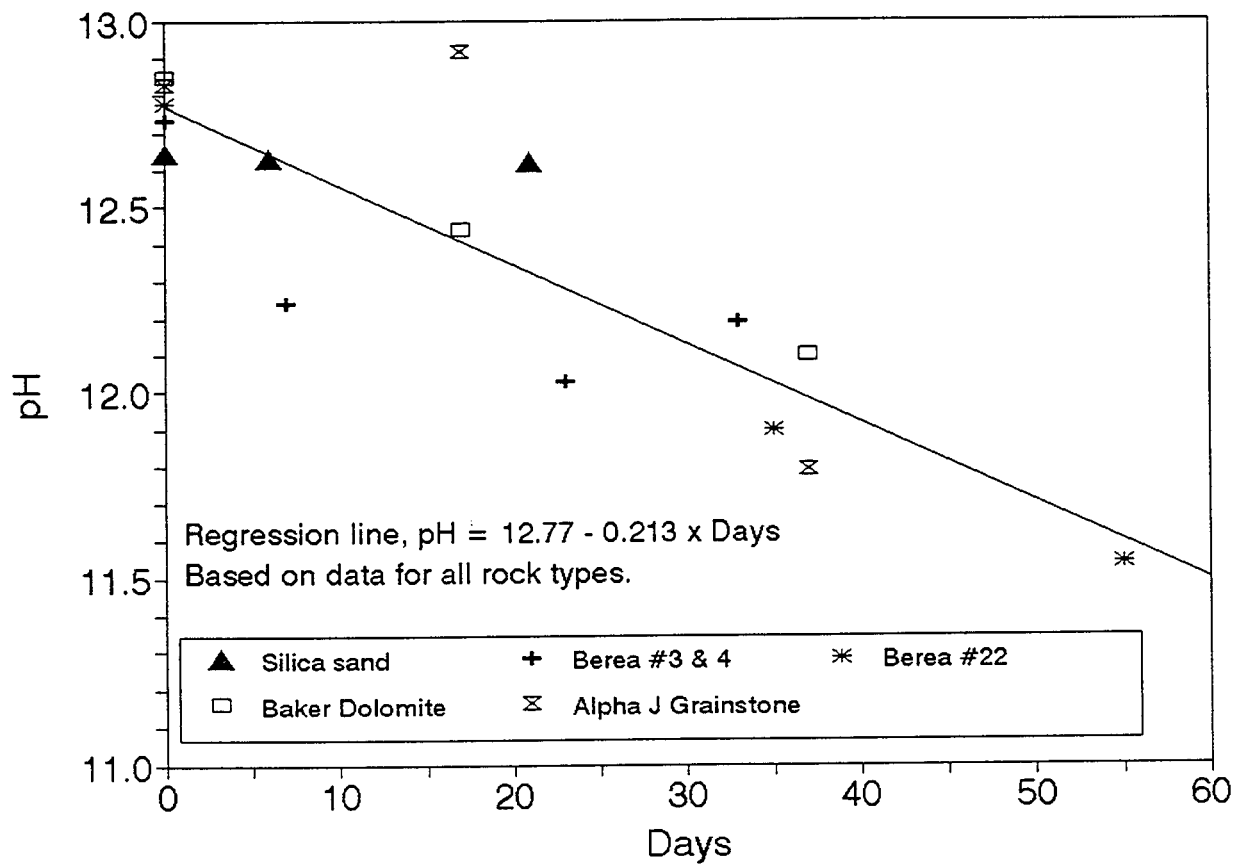


Figure 5.4: Consumption of Hydroxide with Time by the Rock Matrix for Solutions Containing 0.1 M Sodium Hydroxide.

Chapter 6

In Situ Gelation of KUSP1 by Supercritical Carbon Dioxide

Principal Investigators: S. Vossoughi, G.P.Willhite and D.W.Green
Graduate Research Assistant: Milind Raje

INTRODUCTION

Carbon dioxide flooding is one of the various enhanced oil recovery techniques employed in reservoirs where the temperature and pressure conditions are at or above supercritical conditions of carbon dioxide. Supercritical CO₂ is an excellent solvent and miscibility with oil results in efficient displacement of oil where the oil is contacted by CO₂.

Although the microscopic displacement efficiency of the miscible CO₂ displacement is high, the macroscopic sweep efficiency is low due to channeling in the reservoir. Channelling is the result of poor mobility ratio of the crude oil/CO₂ system and gravity override.

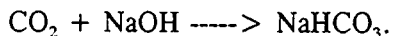
The scope of the research is to increase sweep efficiency of CO₂. The objective of this study is to determine the applicability of using KUSP1 to block CO₂ channels that develop during CO₂ flooding. It is realized that early breakthrough of CO₂ occurs because of its channeling through the oil zone. Plugging these channels should increase the sweep efficiency. This can be achieved by in situ gelation of the polymer in these channels. The polymer dissolves in alkaline solution and forms gel upon reduction of the pH below 11. Reduction of pH can be achieved by the flow of CO₂ through the solution because of CO₂ solubility characteristics in the aqueous phase.

The objective of this study is to analyze the extent of permeability reduction achieved by the in situ gelation and to investigate the reaction mechanism underlying the process.

BACKGROUND

KUSP1 dissolves in alkaline water or brine at pH values of 11.5 and above. A solution containing 2 % KUSP1 at a pH of 13.2 has a viscosity value less than 4 cp (@ 25 °C, 20 s⁻¹). When the pH of the solution is lowered to pH 11, gel is formed. The pH can be lowered by addition of an acid or by injection of CO₂.

If CO₂ is used to lower the pH and is also used as the flooding agent then mobility ratio plays an important role. The primary mechanisms are displacement, diffusion and reaction of CO₂ into the aqueous phase. Therefore, the CO₂ injection rate is critical in determining the performance of the process. The governing reaction is



Hence, 1 mole of CO₂ is required to completely neutralize 1 mole of 1N NaOH. This fact is used to make the material balance. Also the rate of displacement should be lower than the rate of reaction and the rate of diffusion of CO₂ in the aqueous phase. This ensures sufficient time for CO₂ to diffuse and react with NaOH and at the same time the displacement process ensures that fresh NaOH is made available for reaction. In this manner the reaction goes to completion. If the rate of injection is very high, CO₂ would finger through the polymer solution due to the adverse mobility ratio leaving the solution unreacted. Therefore, in situ gel formation is dependent on the rate of injection.

EXPERIMENTAL

Experiments have been conducted at three different CO_2 injection rates in Berea sandstone cores. The flow rates of CO_2 were 0.5 ml/min, 0.1 ml/min and 0.005 ml/min. A new Berea core of 30.2 cm in length and cross sectional area of 20.25 cm^2 was used in each experiment. The pressures and temperatures were maintained above supercritical conditions. The general outline of the experiments is as follows:

Permeability and dispersion runs are carried out. Brine permeability is evaluated from the pressure data. Pressure ports are located at three positions so that the incremental pressure drops are measured in four sections of the core in addition to the measurement of the overall pressure drop of the core.

A core is saturated with polymer solution of pH 13.5.

CO_2 is injected at supercritical conditions using a syringe pump at constant rate.

Effluent production is measured as a function of time.

CO_2 injection is continued until steady pressure readings are obtained.

Brine permeability is determined and a post gelation dispersion run is conducted.

RESULTS AND DISCUSSION

Experiment 1. This experiment was carried out on a high-permeability Berea core (porosity = 19%, pore volume = 115 ml). CO_2 was injected at 0.5 ml/min. The operating conditions were as follows:

$$P = 1100 \text{ psi}$$

$$T = 30 \text{ }^{\circ}\text{C}$$

The core was initially saturated with brine and liquid permeability was determined for each of the four sections of the core. The brine was displaced by the alkaline polymer solution followed by CO_2 injection at 0.5 ml/min. Injection of the CO_2 was continued beyond gas breakthrough until a stable pressure drop was achieved. The total amount of CO_2 injected at breakthrough was 60 ml while the total amount of liquid production was 28 ml. This means that a significant amount of CO_2 was injected, i. e. $60 - 28 = 32$ ml, was consumed by the polymer/alkaline solution in the core.

Brine injection was resumed to determine the liquid permeability of each section after treatment. The permeability modification is depicted in Table 6.1. It is evident from Table 6.1 that significant permeability reduction (more than 70%) was obtained in all the four sections. Injection of the brine was continued to study the stability of the gel. A total of 12 pore volumes was injected in the core and permeability was evaluated after every 2 pore volumes injected. The results are summarized in Table 6.2. The permeability reduction was stable during brine injection.

To investigate the possibility of permeability restoration, 1N NaOH followed by 2N NaOH was injected in the core and permeability was evaluated again. Permeabilities measured following treatment with 2N NaOH are given in Table 6.3. This treatment restored some of the original permeability but it did not return to its original value. This is due to the fact that the NaOH solution is not able to completely contact all the gel formed.

Table 6.1: Permeability Reduction by CO₂ Injection at 0.5 ml/min.

	Initial Permeability	Permeability After CO ₂ injection	Permeability Reduction %
Overall	384 md	86 md	78
1st Section	331 md	88 md	73
2nd Section	423 md	92 md	78
3rd Section	384 md	78 md	80
4th Section	332 md	90 md	73

Table 6.2: Stability of Permeability Reduction.

	Permeability after Pore Volumes (PV) Injected (md)				
	4 PV	6 PV	8 PV	10 PV	12 PV
Overall	90	90	93	85	86
1st Section	89	91	94	91	88
2nd Section	89	92	93	93	92
3rd Section	85	84	85	72	78
4th Section	103	103	103	98	90

Table 6.3: Reversibility of Permeability Reduction.

	Initial permeability (md)	Before NaOH injection (md)	After NaOH injection (md)
Overall	384	86	117
1st Section	331	88	158
2nd Section	423	92	162
3rd Section	384	78	93
4th Section	332	90	145

Experiment 2. This experiment was carried out on a low-permeability Berea core (pore volume = 115) and the CO₂ injection rate was set to 0.1 ml/min. The pressure was 1200 psi and the temperature was 37.8°C. Permeability reduction by the injection of CO₂ into a core saturated with 1N NaOH was investigated in the presence and absence of KUSP1 polymer. Experiment 2 was conducted in two parts.

Experiment 2, Part 1: CO₂ - NaOH system. As in experiment 1 the core was initially saturated with brine and the brine permeability was determined. The brine was then displaced by 1 N sodium hydroxide solution and CO₂ injection was resumed. CO₂ injection was continued beyond the gas breakthrough until a stable pressure drop was achieved. Brine permeability of the core was determined at this time and compared with the initial permeability of the core as presented in Table 6.4.

Table 6.4: Permeability Reduction by CO₂ Injection in the Absence of Polymer.

	Initial Permeability of the Core (md)	Permeability after NaOH/CO ₂ injection (md)	Permeability Reduction (%)
Overall	72	57	21
1st Section	68	44	35
2nd Section	70	60	14
3rd Section	73	67	8
4th Section	53	53	0

The data presented in Table 6.4 suggest that there is about 20% reduction in the overall liquid permeability attributed to the fluid/rock interaction.

Experiment 2, Part 2: CO₂ - Polymer System. The previous experiment was repeated in the presence of KUSP1. The operating conditions and injection rate of CO₂ were maintained the same as in Part 1. It is interesting to note that the amount of CO₂ injected until gas breakthrough was the same as in part 1 as was the amount of effluent produced. The liquid permeability was measured again. The values are compared with the initial permeability of the core in Table 6.5.

Table 6.5: Permeability Reduction by CO₂ Injection in the Presence of Polymer.

	Initial Permeability of the Core (md)	Permeability after CO ₂ injection (md)	Permeability Reduction (%)
Overall	57	8	86
1st Section	44	6	86
2nd Section	60	12	80
3rd Section	67	7	90
4th Section	53	5	91

Permeability reduction is significantly higher than that observed in Part 1 due to fluid-rock interaction. The high level of permeability reduction is undoubtedly due to in situ gelation caused by dissolution of the CO₂ in the KUSP1/NaOH solution.

Experiment 3. This experiment was carried out on a new Berea core of low permeability. The injection rate of CO₂ was lowered to 0.005 ml/min. The operating conditions were the same as in Experiment 2. Results are presented in Table 6.6.

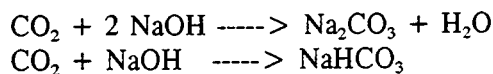
Table 6.6: Permeability Reduction by CO₂ Injection at 0.005 ml/min.

	Initial Permeability of the Core (md)	Permeability after CO ₂ injection (md)	Permeability Reduction (%)
Overall	93	6	94
1st Section	72	4	94
2nd Section	97	5	95
3rd Section	106	10	91
4th Section	101	13	87

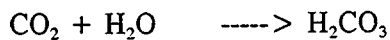
A permeability reduction of over 90% was achieved. Complete plugging of the core even at this low CO₂ injection rate was not possible.

REACTION MECHANISMS

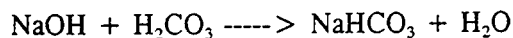
CO₂ reacts with NaOH to form sodium carbonate and sodium bicarbonate. The reactions are:



The pH of NaHCO₃ (pH 8 for 1 M solution) is lower than that of Na₂CO₃ (pH 9 for 1 M solution). Figure 6.1 is a typical pH profile of the effluent during CO₂ injection which indicates that pH drops drastically from the initial 13.5, which is the pH of 1N NaOH, to 8 which corresponds to the pH of NaHCO₃. The absence of a transition zone suggests sodium carbonate was not formed. This is expected because of the excess amount of the CO₂ injected compared to the availability of the sodium hydroxide in the core. Initially CO₂ goes into solution forming carbonic acid by means of the following reaction :



Subsequently, H₂CO₃ reacts with NaOH to form NaHCO₃. The reaction is:



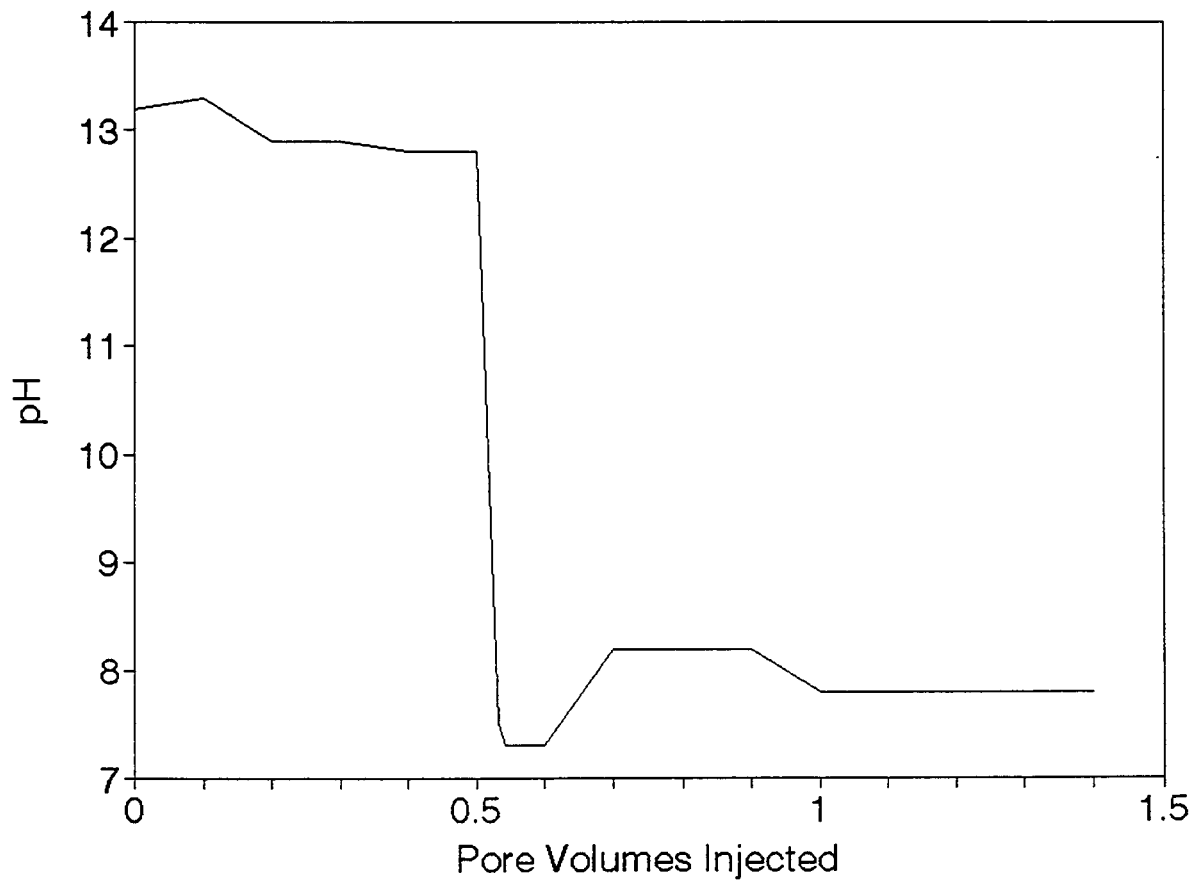


Figure 6.1: Typical Effluent pH During Injection of Carbon Dioxide
In a Berea Core Saturated with KUSP1 and 1 N Sodium Hydroxide.

Adding the above two reactions we obtain the governing reaction as:



Therefore, 1 mole of CO_2 is consumed to completely neutralize 1 mole of 1N NaOH .

OTHER OBSERVATIONS

Effluent liquid productions were collected in test tubes at fixed incremental time periods. A typical liquid production rate is given in Figure 6.2. Figure 6.2 depicts the cyclic nature of the liquid production and it is maximum at the gas breakthrough. The cyclic nature of effluent production suggests the presence of more than one mechanism underlying the process. The primary mechanisms are reaction and displacement. Also present is diffusion of CO_2 in the aqueous medium. In the beginning the effluent production increases indicating gas displacement being the dominating mechanism. However, as more CO_2 is injected, more and more gas/liquid interface is created which helps dissolution of CO_2 into the liquid phase. Most of the injected CO_2 will go into solution instead of displacing the liquid. Consequently the liquid production rate drops. This continues till the liquid immediately near the gas/liquid interface becomes saturated with CO_2 . Again the displacement process starts to dominate and more and more liquid production is observed. This produces new gas/liquid interface which repeats the cycle again. This cyclic process continues until gas breakthrough and beyond. It is interesting to note that the "peaks" of effluent production are increasing as more and more CO_2 is injected. A possible explanation would be that as more and more CO_2 is injected, more and more fingers are formed due to which gas displacement drive becomes more effective as time passes and hence, more fluid will be displaced. At gas breakthrough effluent production attains a maximum since from thereafter a channel is established. Effluent production drops after gas breakthrough since a gas channel is established which prevents effective displacement.

CONCLUSIONS

In situ gelation occurs because dissolution of CO_2 into the aqueous phase causes reduction of pH below the gelation pH level. A significant permeability reduction (in the range of 90%) due to the interaction of KUSP1 and CO_2 was achieved. Complete plugging of the core is not possible even at a very low CO_2 injection rate. This is because CO_2 channels through the liquid phase. The process appears to have potential for the WAG process where the mobility of the CO_2 could be further reduced due to the in situ gelation. However, it is not suitable for the application where complete plugging is required such as plugging the fractures or high permeable streaks.

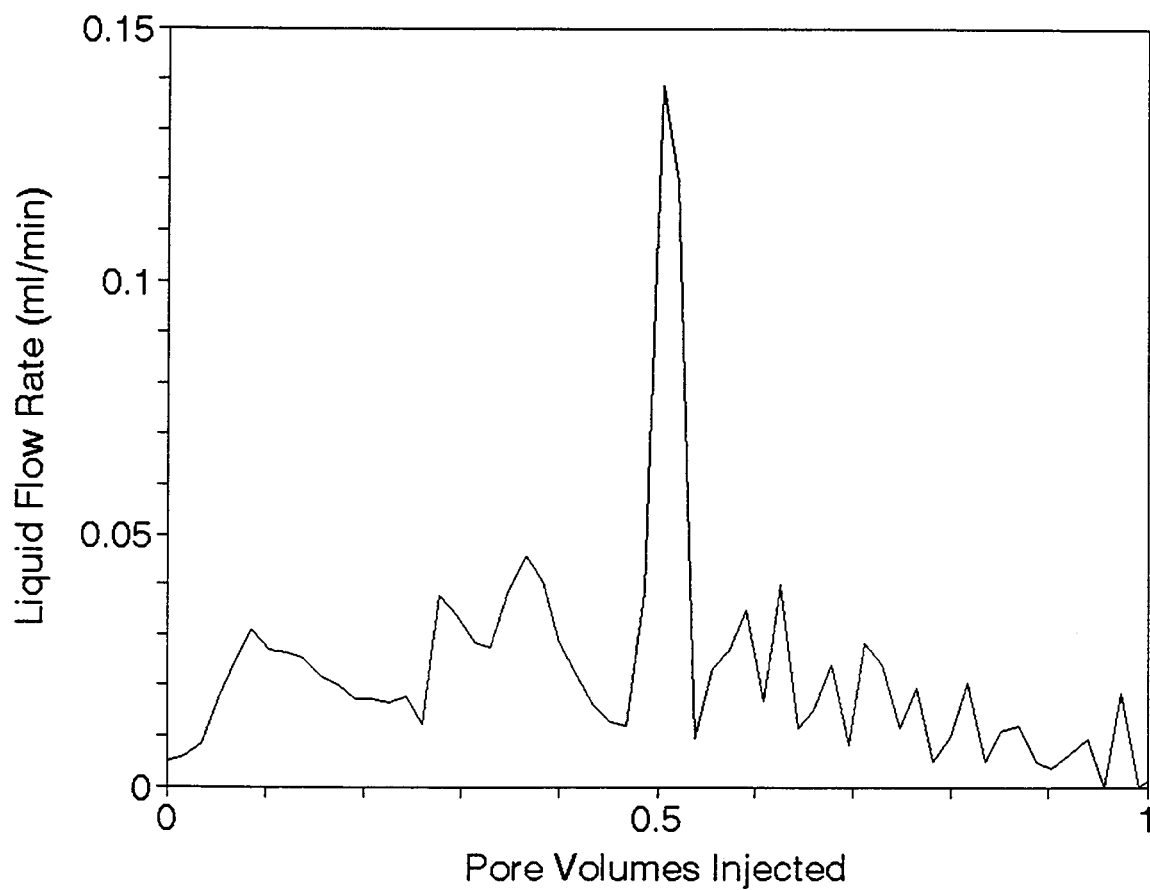


Figure 6.2: Typical Production Rate of Liquid During Injection of Carbon Dioxide In a Berea Core Saturated with KUSP1 and 1N Sodium Hydroxide.

Chapter 7

Effect of Steady Shear on the Gelation of a Polyacrylamide-Chromium(III) System

Principal Investigators: Don W. Green, G. Paul Willhite, C.S. McCool
Graduate Research Assistant: Ajay Kumar

INTRODUCTION

Shear is an important parameter affecting the gelation of systems used in permeability reduction treatments. The gel solution, or gelant, is invariably subjected to shear when it is being pumped through the well and the reservoir rock. This study was conducted to examine the effect of shear on the gelation of a polyacrylamide-chromium(III) gelant.

Experiments were performed using cone-and-plate geometry on a Weissenberg R-19 rheometer and using parallel-plate geometry on a Bohlin CS rheometer. Steady shear experiments and parallel superposition experiments (simultaneous application of oscillatory shear and steady shear) were conducted. Shear rates examined ranged from 0.47 to 47 sec^{-1} . The effect of shear on gelation was interpreted primarily from the time-dependent data of shear viscosity and storage modulus.

BACKGROUND

Previous studies¹⁻⁴ on the effect of shear on gelation of polyacrylamide-chromium systems have reported an *increase* in the rate of gelation at *low* shear rates and a *decrease* in gelation rate at *high* shear rates. This effect of shear is usually interpreted as two opposing mechanisms. A small amount of shear enhances the rate of gelation by increasing interactions between the large polymer molecules. Higher amounts of shear retard gelation by not allowing crosslinks to form or by the scission of previously formed crosslinks.

Shear also affects the final, or equilibrium, viscosity that a gelant will achieve. Viscosities of gels at long reaction times were found to decrease with increasing shear rate. The reproducibility of steady-shear experiments of gelling materials has been difficult, particularly after a "gel" has formed. The cause of these experimental difficulties is presumably due to non-uniform flow between the platens of the rheometer.

EXPERIMENTAL METHODS

Rheological experiments of gelation have been found to be sensitive to experimental technique⁵. The following procedures were followed in this study.

Preparation of stock solutions. All solutions were prepared by weight. The stock polymer solution contained 1.00 weight % polyacrylamide (Aldrich) and 2.66 % NaCl (Fisher Scientific). Water was stirred with a magnetic stir plate and bar so that a vortex was formed. Salt was added and allowed to dissolve. The weighed polymer was slowly dropped on the shoulder of the vortex. The addition of polymer to the solution was slow enough to wet each particle and fast enough to add all the polymer before a good vortex ceased to exist due to the increased viscosity of the solution. Care was taken to avoid formation of polymer agglomerates. The solution was stirred for three days and then was filtered using a 5-micron filter paper under a 20 psig head. Care was taken to insure that the polymer solutions were subjected to

the same conditions. The filtered stock polymer solution was allowed to age for 3-4 days to avoid ageing effects.

Polymer solutions were sometimes found to be infected with bacterial growths. Any drastic change in the pH of the polymer solution or appearance of any kind of turbidity in the solution was assumed to be due to bacterial degradation and such solutions were discarded.

Stock chromium solutions were prepared at a concentration of 400. ppm with hexahydrate chromium chloride (Fisher Scientific) and water. Stock chromium solutions were aged for a minimum of six days before use.

Preparation of gelant. The following steps were followed during preparation of each gel solution:

1. The rheometer was readied prior to preparing a gelant sample.
2. 30.00 grams of polymer solution were adjusted to 25 °C and stirred to form a vortex.
3. pH of the polymer solution was measured.
4. 10.0 ml of chromium solution was added to the stirred polymer solution.
5. pH of the gelant was measured.
6. The pH of the gelant was adjusted to 5.0 using 0.1 N sodium hydroxide. The base was added dropwise to the stirred solution to avoid formation of gel clusters.
7. The gelant sample was placed immediately on the rheometer.

The composition of the gelant was:

7500 ppm	polyacrylamide
100 ppm	chromium
2.0 %	NaCl
5.00	initial pH

Equipment and procedures. A Weissenberg R-19 rheometer was used to obtain the principal rheological data of this study. A 7.5 cm diameter cone-and-plate geometry with cone angle of 0 degrees 57 minutes and 20 seconds was used on the Weissenberg. Strain was fixed at 0.5 for oscillatory measurements. The plates were meticulously cleaned after each experiment.

Four types of experiments were performed on the Weissenberg rheometer. All experiments were conducted at a temperature of 25 °C.

Oscillatory experiments. The sample was subjected to a sinusoidal strain that results in zero net shear applied to the sample. Oscillatory experiments allowed determination of dynamic properties of the sample, e.g. the storage and loss moduli. Oscillatory runs were conducted to check consistency between different polymer and chromium solutions, as well as smooth functioning of the Weissenberg rheometer.

Steady-shear experiments. The sample was subjected to a constant steady shear for the determination of viscosity. Steady-shear experiments were performed on the Weissenberg R-19 rheometer at shear rates that ranged from 0.47 to 47 sec⁻¹. The entire sample was subjected to the same rate of shear deformation by using a cone-and-plate geometry.

Parallel-superposition experiments. The sample was subjected simultaneously to steady shear and oscillatory shear. This experiment allowed for the determination of storage modulus (and shear viscosity) while the sample was under steady shear.

The Bohlin CS (controlled stress) rheometer was used to address the issue of slippage during gelation. Steady-shear experiments were conducted using parallel plates with a diameter of 40 mm and at gap settings of 0.5 and 0.75 mm.

RESULTS AND DISCUSSION

The principal rheological properties considered in this study were the steady-shear viscosity and the storage modulus. These properties were monitored over time as samples were subjected to shear rates that ranged from 0.47 to 47 sec⁻¹. The effect of shear on the gelation process was interpreted from these data.

Shear Viscosity Data. Viscosity was monitored over time in steady-shear experiments and in parallel-superposition experiments. The viscosity behavior was consistent between these two types of experiments. That is, oscillatory shear superimposed on steady shear did not alter the viscosity behavior. Viscosity behavior as a function of time at the selected shear rates are shown in Figure 7.1. The early period of these data are shown in Figure 7.2. Each curve is representative of two or more runs.

Figures 7.1 and 7.2 show that there was an induction period where the shear viscosity increased at slow rates. The induction period lasted an hour or longer and was a function of the applied shear rate. The induction period was observed at all shear rates studied.

For shear rates less than 14.88 s⁻¹, there was an abrupt increase in viscosity at the end of the induction period. The abrupt rise in viscosity occurred sooner at successively higher shear rates up to a shear rate of 2.35 s⁻¹. Further increases in shear rate suppressed the abrupt viscosity rise. Using the abrupt rise in viscosity as a measure of the *gel time*, gelation was accelerated by increasing shear rates to a maximum gelation rate at 2.35 s⁻¹ and retarded for higher shear rates.

The highest viscosity attained decreased with increased shear rate. Viscosity data at long reaction times was questionable and is addressed in a following section on Validity of Data.

Steady-shear viscosity data obtained on the Bohlin CS rheometer using parallel-plate geometry are shown in Figures 7.3 and 7.4. The same trends as seen in data from the Weissenberg were observed. However, the shear rate at which the reversal in gel time occurred was 4.34 s⁻¹, higher than the value observed on the Weissenberg rheometer. This was likely due to the difference in geometries between the rheometers. Unlike using cone-and-plate geometry, the shear rate is a linear function of the radius in the a parallel-plate geometry. The indicated shear rates were the values at 3/4 of the radius. Thus, the sample was subjected to a range of shear rates which probably caused the differences between the data from the two rheometers.

Storage Modulus Data. Storage modulus was monitored in parallel-superposition experiments on the Weissenberg rheometer. The storage modulus as a function of time for selected shear rates are shown in Figure 7.5 and for the early time period in Figure 7.6. An induction period was observed followed by a sharp rise. The increase in storage modulus occurred sooner as shear rate increased up to 2.35 sec⁻¹. Further increases in shear rate lengthened the induction period. The storage modulus showed the same general trend with shear rate as did the viscosity (see Figure 7.2).

Gel Time Data. Easily detectable gel times are used to study the effect of various parameters on gelation. A rapid rise in viscosity and the G'-G" cross-over are two measurements of gel time. Gel times determined from these measurements were compared. Figure 7.7 presents data from a parallel-

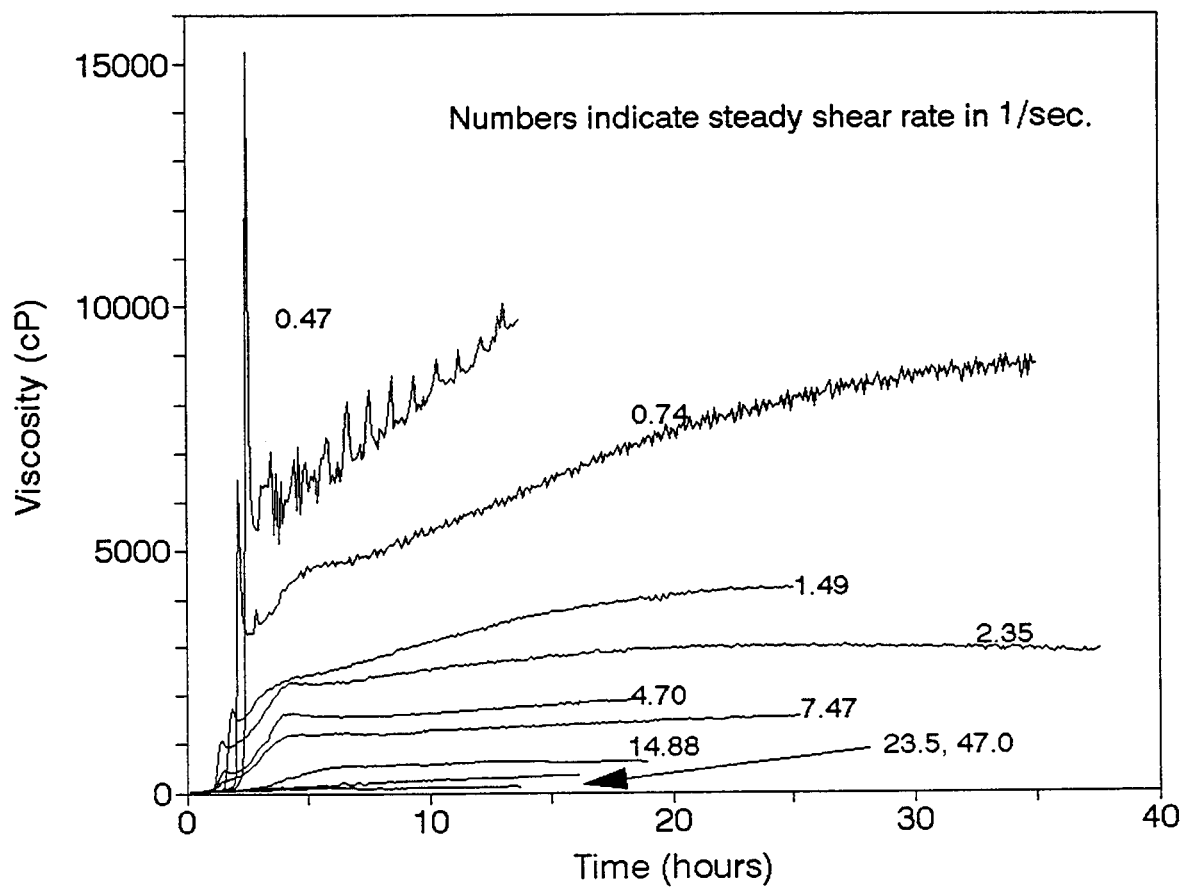


Figure 7.1: Viscosity Behavior During Gelation Under Shear.
Data from Weissenberg Rheometer and for Long Time Periods.

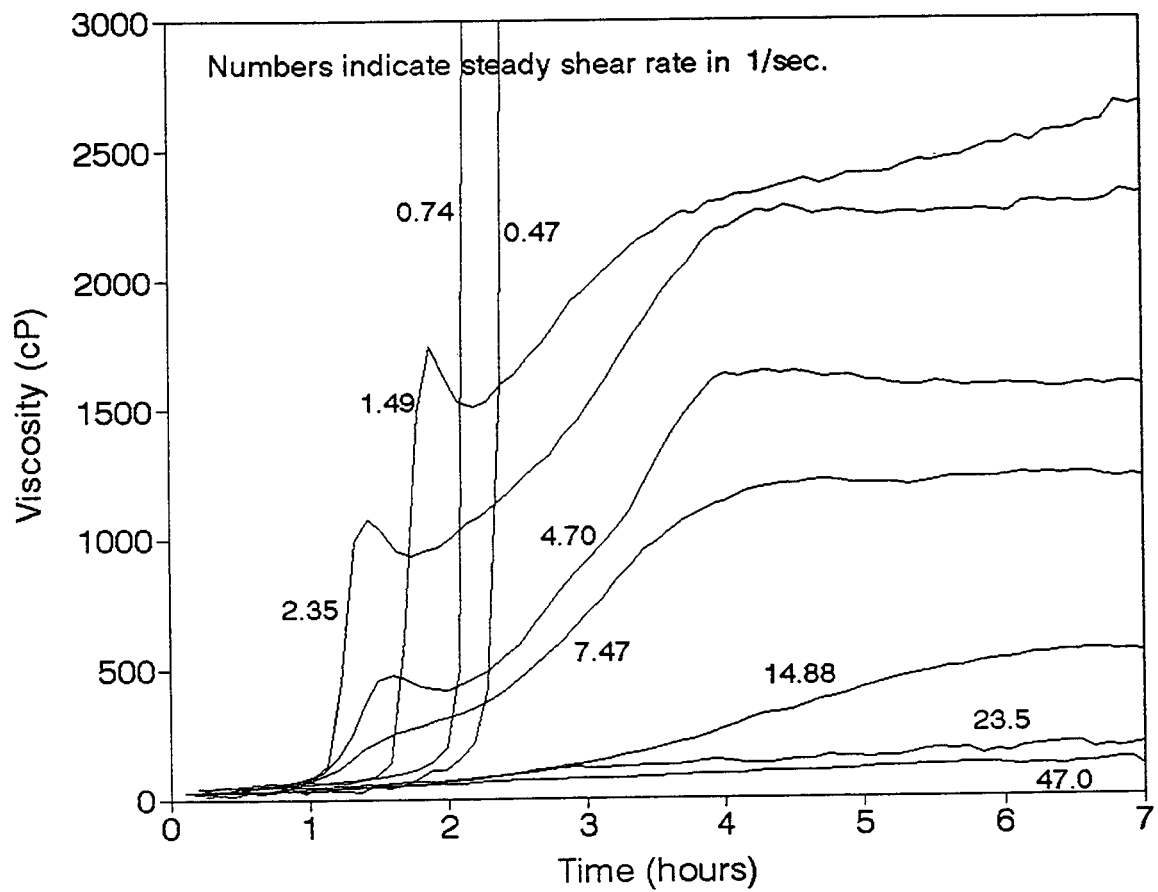


Figure 7.2: Viscosity Behavior During Gelation Under Shear.
Data from Weissenberg Rheometer and for Early Time Periods.

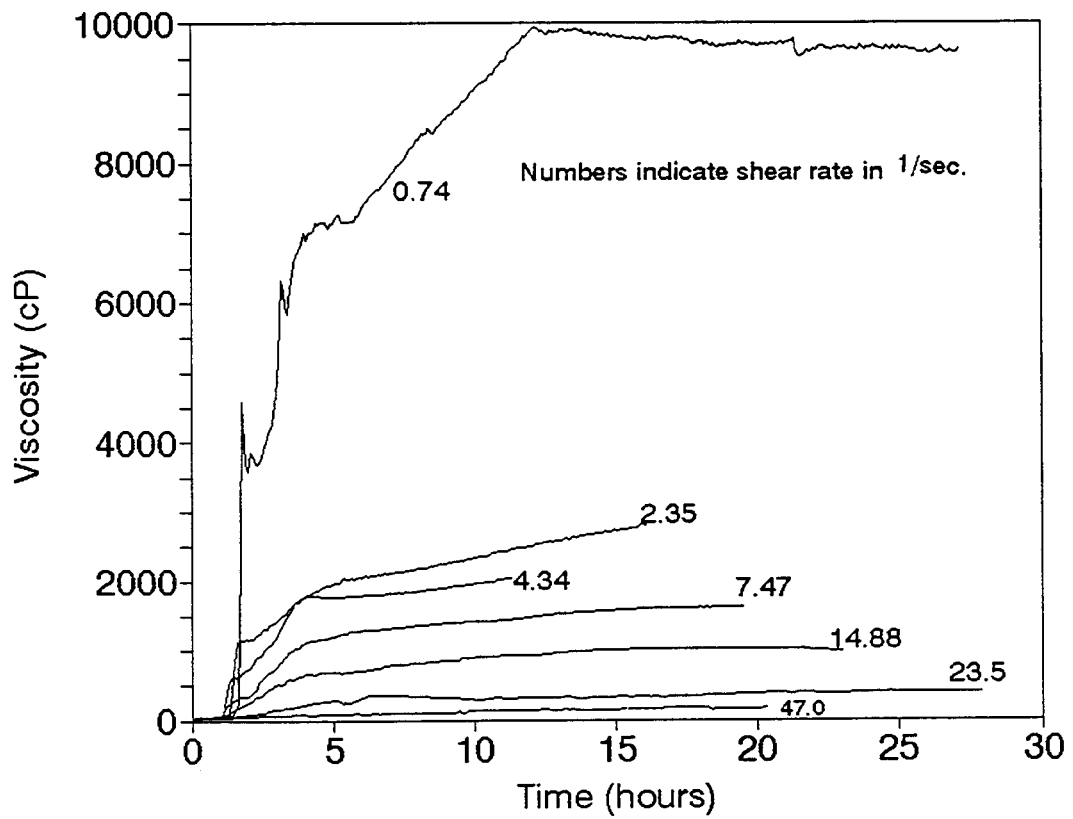


Figure 7.3: Viscosity Behavior During Gelation Under Shear for Long Time Periods.
Data from Bohlin Rheometer (parallel plates, gap = 0.5 mm).

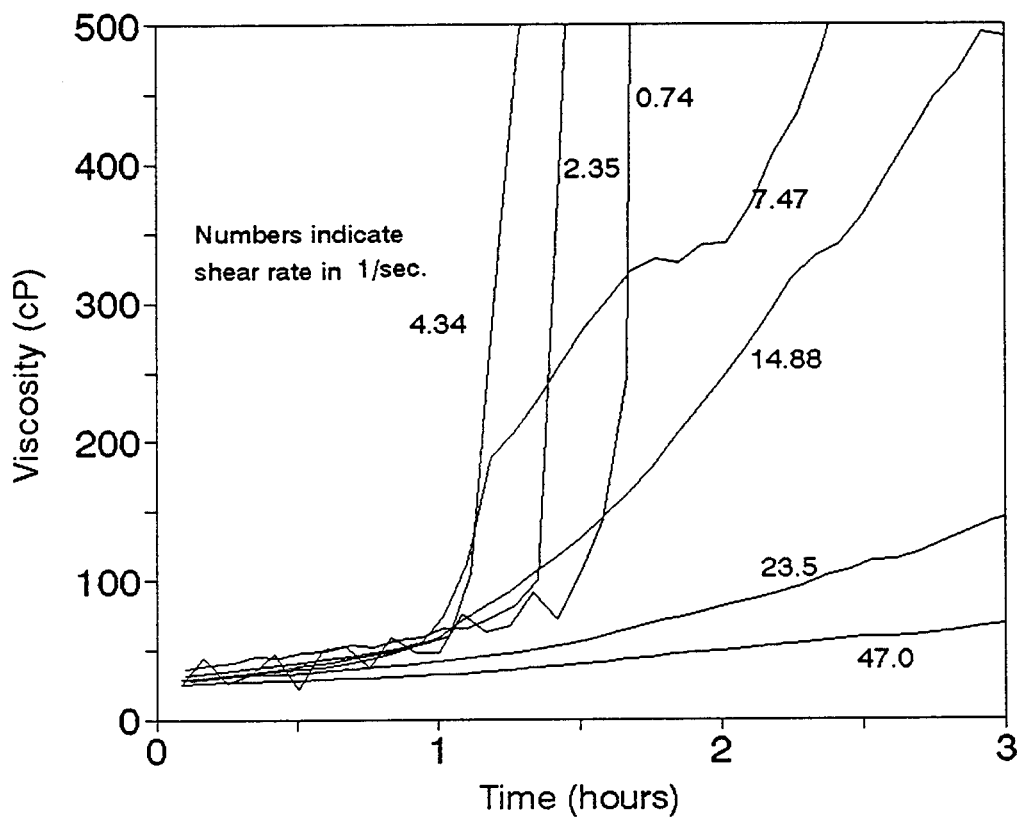


Figure 7.4: Viscosity Behavior During Gelation Under Shear.
Data from Bohlin Rheometer (parallel plates) and for Early Time Periods.

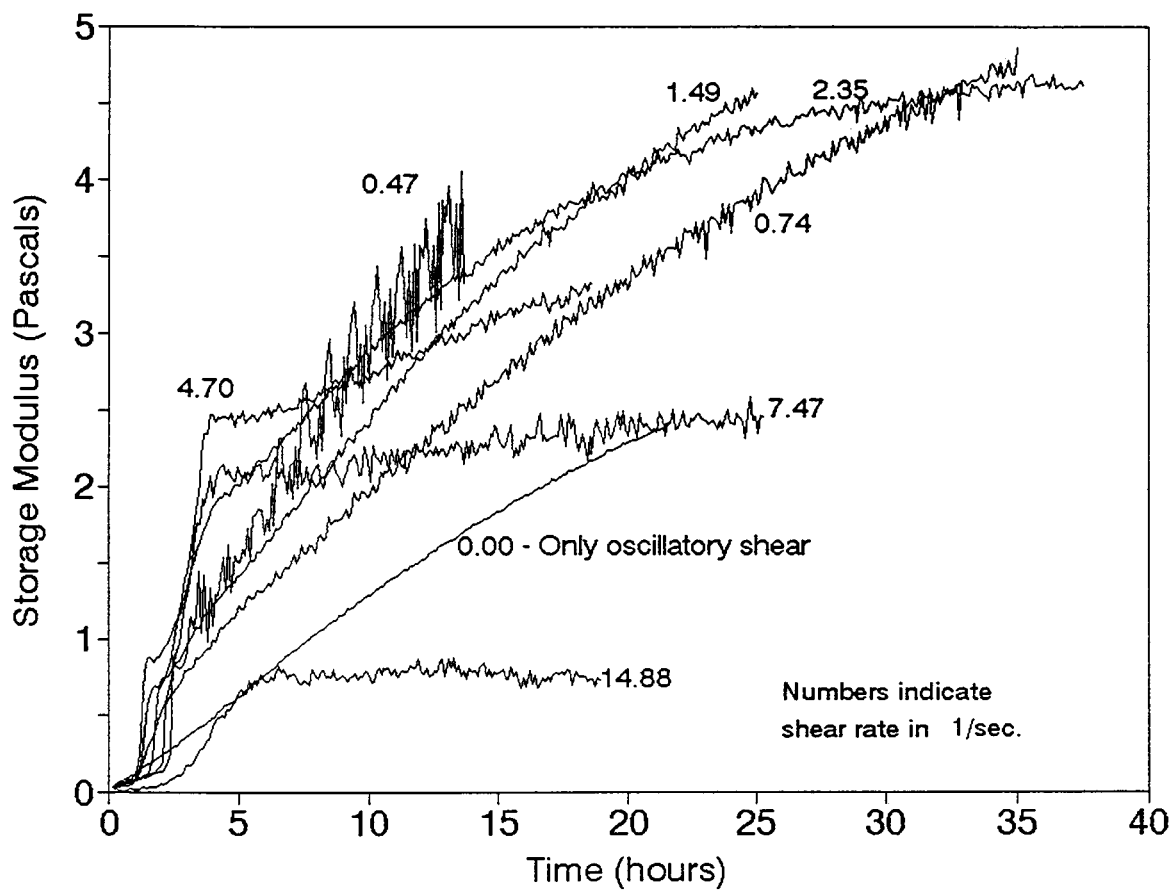


Figure 7.5: Development of Storage Modulus During Gelation Under Shear.
Data from Weissenberg Rheometer and for Long Time Periods.

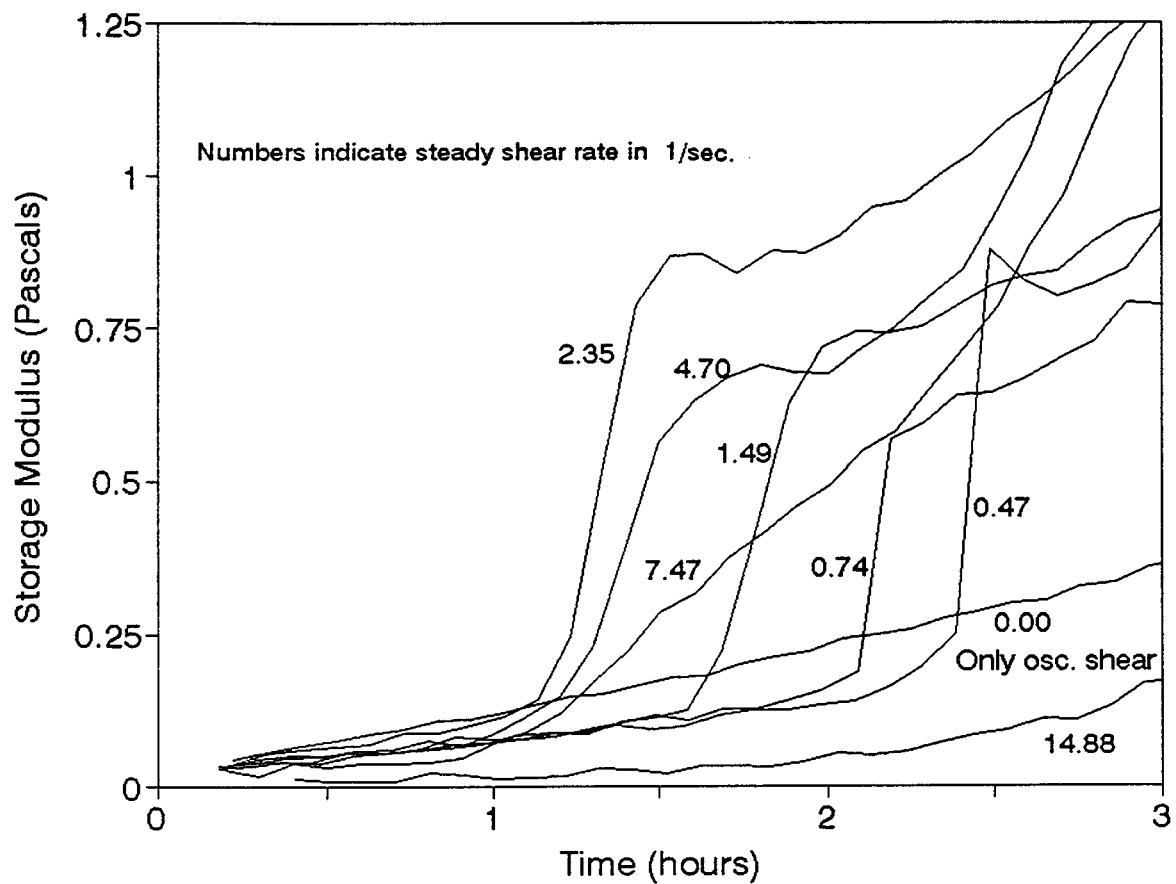


Figure 7.6: Development of Storage Modulus During Gelation Under Shear.
Data from Weissenberg Rheometer and for Early Time Periods.

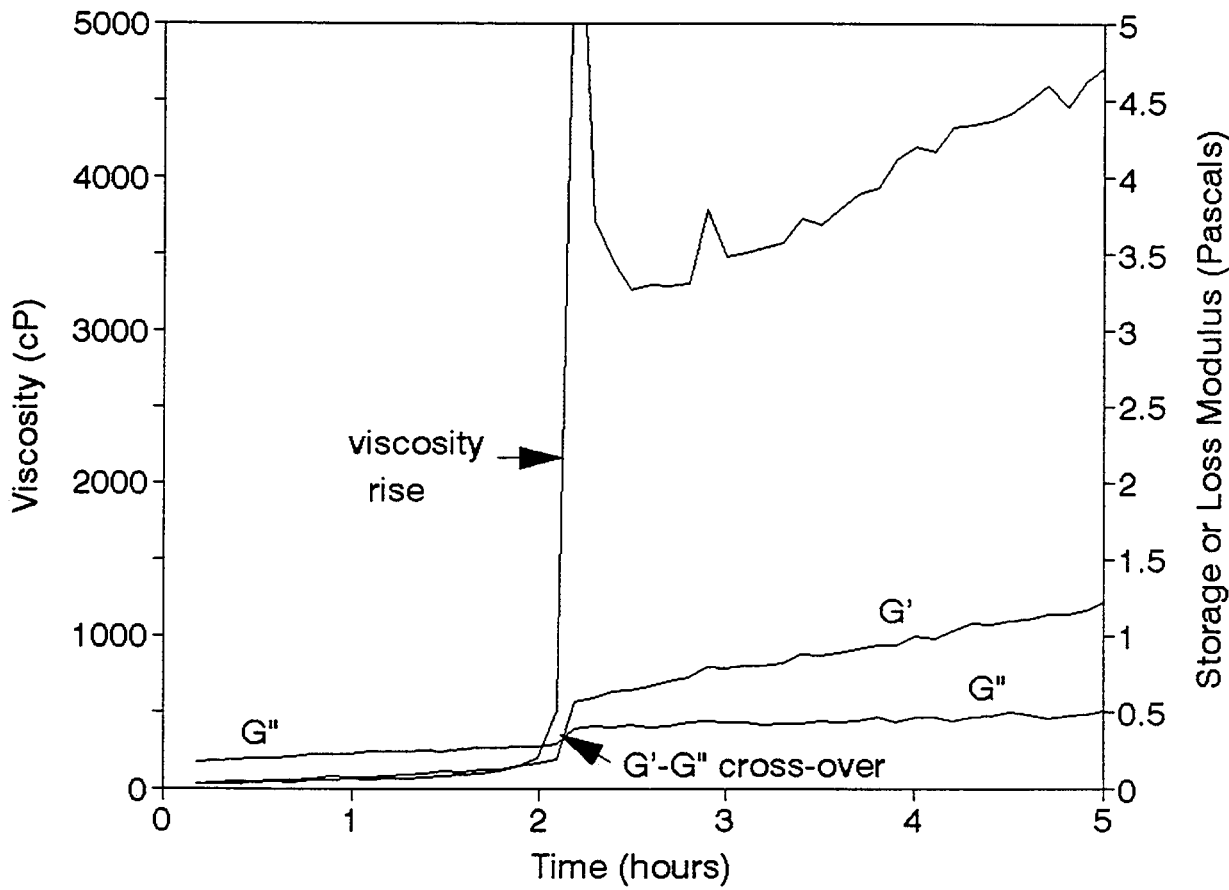


Figure 7.7: Determination of Gel Times from Rheological Data.
Sample Subjected to Shear Rate of 0.74 s^{-1} .

superposition experiment at a shear rate of 0.74 sec^{-1} . Initially, the storage modulus (G') is less than the loss modulus (G''). At 2.15 hours, the storage modulus increased to values greater than the loss modulus. The point where the moduli were equal is termed the $G'-G''$ cross-over. The shear viscosity increased rapidly during this period of time with a maximum slope occurring also at 2.15 hours. Similar data for a run conducted at 14.88 s^{-1} are presented in Figure 7.8. Although the viscosity and storage modulus increased with time, there was no rapid rise in viscosity or $G'-G''$ cross-over for this shear rate.

Gel time data, in terms of rapid viscosity rise and $G'-G''$ cross-over, for all the shear rates studied are presented in Table 7.1. The $G'-G''$ cross-over occurred at the lower shear rates but is absent at higher shear rates. The rapid rise in viscosity corresponded to the maximum slope in the viscosity-time curve at the indicated shear rate. The rapid rise in viscosity was distinct for shear rates of 0.47 , 0.74 , 1.49 and 2.35 sec^{-1} , but less clear for higher shear rates. At the lower shear rates, the viscosity increased several hundred centipoise over one time interval of six minutes. At shear rates of 4.70 sec^{-1} and higher, the viscosity increased approximately linearly over many time intervals and no rapid viscosity increase was identified. The data in Table 7.1 showed that the gel time determined by the $G'-G''$ cross-over and the rapid rise in viscosity were approximately the same. Both of these methods signify growth of structure within the sample.

Validity of Data. Replicate runs were conducted at each shear rate. Comparison of the replicate runs showed that the data were reproducible up to the time when the rapid rise in viscosity occurred. After the rapid rise, the data deviated for many data sets. Viscosity behavior for replicate runs at a shear rate of 0.74 s^{-1} are shown in Figure 7.9. Deviations in the viscosity occurred after the rapid rise in viscosity at 2.15 hours. These deviations were interpreted to be caused by slip. This interpretation was supported by visual inspections of the samples at the end of the runs. These inspections showed that the sample was a connected mass. Samples were lifted off the platen with a cable tie, except at the highest shear rate of 47.0 sec^{-1} . Also, the sample did not stick to either platen for shear rates higher than 1.49 sec^{-1} . Sometimes, the sample adhered to the lower platen at shear rates of 0.47 and 0.74 sec^{-1} . For comparison, samples subjected to only oscillation wound stick to both the platens and when the platens were separated, the sample formed strands that connected the two platens. One experiment was stopped at the time the viscosity started the rapid rise. The sample was quite viscous but it was not a single mass that could not be lifted from the plates with a cable tie.

The visual observations of the samples showed that significant gel structure formed at the time of the rapid viscosity increase. The absence of adhesion of the sample to the platens and gelled nature of the sample indicated that slip occurred between sample and the platens which, in turn, produced meaningless data. It was concluded that accurate steady-shear data cannot be obtained for samples with significant structure, that is, a gel.

The presence of slip can be detected by measuring viscosities using the parallel-plate geometry.⁶ Viscosities measured at the same shear rate but at different gap settings should be the same in the absence of slip. Experiments were conducted on the Bohlin CS rheometer at seven different shear rates that ranged from 0.47 to 14.88 s^{-1} . Gap settings of 0.50 mm and 0.75 mm for each shear rate were used. Typical data for these runs are shown in Figure 7.10 for a shear rate of 14.88 s^{-1} . The data are reproducible up to approximately three hours after which the data deviate. Results obtained using the Bohlin rheometer confirmed the data obtained on the Weissenberg rheometer.

The shear stress at which slip occurred appeared to be the same for the runs where a rapid viscosity rise was observed. Shear stress (instead of viscosity) is plotted as a function of time for the experiments

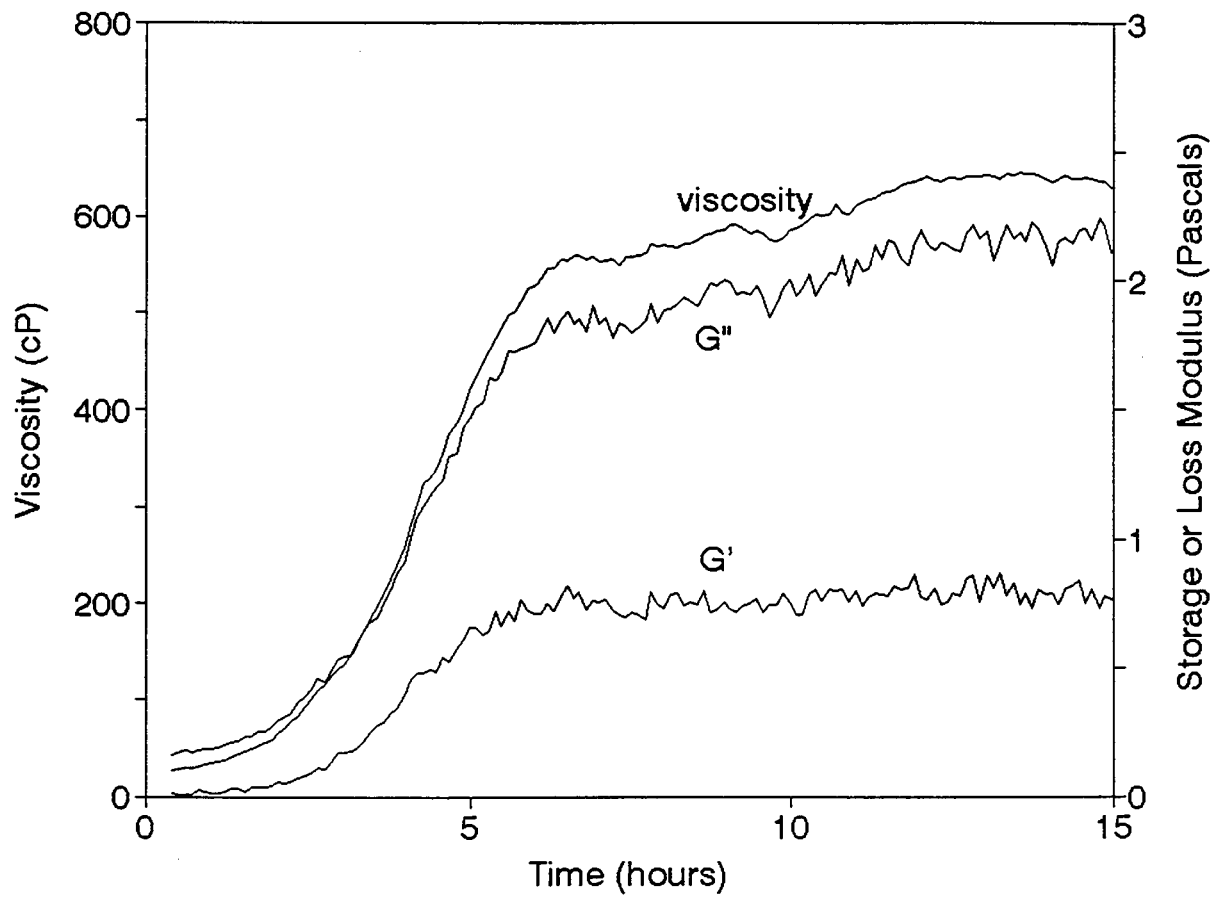


Figure 7.8: Rheological Data for Sample Subjected to a Shear Rate of 14.88 s^{-1} .
Rapid Rise in Viscosity and $G'-G''$ Cross-over Not Observed.

Table 7.1: Gel Times as determined by G'-G" Cross-over and Rapid Rise in Viscosity.

Shear Rate (sec ⁻¹)	Time @ G'-G" Cross-over (hours)	Time @ Rapid Viscosity Rise (hours)
0.0	2.76	-
0.47	2.44	2.44
0.74	2.15	2.15
1.49	1.74	1.74
2.35	1.33	1.28
4.70	2.64	no rapid rise
7.47	no cross-over	"
14.88	"	"
23.5	"	"
47.0	"	"

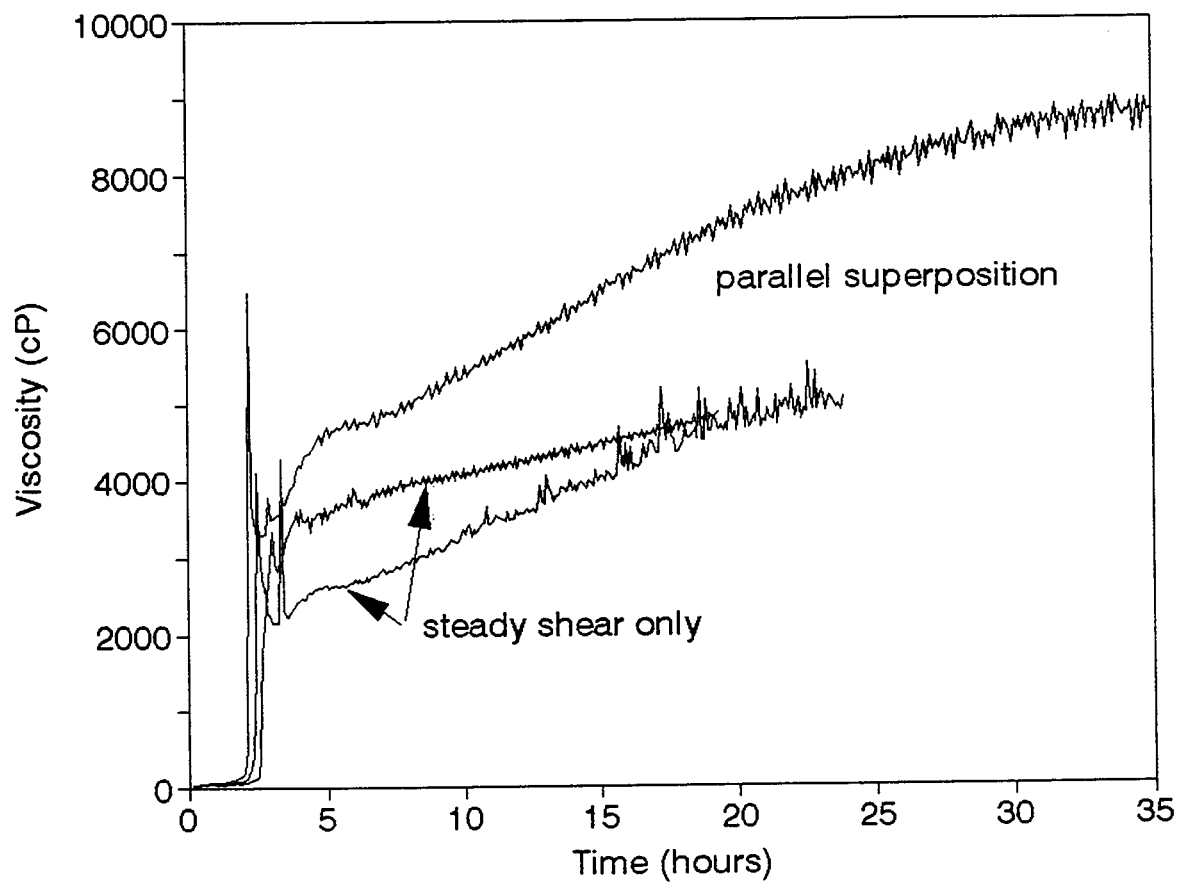


Figure 7.9: Comparison of Viscosity Behavior for Replicate Experiments.
Sample Subjected to Shear Rate of 0.74 s^{-1} on Wiesseberg Rheometer.

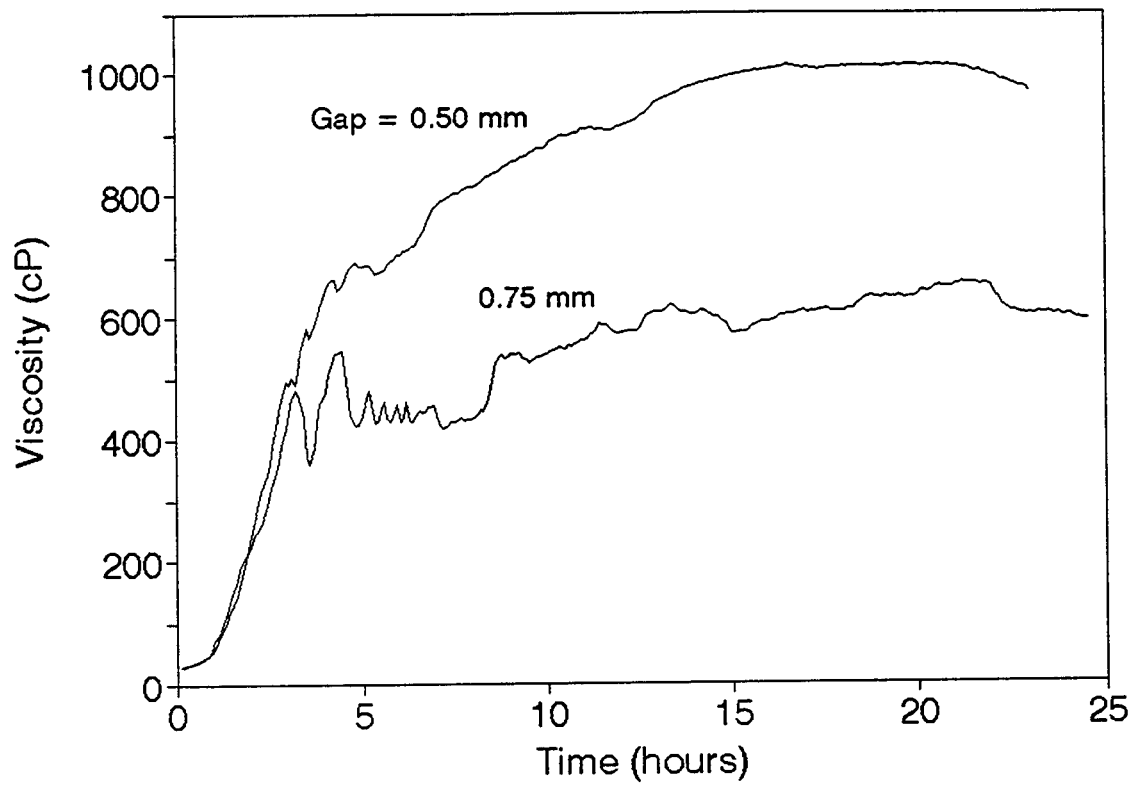


Figure 7.10: Comparison of Viscosity Behavior at Two Gap Settings Using Parallel-Plate Geometry.
Sample Subjected to Shear Rate of 14.88 s^{-1} on Bohlin Rheometer.

conducted at shear rates between 0.47 and 4.7 s^{-1} in Figure 7.11. It appears that slip occurred at a shear stress of between 2 and 3 Pascals. Similar results were obtained on the Bohlin rheometer using parallel-plate geometry. The significance of this value of shear stress is not presently understood.

Oscillatory Shear Experiments. Figure 7.12 shows two typical runs at 1.0 Hz. Such runs were performed periodically to test reproducibility and to indicate consistency between different polymer and chromium solutions, as well as proper functioning of the Weissenberg rheometer. Storage modulus values within about 10 percent for different oscillatory shear experiments were considered reproducible.

SUMMARY

Several characteristic responses were observed when a chromium(III)-polyacrylamide gel system was subjected to continuous steady shear during gelation on a rheometer using a cone-and-plate geometry. These responses and our interpretation of the gelation process under shear are summarized below.

- * There is an induction period where small increases in shear viscosity and storage modulus occur. Polymer aggregates formed by the gelation process are small and do not contribute significantly to the shear viscosity and storage modulus during the induction period.
- * There is an abrupt increase in viscosity and storage modulus at the end of the induction period for shear rates less than 14.88 s^{-1} . This point represents the onset of gelation caused by the rapid formation and crosslinking of aggregates.
- * Gelation was accelerated by increased shear rate, reaching a maximum rate at 2.35 s^{-1} , and was retarded for higher shear rates. No gelation occurred when shear rates are high, on the order of 40 s^{-1} .
- * When the gel was formed under continuous shear, the gelled material did not adhere to both platens and could be removed from the platens as a single mass. We conclude that there was slip between the gel and the platens during the later stages of the gelation process. Slip probably began after the abrupt increases in viscosity and storage modulus were observed.

REFERENCES

1. Aslam, S., Vossoughi, S. and Willhite, G.P., "Viscometric Measurement of Chromium(III)-Polyacrylamide Gels by Weissenberg Rheogoniometer," SPE/DOE Paper No. 12639, SPE/DOE Fourth Symposium on Enhanced Oil Recovery, Tulsa, OK (April 15-18, 1984).
2. Bhaskar, R.K., "Transient Rheological Properties of Chromium/Polyacrylamide Solutions Gelling under Superposed Steady and Oscillatory Shear Strains," Ph.D. Dissertation, University of Kansas (1988).
3. Kote, K., "Rheological Study of Cr(III)/Polyacrylamide Gels by Small Amplitude Oscillatory Shear," M.S. Thesis, University of Kansas (1984).
4. Stinson, J.A., "Effect of Shear Rate on the Formation of Chromium-Polyacrylamide Gels," M.S. Thesis, University of Kansas (1984).
5. Yoshimura, A.S. and Prud'homme, R.K., "Viscosity Measurements in the Presence of Wall Slip in Capillary, Couette, and Parallel-Disk Geometries," *SPE Reservoir Engineering* (May 1988).
6. Khanna, P., "A Study of Rheological Methods to Monitor Gelation of Polyacrylamide/Chromium(III) Gels," M.S. Thesis, University of Kansas (1995).

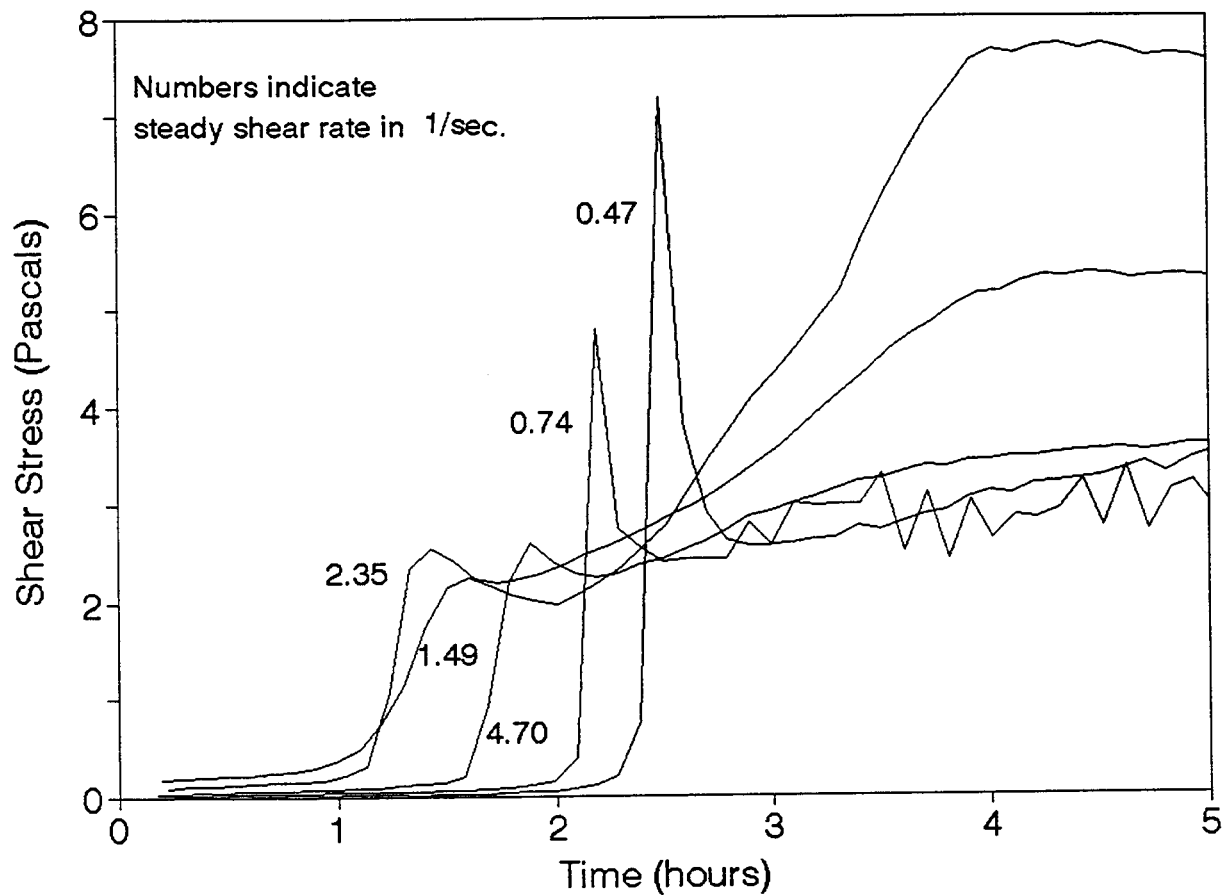


Figure 7.11: Stress as a Function of Time for Selected Shear Rates.
Data from Weissenberg Rheometer.

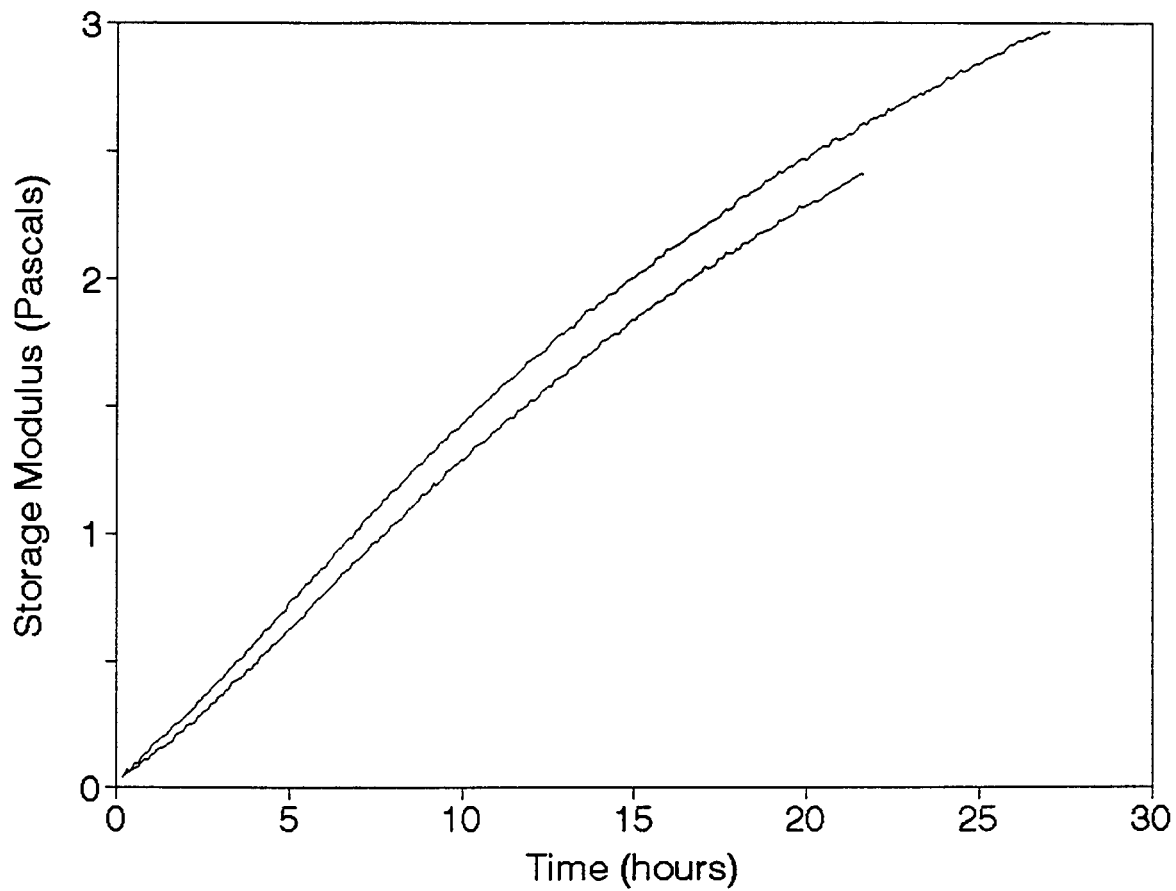


Figure 7.12: Development of Storage Modulus with Time for Replicate Samples Subjected to Oscillatory Shear Only.
Data from Weissenberg Rheometer.

Chapter 8

Investigation of the Polyacrylamide-Aluminum Citrate Gel System

Principal Investigators: G.P. Willhite, D.W. Green and C.S. McCool

Graduate Research Assistants: Raja Ranganathan, Robert Lewis

INTRODUCTION

In-depth placement of a gel system is an effective method of improving the subsequent water flood recovery in highly layered reservoirs. Conventional matrix gel treatments are usually limited to regions close to the wellbore, as the gelant can not propagate deep into the reservoir before it gels. The polyacrylamide-aluminum citrate "colloidal dispersion" gel system is claimed^{1,2} to penetrate deep into reservoirs. This claim was primarily based on field performance with little supporting laboratory work. The scope of this investigation is the understanding of the process by which this colloidal dispersion system reduces permeability.

The polyacrylamide-aluminum citrate system in the form of a colloidal dispersion gel was developed by TIORCO Inc., Englewood, CO. The formulation consists of low concentrations of HiVis 350°, a partially hydrolyzed polyacrylamide, and TIORCO 677°, a chelated aluminum citrate solution. Typical concentrations used in this system are 300 ppm polymer and 15 ppm Al³⁺. These systems are reported to be slow forming which allows large volumes that can be injected during field applications with the intent of altering flow patterns distant from the wellbore. It is speculated that polymer colloids, or gel aggregates, are formed which are then apparently filtered from solution by the rock, thereby reducing the permeability.

Comparison of different formulations of this gel system in the laboratory has been accomplished using a parameter termed the transition pressure. The transition pressure is a measure of the gel strength and is determined using a TGU apparatus³ that was developed at TIORCO Inc.

The objectives of this work are to determine the rheological properties of the system, to determine the size and rate of aggregate formation, and to determine how the system propagates and reduces permeability in porous media. Understanding the fundamental features of this system will improve the application of this technology to improved oil recovery. This chapter reports the progress made to accomplish these objectives.

RESULTS AND DISCUSSION

This investigation was divided into the following tasks.

1. Testing the gels and polymer solutions using a TGU apparatus that was constructed in our laboratory. This testing was conducted to confirm consistent formulation of solutions with those reported in the literature.
2. Determine viscosity of HiVis 350 polymer solutions as a function of concentration and shear rate.
3. Determine the size distribution of the polymer aggregates as a function of time.
4. Determine the behavior of the gel system in porous media.

Progress of each task is reported separately.

TGU Measurements. The TGU apparatus consists of a polyethylene tube with a screen pack (five 100-mesh stainless-steel screens) attached to one end. A test is performed by loading a solution into the tube and applying pressure to force the solution through the screen pack. The pressure and the time (Δt) required for 25 cc of the solution to flow through the screen pack is recorded. This test is conducted at several pressures on a gel solution and on a similar solution without the aluminum crosslinker. A TGU quantity is defined as the ratio of the times for the gel solution and the uncrosslinked polymer solution to flow through the screen packs at the same test pressure.

$$TGU = \frac{\Delta t_{gel\ soln}}{\Delta t_{polymer\ soln}} \quad (8.1)$$

A transition pressure for a particular gel solution was determined by plotting the polymer flow rate (in ml/sec) and the TGU values (dimensionless) as functions of the test pressures. The pressure at which these curves crossed was designated as the transition pressure. It has been proposed that these gels undergo a transformation from a squeeze flow to a free fluid-like flow through the screen pack at the transition pressure. The transition pressure is a measure of gel strength in that higher transition pressures denote stronger gels.

Gel solutions and uncrosslinked polymer solutions contained 0.5% KCl and were prepared from a stock solution containing 3000 ppm HiVis 350° polymer. Formulations consisted of polymer concentrations of 300, 600, 900 and 1200 ppm. Gel solutions contained aluminum citrate (TIORCO 677°) to achieve polymer-to-aluminum ratios of 20:1 and 40:1. Tests using TGU apparatus were conducted as a function of time from mixing.

Typical TGU and flow-rate curves are shown in Figure 8.1 for two times after mixing for a polymer concentration of 900 ppm and polymer-to-aluminum ratio of 20:1. The intersection of the TGU and the flow rate curve denotes the transition pressure which was 18 psi for a sample that was 8 hours old. Development of structure was indicated by the increase in transition pressure with time. Transition pressures determined for samples containing 600, 900 and 1200 ppm polymer were consistent with values reported in the literature.³

Transition pressure data for a 300 ppm polymer, 15 ppm aluminum gel system are presented as the top curve in Figure 8.2. The data indicated that *gelation* occurred within the first 12 to 24 hours. Gelation was in the form of aggregation with little visible structure as the sample did not indicate strong gel-like behavior. After 24 hours, the transition pressure increased marginally. The transition pressure obtained for this gel formulation was consistent with published data.³

Initial tests on solutions at a polymer concentration of 300 ppm exhibited anomalous behavior. The transition pressure increased initially to 8 psi at 24 hr and, thereafter, declined with time as shown in Figure 8.2. Visual observation of the gel indicated it to be water-like in appearance which indicated degradation of the gel. Flow-rate data for the uncrosslinked polymer solutions of 300 ppm concentration also indicated a similar degradation. Viscosity of the polymer and the gel solutions declined over the same time period.

The cause of the degradation of the solutions at polymer concentrations of 300 ppm was investigated. Tests conducted at TIORCO, Inc. determined that the water used in our laboratory produced the degradation problem. The laboratory water contained trace levels of chlorine (1/4 ppm). Subsequent tests showed that the addition of trace amounts of chlorine degraded gel solutions at the low polymer concentration of 300 ppm.

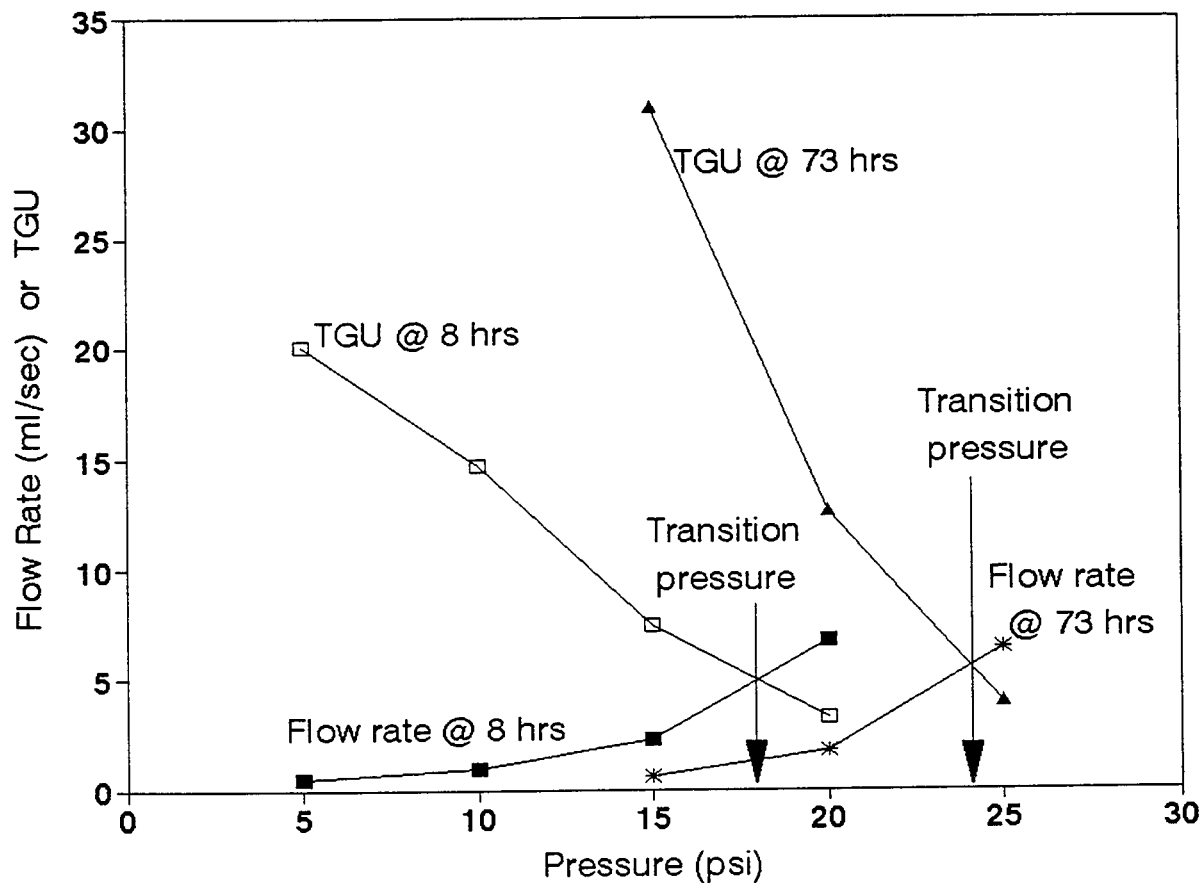


Figure 8.1: Transition Pressures Determined from TGU and Flow Rate Curves.
 Solution Composition: 900 ppm HiVis 350, 45 ppm Al^{+++} and 0.5% KCl.

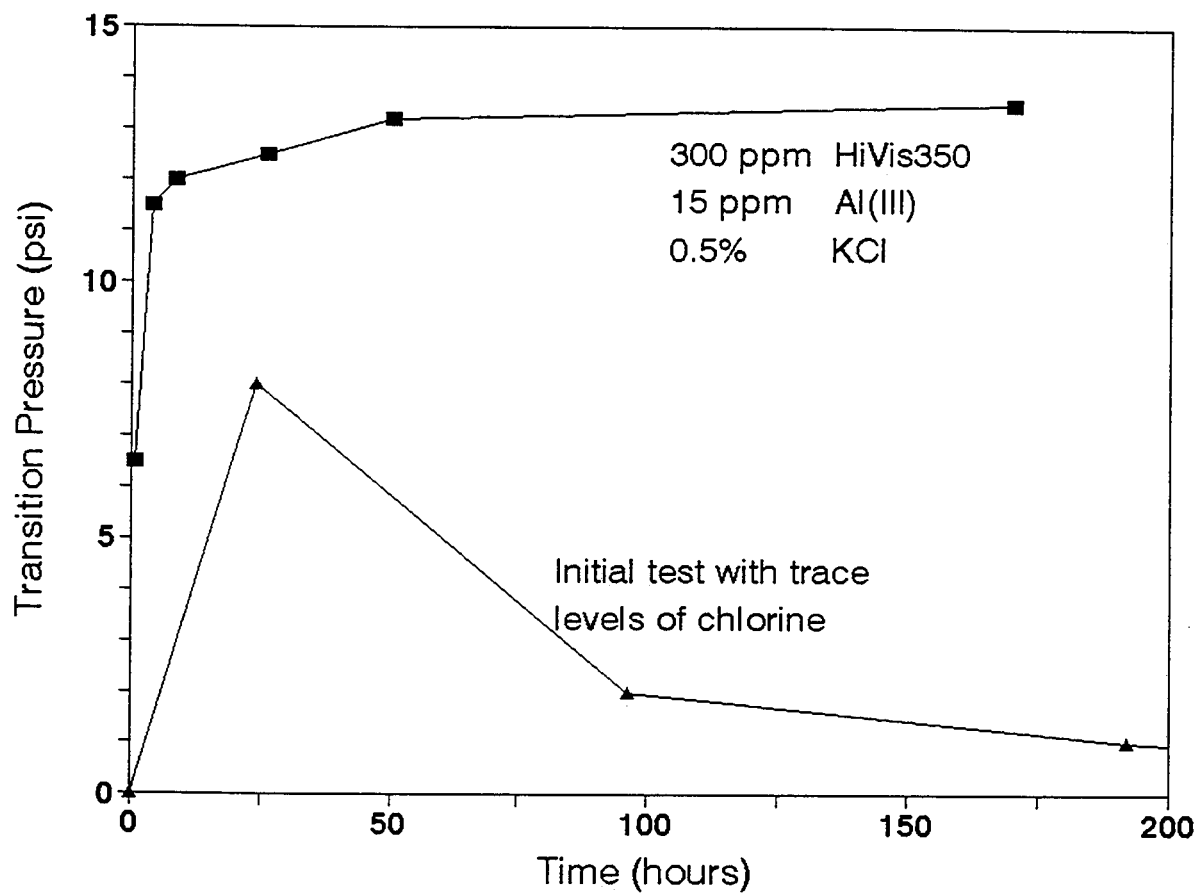


Figure 8.2: Development of Transition Pressure with Time.

Solution Composition: 300 ppm HiVis 3500, 15 ppm Al^{+++} and 0.5% KCl.

Viscometry Measurements. Viscosity was measured on HiVis 350 polymer solutions (uncrosslinked) as a function of polymer concentration, shear rate and time. Solutions were prepared with polymer concentrations of 3000, 1500, 900, and 300 ppm in 0.5% KCl. The viscosity data for the solution containing 900 ppm are presented in Figure 8.3. The viscosity was shear thinning and a minor reduction in viscosity occurred over the time period studied.

The viscosity data when the solutions were one-day old were correlated as a function of polymer concentration and shear rate with Equation 8.2.

$$\eta = K \cdot \gamma^{n-1} \quad (8.2)$$

where

η	=	viscosity, (cp)
γ	=	shear rate, (sec^{-1})
K	=	$1.739 \times 10^4 C^{1.903}$
$1/n$	=	$0.2916 C^{0.2676}$
C	=	polymer concentration, (ppm)

This range of shear rates over which the data were correlated were:

Polymer Concentration (ppm)	Shear rate (s^{-1})	
	minimum value	maximum value
3000	0.01	200
1500	0.1	100
900	0.5	20
300	5.0	40

The experimental data and the correlation, which is represented by the solid lines, are shown in Figure 8.4. The correlation represented the viscosity data well except for the 300 ppm polymer solution.

Measurement of Size Distributions of Gel Aggregates. The objective of this work is to study the development of structure, or aggregate growth, during the gelation reaction between polyacrylamide and aluminum(III). The size distribution of the formed aggregates as a function of reaction time is the key data required to accomplish this objective. A procedure to determine the size distribution was developed previously.⁴ The basic steps of the technique are (1) quench the gelation reactions by dilution, (2) separate the gel aggregates by size using membrane dialysis, and (3) analyze the dialysis products for polymer concentration. Details of this procedure are given reference 4.

The work to date has focused on finding a suitable analytical procedure for determining the concentration of polymer. Two methods have proven unsatisfactory. Problems developed with a size-exclusion chromatography/UV detection method due to polymer retention and plugging in the column. This problem was specific to the HiVis 350 polymer. The analytical procedure worked fine with other polyacrylamides of lower molecular weights. Example chromatograms for the HiVis 350 polymer and a well behaved polyacrylamide are shown in Figure 8.5. The HiVis 350 polymer produced a long tail which indicated

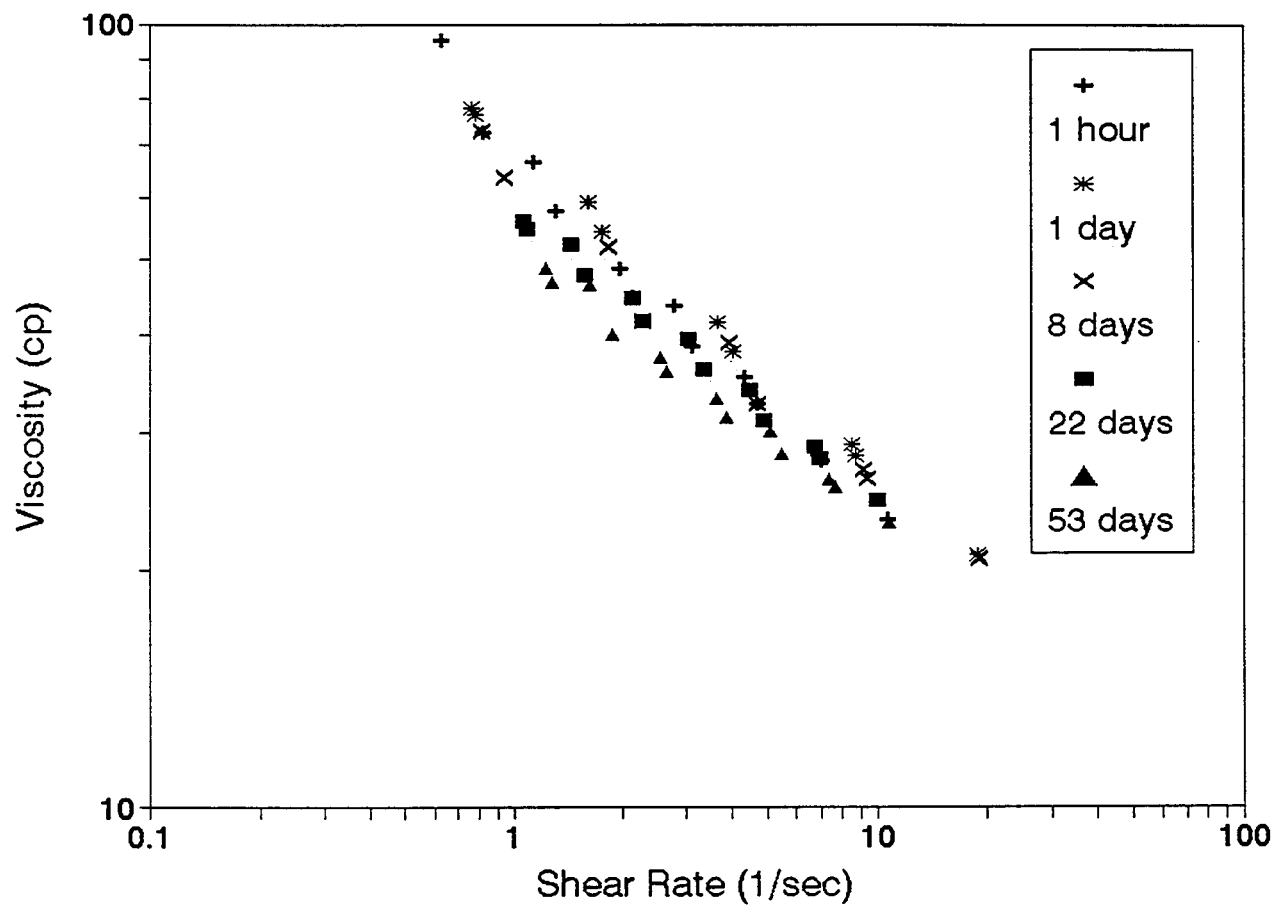


Figure 8.3: Viscosity as a Function of Shear Rate and Age.
Solution Composition: 900 ppm HiVis 3500 and 0.5% KCl.

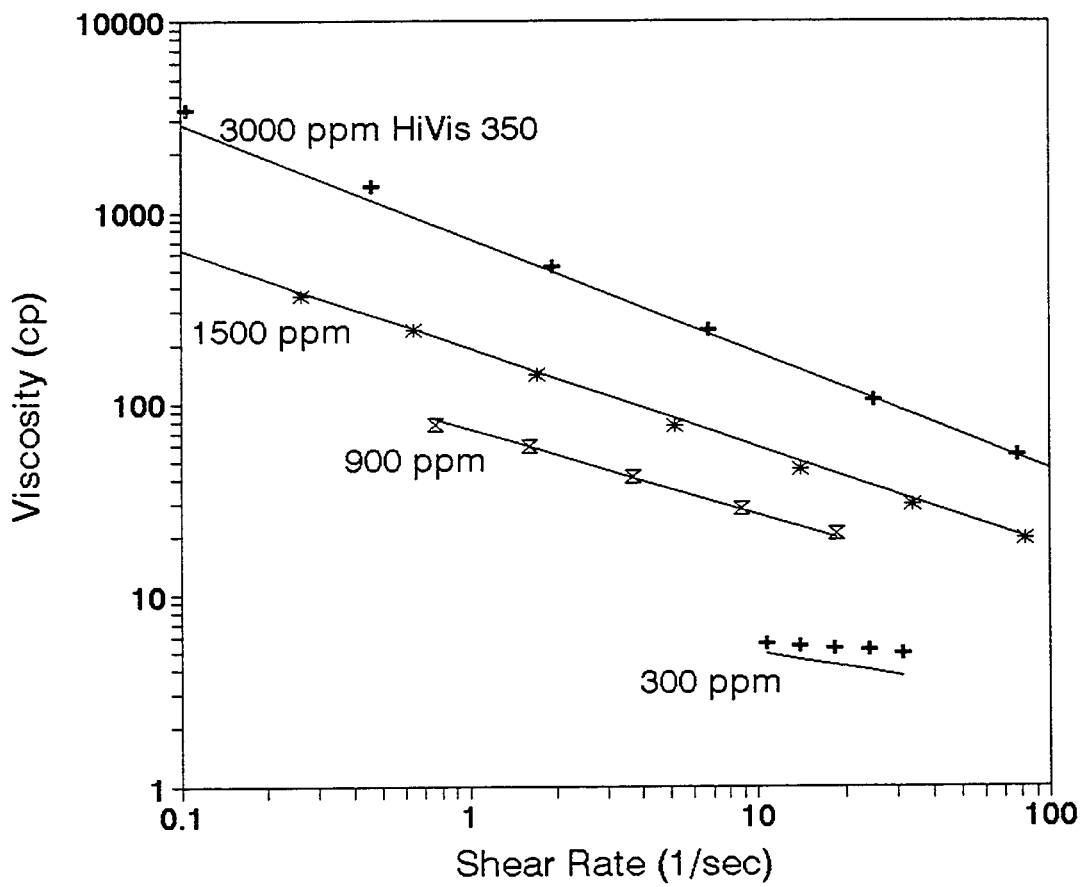


Figure 8.4: Comparison of Experimental Viscosity Data with Correlation.
Solution Composition: HiVis polymer and 0.5% KCl.

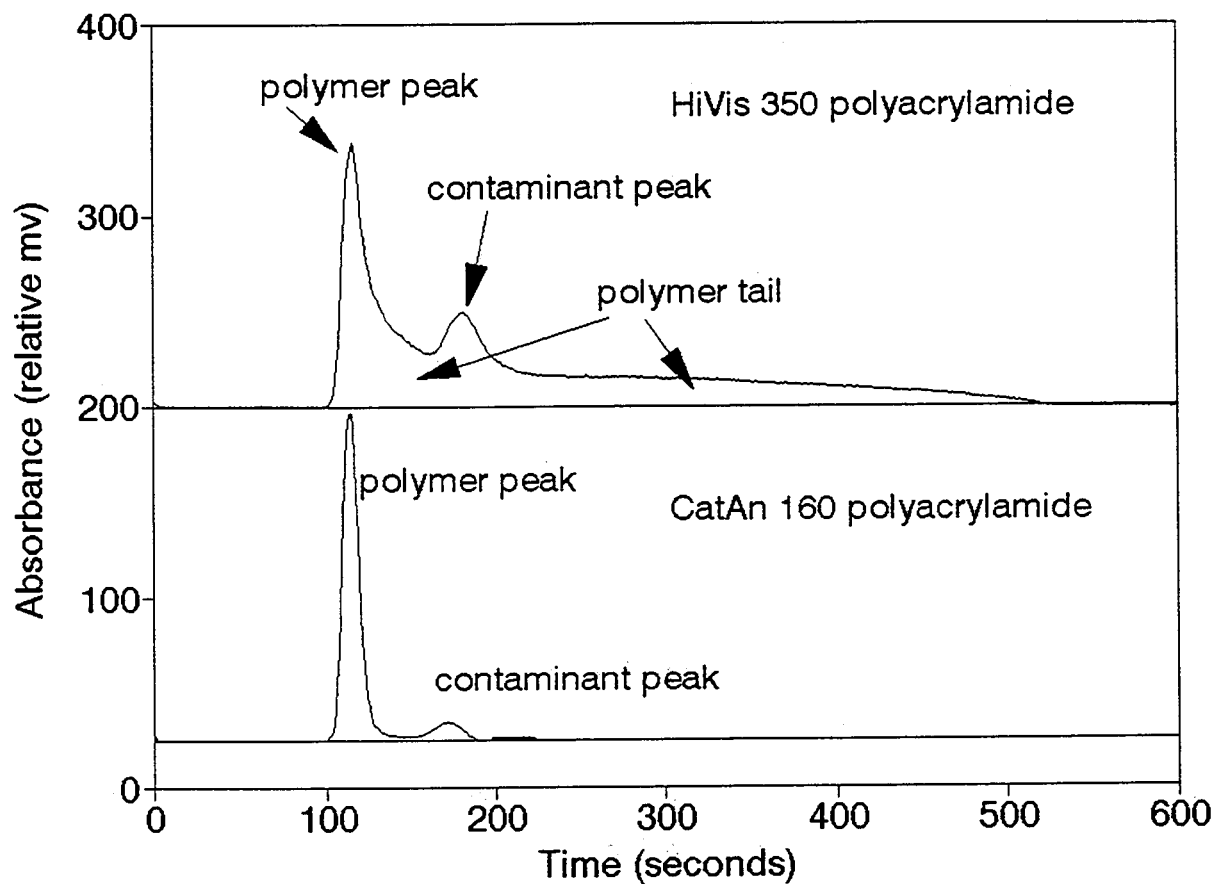


Figure 8.5: Comparison of Chromatograms for Two Polyacrylamides.

a significant amount of very large polymer molecules. Three column packings were examined. Problems persisted with a column packing using a large particle size of 80/120 mesh.

An alternate method for polymer analysis is based on the turbidimetric reaction between polyacrylamide and bleach.⁵ This method was also rejected because of interactions between the reagents and the aluminum citrate. A third method⁶ will be examined in future work.

Flow Experiments in Porous Media. An initial flow experiment with the HiVis 350 polyacrylamide-aluminum citrate system was conducted in a four-foot long, 1.5" ID sandpack. Six pressure ports divided the sandpack into seven sections. Pressure drops were measured across each section of the sandpack and across the entire sandpack length. Permeability of the sandpack was 3.65 darcies. A polymer solution and an aluminum citrate solution were mixed in-line and injected into the sandpack. The injected solution contained 300 ppm polymer and 15 ppm aluminum and was injected at a frontal advance rate of 1 ft/day. About 0.6 pore volumes of solution were injected over 55 hours. At approximately 53 hours, the pressure drop measured over the entrance section of the sandpack increased rapidly. Injection was terminated due to excessive pressure. Inspection showed that a blob of gel material had formed just inside the screen placed at the inlet of the sandpack. Screens were used to contain sand in the holder.

Pressure-drop data from the remaining sections of the sandpack showed that the gel solution propagated through the sandpack without any significant buildup of flow resistance. The apparent viscosity in these sections increased to values of approximately 8 cp as the gel solution flowed through each section. The calculated apparent viscosities were consistent with viscosity of the uncrosslinked gel solution. No reduction in permeability of the sandpack was observed during the 55 hours of injection even though structure development in a bulk gel was nearly complete within 25 hours (see Figure 8.2).

The plugged endscreen was removed and the sandpack recompleted. An uncrosslinked 300 ppm polymer solution was injected to displace the resident gel solution through the sandpack. Two hours after the gel solution was detected in the effluent, the pressure drop in the last section of the sandpack increased sharply. Again, a gel blob had formed on the downstream side of the screen that was placed at the outlet. This problem of gel formation as the gel solution flows through screens will be addressed in future work.

SUMMARY

1. Small concentrations of chlorine (< 1/4 ppm) degrade HiVis 350 polymer solutions and gels prepared at polymer concentrations of 300 ppm. Chlorine must be eliminated from the solutions before reproducible and stable viscometry and TGU measurements can be obtained.
2. Viscosity has been characterized for HiVis 350 in 0.5% KCl brine. These data have been correlated as a function of shear rate and concentration.
3. Two standard methods for the determination of polyacrylamide concentration were not suitable for polymer solutions and gel solution prepared with HiVis 350 and aluminum citrate.
4. Plugging of the screens used at the ends of the sandpacks was observed during initial flow tests of the HiVis 350-aluminum citrate gel system. No significant permeability reduction was observed in the sand during flow.

REFERENCES

1. Mack J.C. and Smith J.E., "In-Depth Colloidal Dispersion Gels Improve Oil Recovery Efficiency," SPE paper 27780, presented at the SPE/DOE Ninth Symposium on Improved Oil Recovery, Tulsa, OK (April 17-20, 1994).
2. Fielding, R.C., Gibbons, D.H. and Legrand, F.P., "In-Depth Drive Fluid Diversion Using an Evolution of Colloidal Dispersion Gels and New Bulk Gels: An Operational Case History of North Rainbow Ranch Unit," SPE paper 27773, presented at the SPE/DOE Ninth Symposium on Improved Oil Recovery, Tulsa, OK (April 17-20, 1994).
3. Smith, J.E., "The Transition Pressure: A Quick Method for Quantifying Polyacrylamide Gel Strength," SPE paper 18739, presented at the SPE International Symposium on Oilfield Chemistry, Houston, TX (Feb. 8-10, 1989).
4. McCool, C.S., "An Experimental Study of the In Situ Gelation of a Polyacrylamide-Chromium(III)-Thiourea System in a Porous Medium," PhD dissertation, University of Kansas (1988).
5. Foshee, W.C., Jennings, R.R. and West T.J., "Preparation and Testing of Partially Hydrolyzed Polyacrylamide Solutions," SPE paper 6202, presented at the 1976 Annual Technical Conference and Exhibition, New Orleans (Oct. 3-6).
6. Allison, J.D., Wimberly, J.W. and Ely T.L., "Automated and Manual Methods for the Determination of Polyacrylamide and Other Anionic Polymers," *SPE Reservoir Engineering*, (May 1987) 184-188.

Chapter 9

Simulation of Alkali-Sandstone Interactions in Core-Flood Experiments

Principal Investigators: G.P. Willhite, D.W. Green, C.S. McCool
Graduate Research Assistant: Vikas Midha

INTRODUCTION

Fluid-rock interactions play a key role in gelled polymer treatments. This study considers the mathematical modeling of the effect of fluid-rock interactions on the pH of alkaline solutions in sandstone cores. A one-dimensional flow model incorporating the kinetics of silica dissolution and sodium/hydrogen ion-exchange equilibria was developed. Since a detailed description of the mathematical model is available in References 1 and 2, only a brief summary of the governing equations is presented here.

Previous work in this study considered the individual effects of the silica dissolution reaction and sodium/hydrogen ion-exchange in core-flood experiments. In order to study the simultaneous effects of the two reactions, a set of core-flood experiments reported in the literature was simulated with the proposed flow model. These experiments were selected to encompass the large range of physical conditions which cannot be simulated using local-equilibrium models such as the UTCHEM simulator.^{3,4}

MATHEMATICAL MODEL

The generalized equation of continuity for the i^{th} chemical species accounting for adsorption, convection, dispersion, and chemical reaction in the fluid phase is given by:

$$\frac{\partial C_i}{\partial \tau} + \sum_{i=1}^{i=N} \alpha_i \frac{\partial C_i}{\partial \tau} = -\frac{\partial C_i}{\partial \xi} + \frac{1}{Pe} \frac{\partial^2 C_i}{\partial \xi^2} + Da_i f_i(C), \dots \dots \dots \quad (9.1)$$

where τ and ξ are dimensionless time and distance defined by:

$$\tau = t \frac{v}{\phi L}, \dots \dots \dots \quad (9.2)$$

and

$$\xi = \frac{x}{L}. \dots \dots \dots \quad (9.3)$$

$f_i(C)$ denotes the dimensionless rate expression for the i^{th} chemical species. The initial condition and boundary conditions are:

$$1) \tau = 0 \quad C_i = C_{\text{initial}} \quad \text{for all } \xi, \dots \dots \dots \quad (9.4)$$

$$2) \xi = 0 \quad C_i = C_{\text{inj}} \quad \text{for all } \tau > 0, \dots \dots \dots \quad (9.5)$$

$$3) \xi = 1 \quad \frac{\partial C_i}{\partial \xi} = 0 \quad \text{for all } \tau > 0. \quad \dots \dots \dots \quad (9.6)$$

Equation 9.1 is characterized by the following groups of parameters:

(1) The Peclet Number, Pe , which characterizes the physical dispersion in the core and is defined by:

$$Pe = \frac{Lv}{K_f \phi}. \quad \dots \dots \dots \quad (9.7)$$

(2) The Damkohler Group, Da_i , given by:

$$Da_i = \frac{k_i \alpha_s \rho_s (1-\phi)}{\phi} \frac{L\phi}{v}. \quad \dots \dots \dots \quad (9.8)$$

This group physically represents the ratio of the characteristic residence time to the characteristic reaction time for the silica-dissolution reaction. A high value of Da , therefore, signifies relatively more time is available for reaction with greater silica dissolution in the core.

(3) The dimensionless retardation factors, α_{Na^+} and α_{OH^-} defined as:

$$\alpha_{Na^+} = \left(\frac{\alpha_s \rho_s (1-\phi)}{\phi} \right) \frac{n_T K_f C_{OH^-}}{(1 + K_f C_{Na^+} C_{OH^-})^2}, \quad \dots \dots \dots \quad (9.9)$$

$$\alpha_{OH^-} = \left(\frac{\alpha_s \rho_s (1-\phi)}{\phi} \right) \frac{n_T K_f C_{Na^+}}{(1 + K_f C_{Na^+} C_{OH^-})^2}. \quad \dots \dots \dots \quad (9.10)$$

These parameters characterize the chromatographic retardation of the Na^+ and OH^- species in the core due to sodium/hydrogen ion-exchange in the core.

The complete flow model consists of the set of continuity equations with the corresponding reaction expressions for the Na^+ , OH^- , H_4SiO_4 , $H_3SiO_4^-$ and $H_2SiO_4^{2-}$ species. The hydrogen-ion concentration is calculated by the following equilibrium relation :

$$C_{H^+} = \frac{K_w}{C_{OH^-}}. \quad \dots \dots \dots \quad (9.11)$$

The Cl^- concentration is found by an overall charge balance in the fluid phase :

$$C_{\text{Cl}^-} = C_{\text{Na}^+} + C_{\text{H}^+} - C_{\text{OH}^-} - C_{\text{H}_3\text{SiO}_4^-} - 2C_{\text{H}_2\text{SiO}_4^{2-}} \dots \dots \dots \quad (9.12)$$

The governing set of partial differential equations given by Equations 9.1 through 9.12 were solved numerically using finite-difference approximations.^{1,2}

RESULTS AND DISCUSSION

Before discussing the results, it is important to recognize some of the problems encountered in the simulations. First, it was necessary to consider only those experiments that satisfied all the restrictions in the model. For example, the silica dissolution kinetics are valid only for pH values less than 13. At higher pH values, the precipitation of various oligomers will take place which is not considered in the model. Similarly, the clay content of the core was assumed to be low so that the dissolution and precipitation of clay minerals was negligible.

Second, some key physical parameters like the dispersion coefficient of the core, specific area of the solid particles and the values of the reaction parameters are not known a priori. The rate constant k_1 is a function of temperature, pH and ionic strength of the solution. An empirical relation given by House and Orr³ provides estimates of k_1 as a function of pH but does not describe its strong dependence on temperature and ionic strength. Similarly, the ion-exchange parameters n_T and K_1 are specific to a given core at a fixed temperature. Some of typical values of n_T for sandstone cores are of the order of 0.1-1.0 meq/(100g solid) and reported values of K_1 vary from 10^{-2} to 10^{-6} N².^{6,7,8} The ion-exchange reaction is a mildly exothermic in nature so the value of K_1 is expected to decrease at higher temperatures. Once again, these values provide, at best, only an estimate of the order of magnitude of n_T and K_1 .

It was necessary to estimate many of the parameters required in the model for simulating the experiments reported in the literature. For simplification purposes, typical values of the system parameters are adopted as a reference set of parameters. These values are shown in Table 9.1. A lumped correction factor for the Damköhler Group (Da) in Equation 9.8 was used to account for the total correction in the overall rate of silica dissolution due to temperature and specific area. Higher temperatures will increase the magnitude of k_1 and will result in a correction factor greater than unity. The specific area, a_s , determines the total surface area for the dissolution reaction and a specific area less than the reference value of 2 m²/g will produce a correction factor less than unity. The lumped correction factor, the ion-exchange parameters and the dispersion were estimated simply by matching the results from the model with experimental data.

The first experiment considered for simulation purposes consisted of a caustic flood of a Berea sandstone core at 50°C conducted by Radke and Jenson⁸ to study the sodium/hydrogen ion-exchange reaction. Hence, a high flow rate was used to reduce the effects of silica dissolution on the pH profile. The physical parameters of the experiment are summarized in Table 9.2.

Figure 9.1 shows the histories of the reduced concentrations of the Na^+ and the OH^- species (concentrations are normalized by injected values) predicted by the model compared to the experimental results. The model predicts the formation of a coherent ion-exchange wave which appears in the effluent after a delay of 2.4 PV. At the high pH values of the ion-exchange wave, hydroxide ions are consumed by the silica dissolution reaction. This consumption is small due to the short residence time of the experiment. The model also predicts the formation of the intermediate plateau in the concentration history

Table 9.1: Summary of the reference physical parameters used in the simulations.

Porosity :	0.20
Specific surface area :	2 m ² /g
Solid density :	2.5 g/cm ³
Rate constant k_1 :	$10^{(-14.55+0.361\text{pH})}$ (moles/m ² .sec.) for pH < 11 10^{-7} (moles/m ² .hr.) for pH > 11
Equilibrium quotient Q_1 :	1 E4 moles/liter
Equilibrium quotient Q_2 :	2 E4 (moles/liter) ⁻¹
Equilibrium quotient Q_3 :	10 (moles/liter) ⁻¹
Equilibrium constant F_K :	1.0

Table 9.2: Summary of the physical parameters for the alkaline flood by Radke and Jenson⁸.

Porosity :	0.21
Solid density :	2.56 g/cm ³
Superficial velocity :	3.47 m/day
Core length :	44.7 cm
Initial brine :	1% NaCl (pH=9.45)
Injected solution :	2.08% NaCl, 0.02% NaOH (pH=11.69)

of the Na⁺ species. This plateau corresponds to breakthrough of the intermediate region between the ion-exchange wave and the salinity wave in the effluent. There appears to be some discrepancy between the predicted value of Na⁺ concentration and the experimental value. The reason for this discrepancy is not completely understood. In addition, there is a significant amount of dispersion in the experimentally determined concentration histories which are not shown by the simulated profiles. A part of this disparity is probably due to some inaccuracies in the estimation of parameters in the simulation. Radke and Jenson also propose that extraneous dispersion may be caused by internal-diffusion resistances which reduce the accessibility of the mineral exchange sites for sodium and hydrogen species. These mass-transfer limitations were not considered in the proposed model.

It is instructive to examine the parameters used in the simulations. A correction factor of 5 was applied to the reference Damkohler Group to account for the increased rate of silica dissolution at the elevated temperature. It was found that an ion-exchange capacity, n_T , of 0.125 meq/100g solid and an equilibrium constant, K_i , of 10^4 N⁻² were required to match the experimental data. These values are well within the expected range of values for these parameters.

In this particular example, it is possible to further test the validity of the ion-exchange parameters used in the simulation. Radke and Jenson conducted a series of similar experiments at different concentrations of NaOH to estimate the values of n_T and K_i for their system. The sodium-ion uptake was fit by the ion-exchange isotherm to yield an n_T value of 0.18 meq/100g solid and a K_i value of $10^{3.3}$ N⁻².⁸ Given the

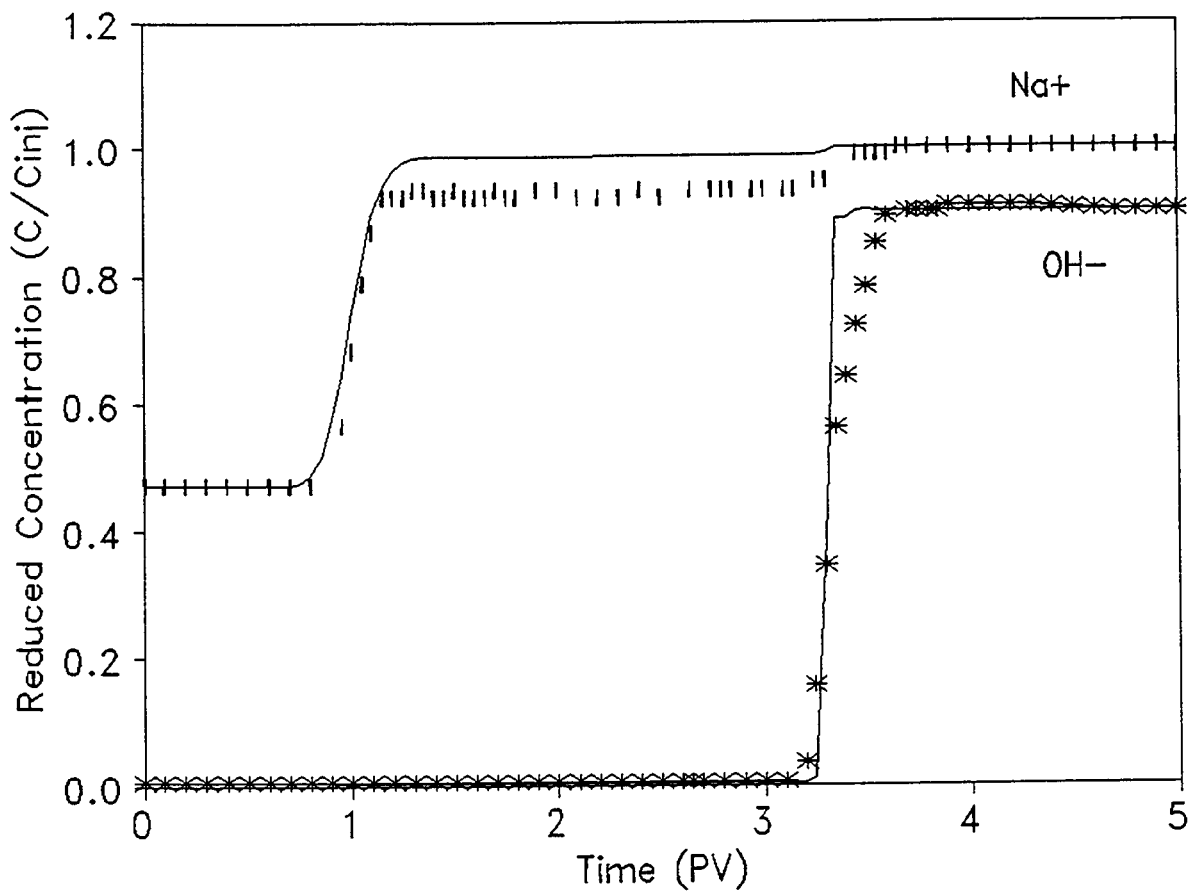


Figure 9.1: Simulated histories of the reduced concentrations of sodium and hydroxide compared to experimental data by Jenson and Radke⁸ (correction factor = 5, $K_t = 1E4$ (moles/liter)⁻², $n_T = 0.125$ meq/(100g solid)).

amount of scatter between the experimental data and their fitted isotherm, the values of n_T and K_i used in the simulations seem quite reasonable.

The second case consisted of the simulation of an alkaline flood of a Berea core at 23°C conducted by Novosad and Novosad⁹ to study the effect of flow rate on the hydroxide- and sodium-ion concentration histories. The experimental conditions are summarized in Table 9.3.

Table 9.3: Summary of the physical parameters for the alkaline flood by Novassad and Novassad⁹.

Porosity :	0.19
Core length :	10 cm
Superficial velocity :	4 cm/hr
Initial brine :	1 N NaCl
Injected solution:	0.06 N NaCl, 0.04 N NaOH
Total sodium uptake :	0.4 (meq/100g)

It was necessary to estimate the ion-exchange parameters K_i , n_T and the correction factor for the Damkohler Group. The equilibrium constant at 23°C is expected to be relatively high and a value of 10^4 N² was arbitrarily selected. Under these conditions, the sodium-ion uptake at high pH values is approximately equal to the total cation-exchange capacity of the sand. Hence, the value of n_T is estimated to be 0.4 meq/100g sand. A correction factor of 6 was required to describe the silica dissolution reaction in the core. At the given temperature, this value is relatively high and may be due to differences in the specific area from its reference value.

Figure 9.2 shows the experimental data compared to the profiles predicted by the model. The calculated sodium-ion history shows a good match with the experimental data. Due to the large amount of dispersion, mixing between the salinity wave and the ion-exchange wave takes place and a distinct intermediate region is not formed. Based on the theoretical considerations, the ion-exchange wave for the hydroxide species is expected to be coherent with the sodium ion-exchange wave. Thus, the model predicts a steady concentration of hydroxide in the effluent after a delay of 2 PV. The experimental values for the hydroxide-ion history, however, show considerable scatter even after the sodium-ion profile attains a constant value. Silica dissolution within the core is significant and the model predicts a steady concentration of hydroxide which is significantly less than the injected value. On halving the flow rate after 4.5 PV, the contact time for the injected solution is doubled and there is a greater consumption of hydroxide ions by the dissolution reaction. The experimental results also show a drop in the hydroxide concentration, but the decrease is greater than what is predicted by the model. As the hydroxide-ion concentration in the fluid phase decreases, the concentration of the adsorbed sodium ions (in equilibrium with the fluid-phase concentrations) also decreases. Hence, there is a slight increase in the fluid-phase concentration of the Na⁺ ions when the flow rate is reduced. This increase, however, is too small to be measured in the experiment.

The final example considers the effect of flow rate on the silica dissolution reaction in greater detail. Bunge and Radke⁶ reported results from alkaline floods in a Huntington Beach sand core at four different flow rates by Lieu.¹⁰ A single set of parameters must be used to characterize all the profiles. A low value of K_i equal to 10^2 N² was selected in order to be consistent with the high temperature of 85°C. The cation-exchange capacity used in the simulations was 1.25 meq/(100g solid) which is relatively high but still acceptable. It was also necessary to decrease the rate of the silica dissolution reaction by using a

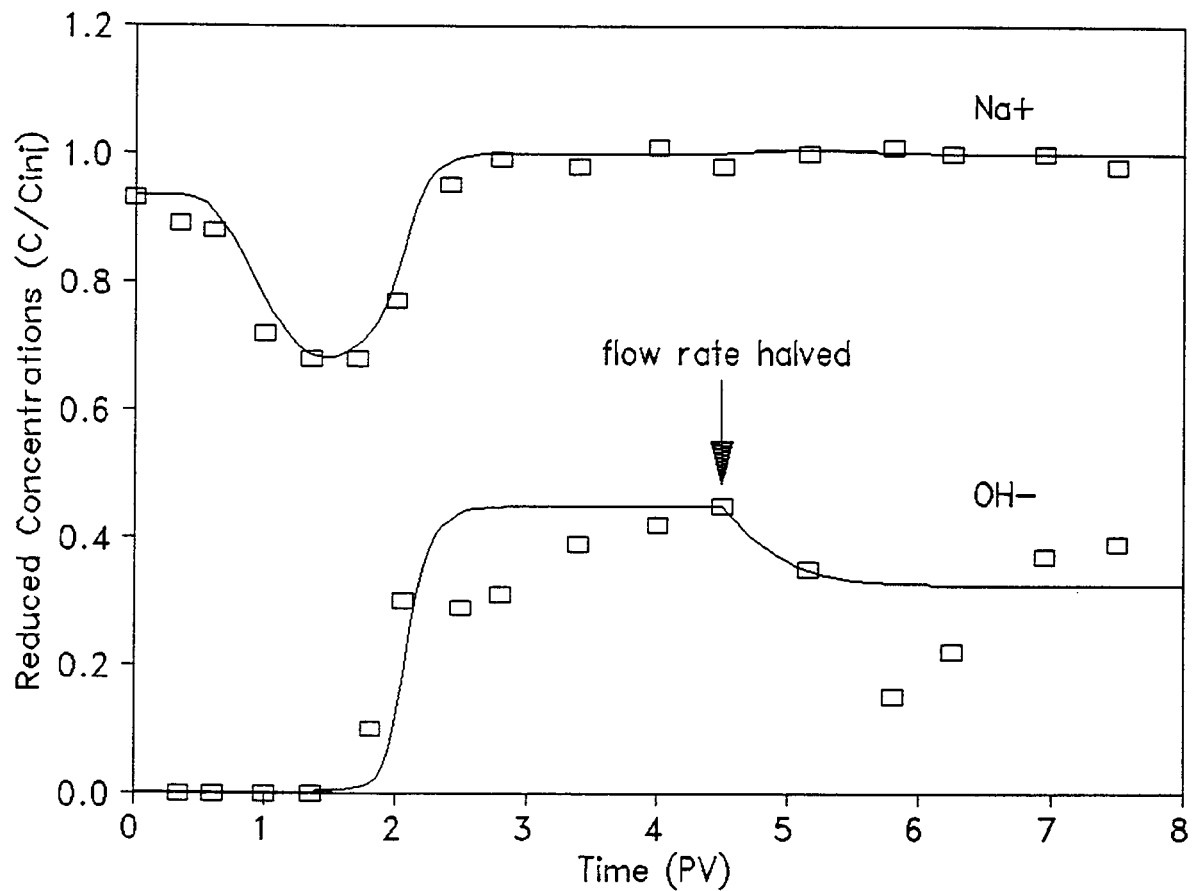


Figure 9.2: Simulated histories of the reduced concentrations of sodium and hydroxide compared to experimental data from Novassad and Novassad⁹ (correction factor=6, $K_l = 1E4$ (moles/liter)², $n_T = 0.4$ meq/100g solid).

correction factor of 0.14 to fit the data. This is surprising considering the elevated temperature of the experiment, but is acceptable given the uncertainty regarding the physical characteristics of the rock.

Figure 9.3 shows that there is good agreement between the hydroxide ion history predicted by the model and the experimental data. As the flow rate is reduced, the residence time of the injected solution is increased. This results in progressively more consumption of hydroxide ions by the silica-dissolution reaction. The ion-exchange reaction results in a delay of about 2.5 PV before the breakthrough of the injected hydroxide concentrations. This delay is independent of the flow rate and suggests the validity of the assumption of local equilibrium for the sodium/hydrogen ion-exchange reaction. There are, however, some minor discrepancies between the predicted profiles and experimental data at low hydroxide concentrations. A better fit would require some adjustment of the parameters for dispersion and the ion-exchange reaction but, due to the lack of sufficient data in this region, it was not attempted.

CONCLUSIONS

The simulation of three independent core-flood experiments shows that the proposed model describes all the essential features seen in experimental results. In each case, the estimated values of the reaction parameters correspond to typical values suggested in the literature. Furthermore, a single set of parameters was used to simultaneously describe all the concentration profiles in an experiment. These results, therefore, establish the validity of the assumptions in the model and the underlying mechanisms for silica dissolution and sodium/hydrogen ion exchange.

NOMENCLATURE

a_s	specific surface area of the solid particles (m^2/g).
C	vector representing the concentrations of all the transported species (moles/liter PV).
C_i	concentration of i^{th} species in the fluid phase (moles/liter PV).
C_{inj}	injected value of concentration (moles/liter PV).
Da	Damkohler Group (moles/liter).
$f_i(C)$	reaction rate expression in terms of the species concentrations (dimensionless).
k_1	surface reaction rate constant (moles/ $m^2 \cdot hr$).
K_d	dispersion coefficient (m^2/hr).
K_I	equilibrium constant for sodium/hydrogen ion-exchange reaction (moles/liter) ² .
K_w	equilibrium quotient for water (moles/liter) ² .
L	length of the core (m).
n_{Na^+}	concentration of the adsorbed form of the Na^+ species on the rock (meq/ m^2 solid).
n_{OH^-}	concentration of the adsorbed form of the OH^- species on the rock (meq/ m^2 solid).
n_T	total cation exchange capacity of the rock (meq/ m^2 solid).
Pe	Peclet Number (dimensionless).
$R_i(C)$	rate of generation of the i^{th} species per unit volume (moles/liter.hr).
t	time (hr).
v	superficial velocity of injected brine (m/hr).
x	distance (m).

Greek symbols

α_{Na^+}	retardation factor for the Na^+ species (dimensionless).
α_{OH^-}	retardation factor for the OH^- species (dimensionless).
ξ	dimensionless distance in x direction.
ρ_s	bulk density of the rock (g solid/liter solid).
τ	dimensionless time.
ϕ	porosity of the core (dimensionless).

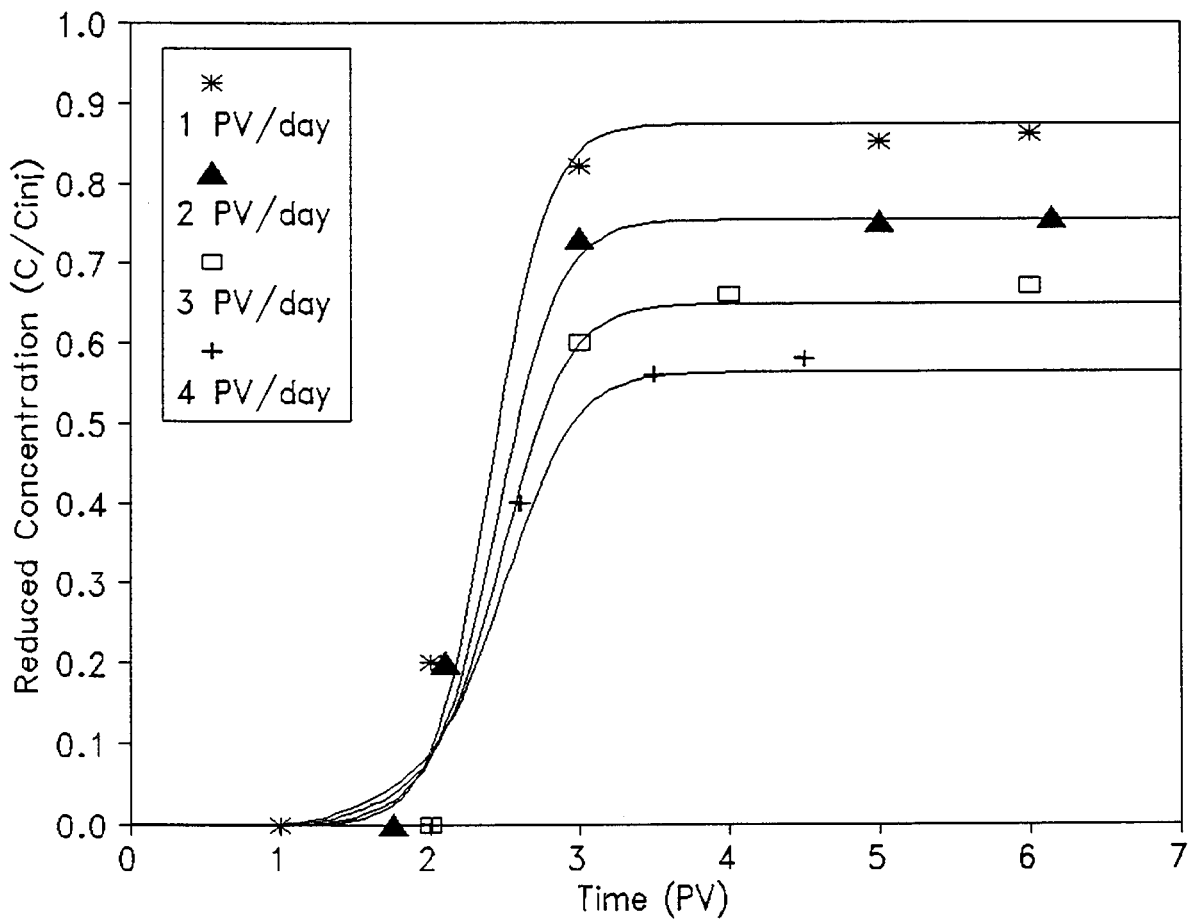


Figure 9.3: Simulated histories of the reduced hydroxide concentrations compared to experimental data reported by Bunge and Radke⁶ (correction factor = 0.14, $K_i = 1E2$ (moles/liter)², $n_T = 1.25$ meq/100g solid).

REFERENCES

1. Midha, V., "Mathematical Modeling of Fluid-Rock Interactions During the Flow of Alkaline Solutions Through Porous Media," M.S. Thesis, University of Kansas, 1994.
2. Green, D.W. and Willhite, G.P., "Improving Reservoir Conformance Using Gelled Polymer Systems," Annual Report, DOE Contract No. DE-AC22-92BC14881 (August 1994).
3. Bhuyan D., Lake, L.W. and Pope, G.A., "Mathematical Modeling of High pH Chemical Flooding," *SPERE*, (May 1990) 212-220.
4. Bhuyan, D., "Development of an Alkaline-Surfactant-Polymer Compositional Reservoir Simulator," Ph.D Dissertation, The University of Texas at Austin (Dec. 1988).
5. House, W.A. and Orr, D.R., "Investigation of the pH Dependence of the Kinetics of Quartz Dissolution at 25°C," *J. Chem. Soc. Faraday Trans.*, (1992) 233-241.
6. Bunge, A.L. and Radke, C.J., "Migration of Alkaline Pulses in Reservoir Sands," *SPEJ*, (Dec. 1982) 998-1012.
7. Bunge, A.L. and Radke, C.J., "The Origin of Reversible Hydroxide Uptake on Reservoir Rock," *SPEJ*, (Oct. 1985) 711-718.
8. Radke, C.J. and Jenson J.A., "Chromatographic Transport of Alkaline Buffers Through Reservoir Rock," *SPERE*, (Aug. 1988) 849-856.
9. Novosad, Z. and Novosad, J., "The Effect of Hydrogen Ion Exchange on Alkalinity Loss in Alkaline Flooding," *SPEJ*, (Feb. 1984) 49-52.
10. Lieu, V.T., "Long-Term Alkaline Consumption in Reservoir Sands," Second Progress Report for the City of Long Beach, THUMS Long Beach Co., DOE Contract No. DE-AC-03-76Et-12407 (June 1980).

